DNA biosensors

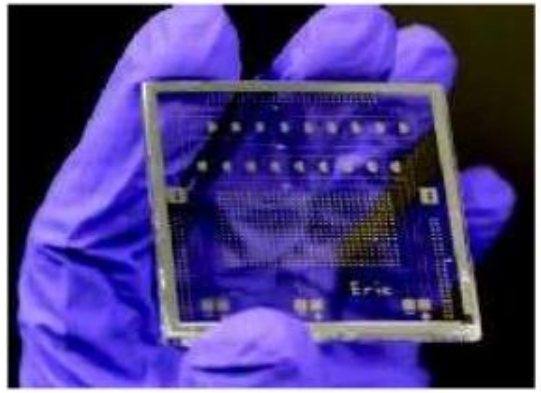

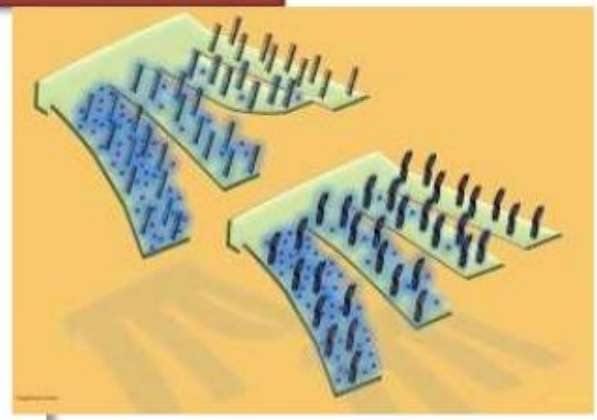

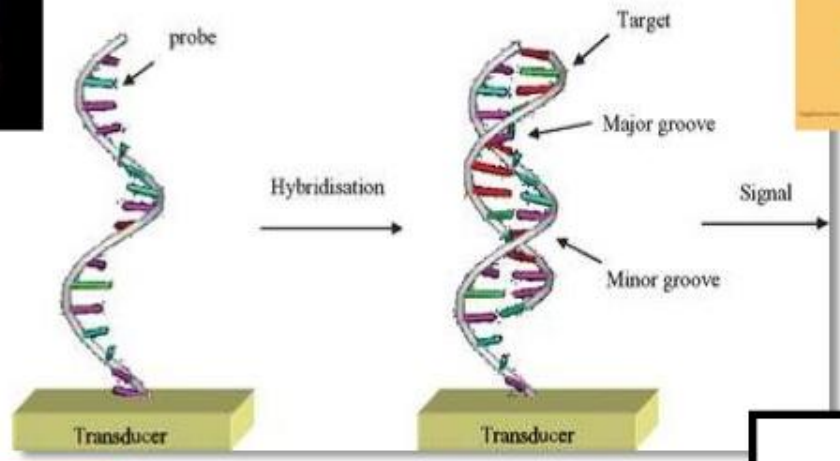

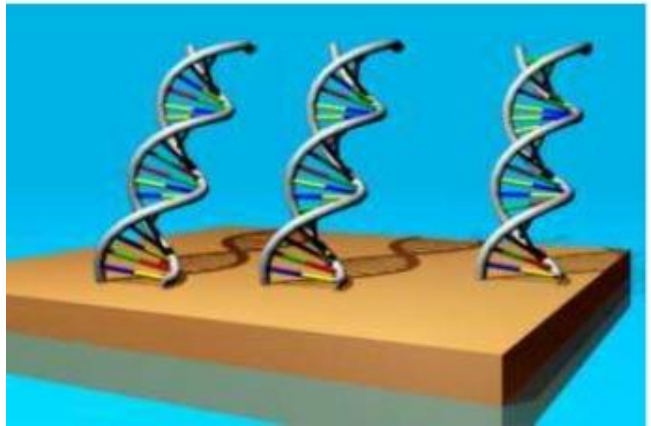

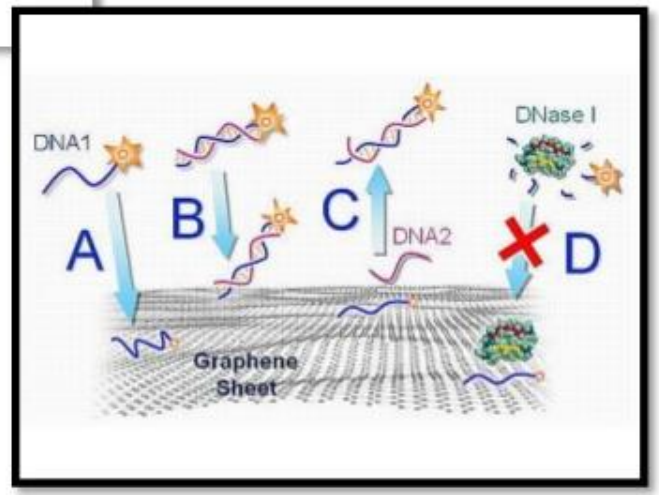

Principles of DNA biosensors

❖Nucleic acid hybridization

- **Perfect match**
  stable dsDNA, strong hybridization

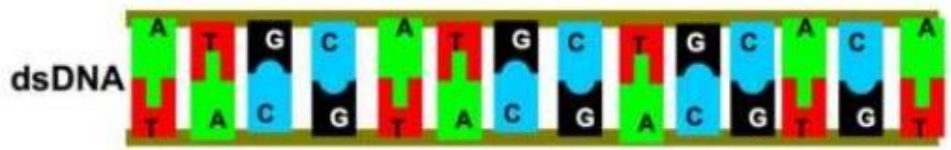

- **One or more base mismatches**
  weak hybridization

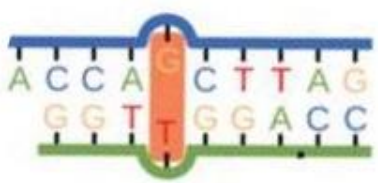

❖ Forms of DNA Biosensors

- Electrodes
- Chips
- Crystals

❖ Types of DNA Based Biosensors

- Optical
- Electrochemical
- Piezoelectric

Immobilization of DNA Probe onto Transducer Surface

- **simple adsorption**
  onto carbon surfaces

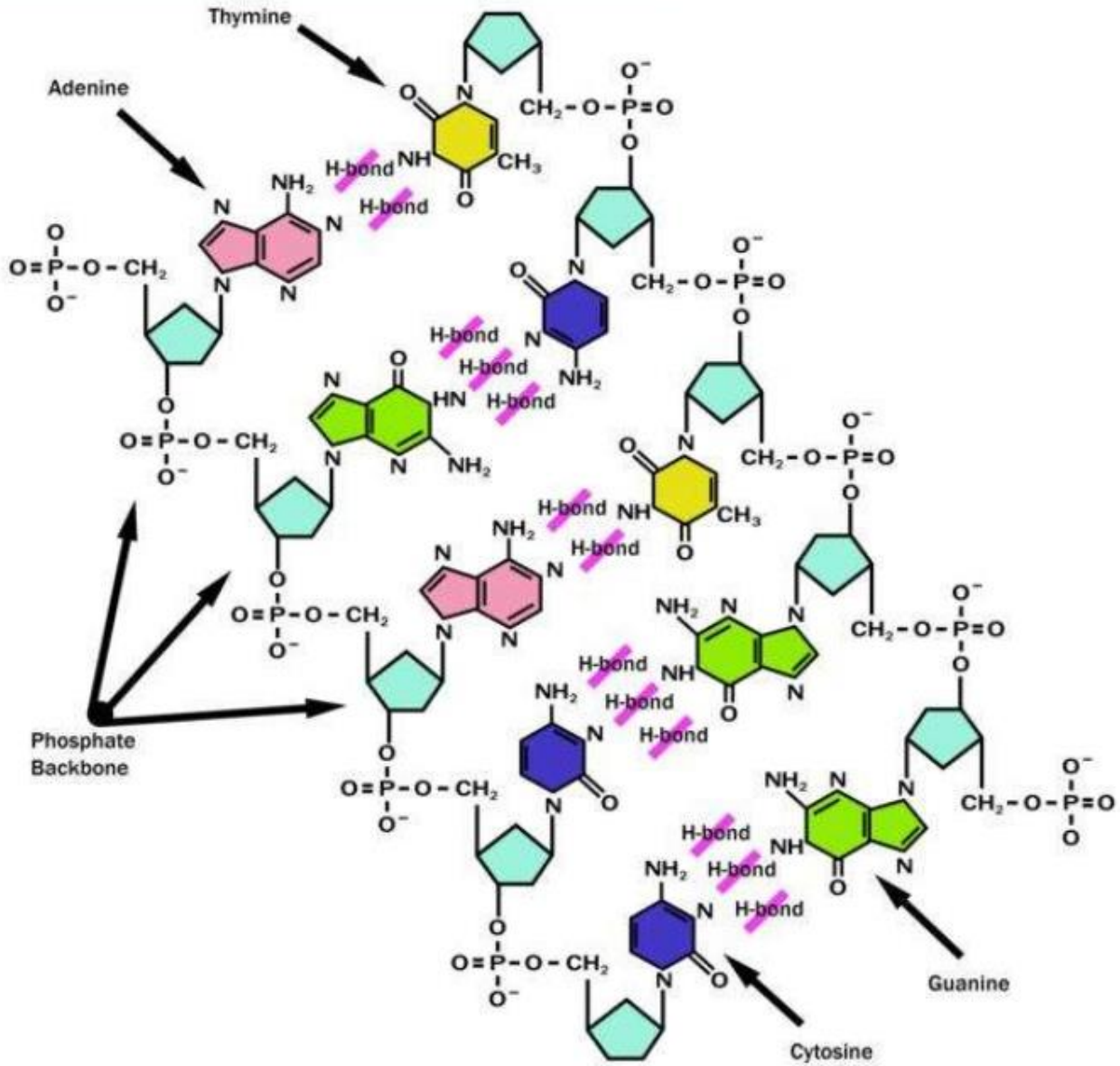

Immobilization of DNA Probe onto Transducer Surface

- Thiolated DNA for self assembly onto gold (or platinum) transducers

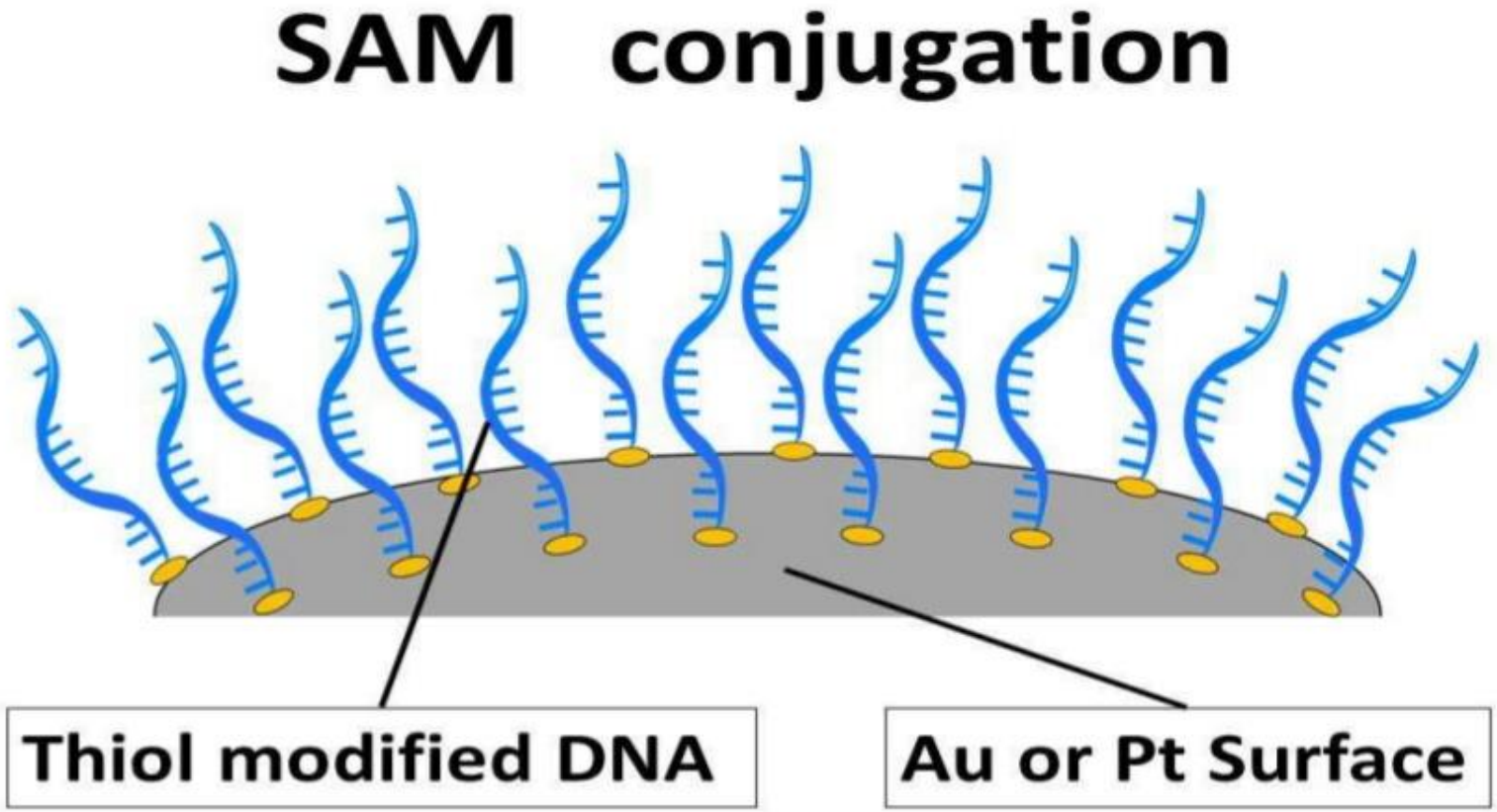

Immobilization of DNA Probe onto Transducer Surface

- Covalent linkage to the gold surface via functional **alkanethiol-based** monolayers

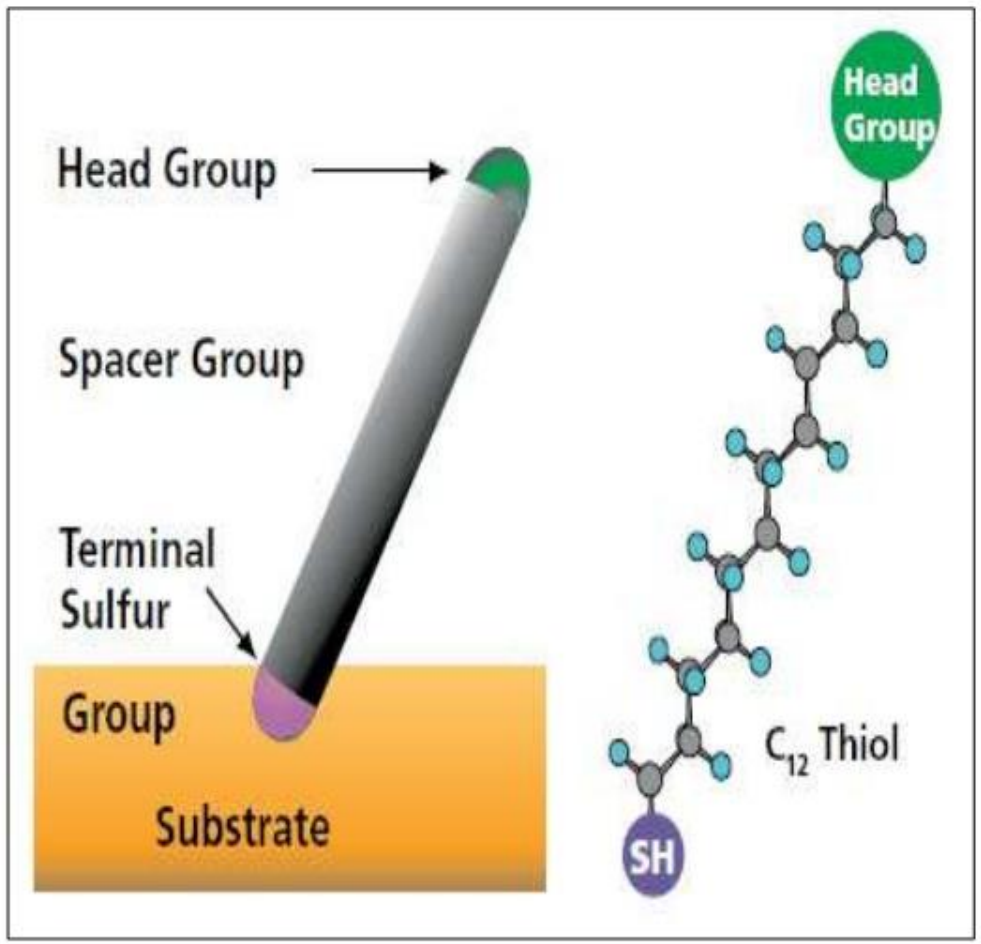

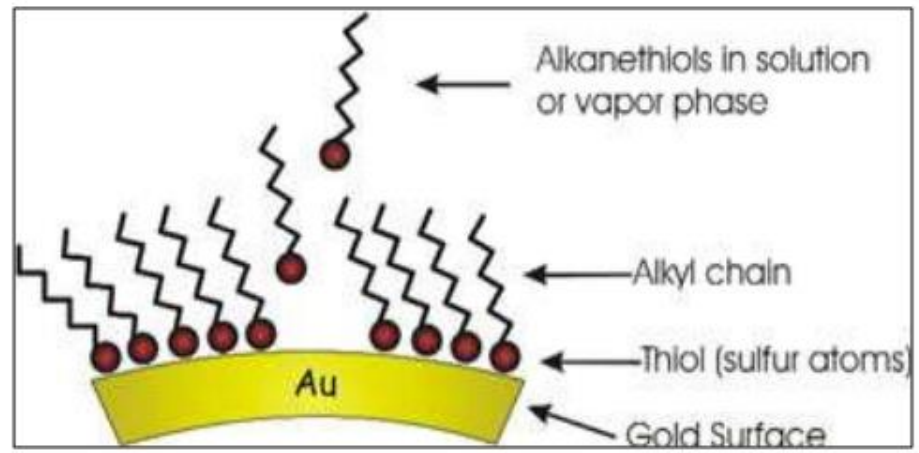

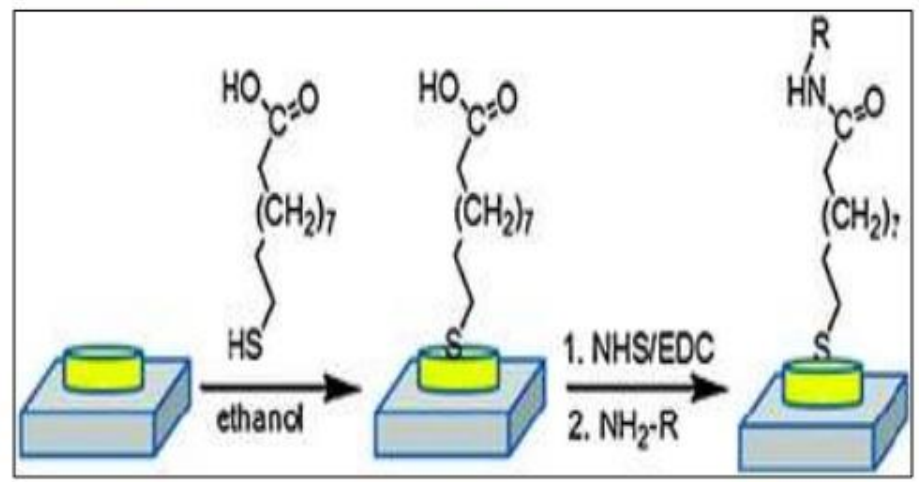

Immobilization of DNA Probe onto Transducer Surface

- Use of biotinylated DNA for complex formation with a surface-confined avidin or streptavidin

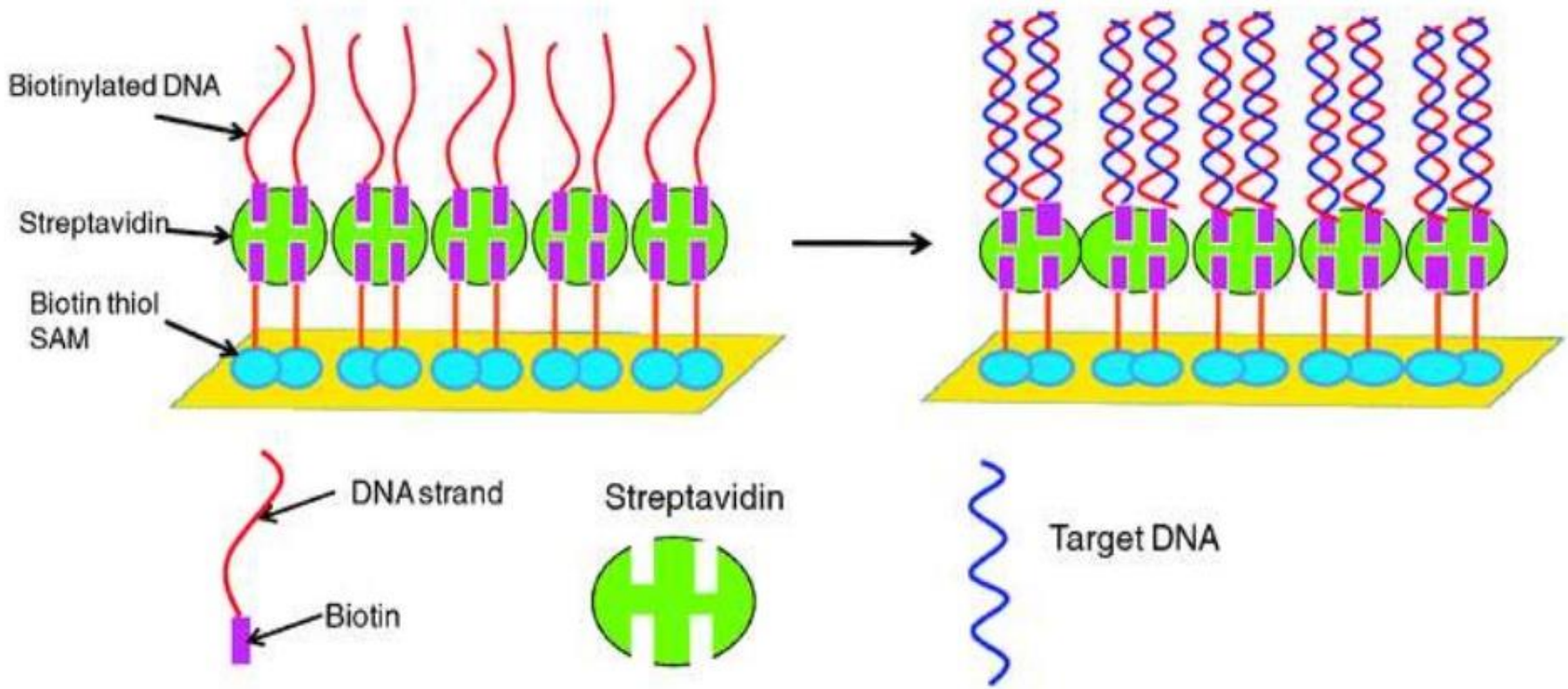

UNIVERSITÀ degli STUDI di CATANIA
DIPARTIMENTO DI SCIENZE CHIMICHE
Viale Andrea Doria, 6 – I-95125Catania

Tecniche innovative ed ultrasensibili PCR-free per la diagnosi precoce di acidi nucleici in biopsia liquida

Noemi Bellassai

Webinar, ***28 Aprile 2021***

Liquid biopsy

Non-invasive test based on the **detection of biomarkers** related to specific disease circulating in body fluids (blood, plasma, serum, urine, saliva, synovial fluid etc.).

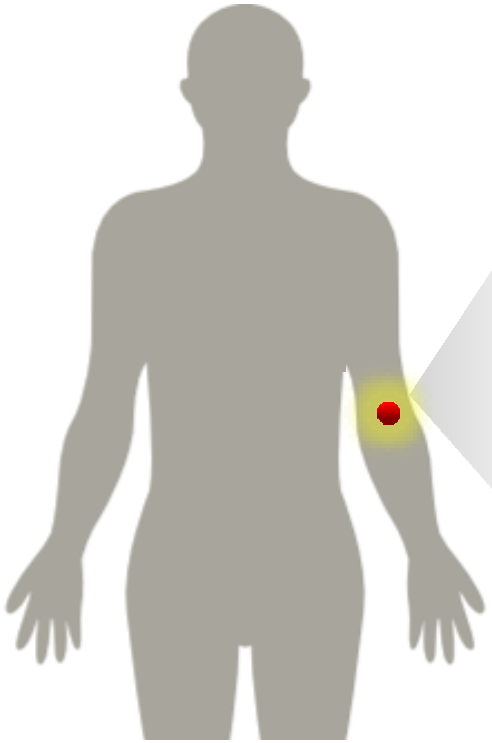

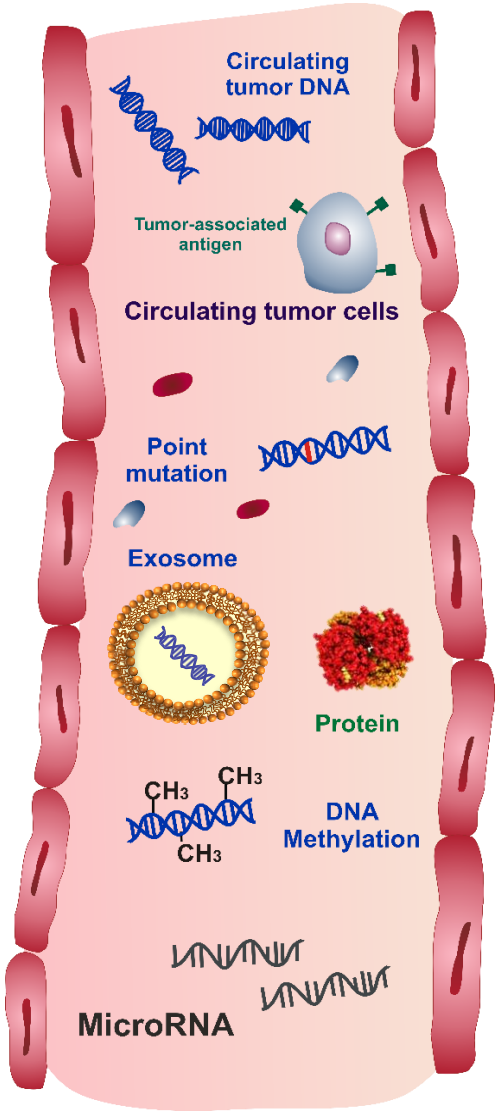

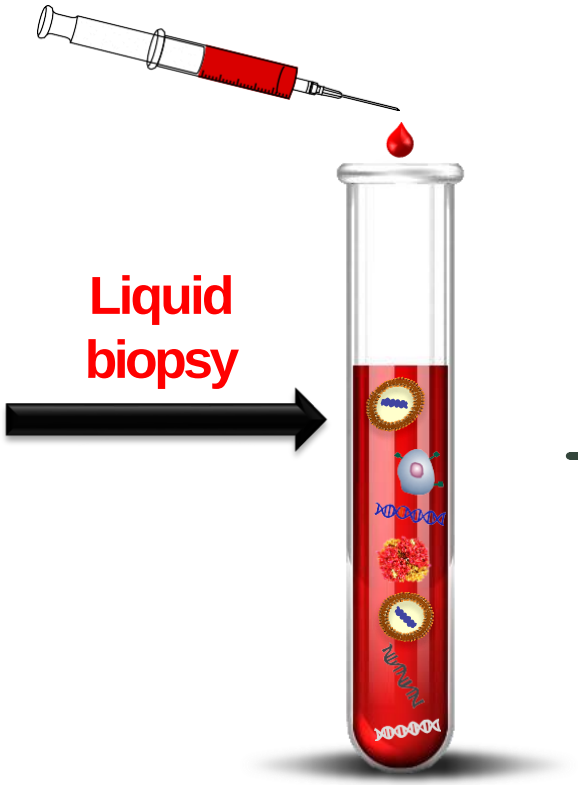

- ctDNA
- miRNA
- Protein
- CTCs

Bellassai et al., Front Chem **2019**, 7, 570

Liquid biopsy

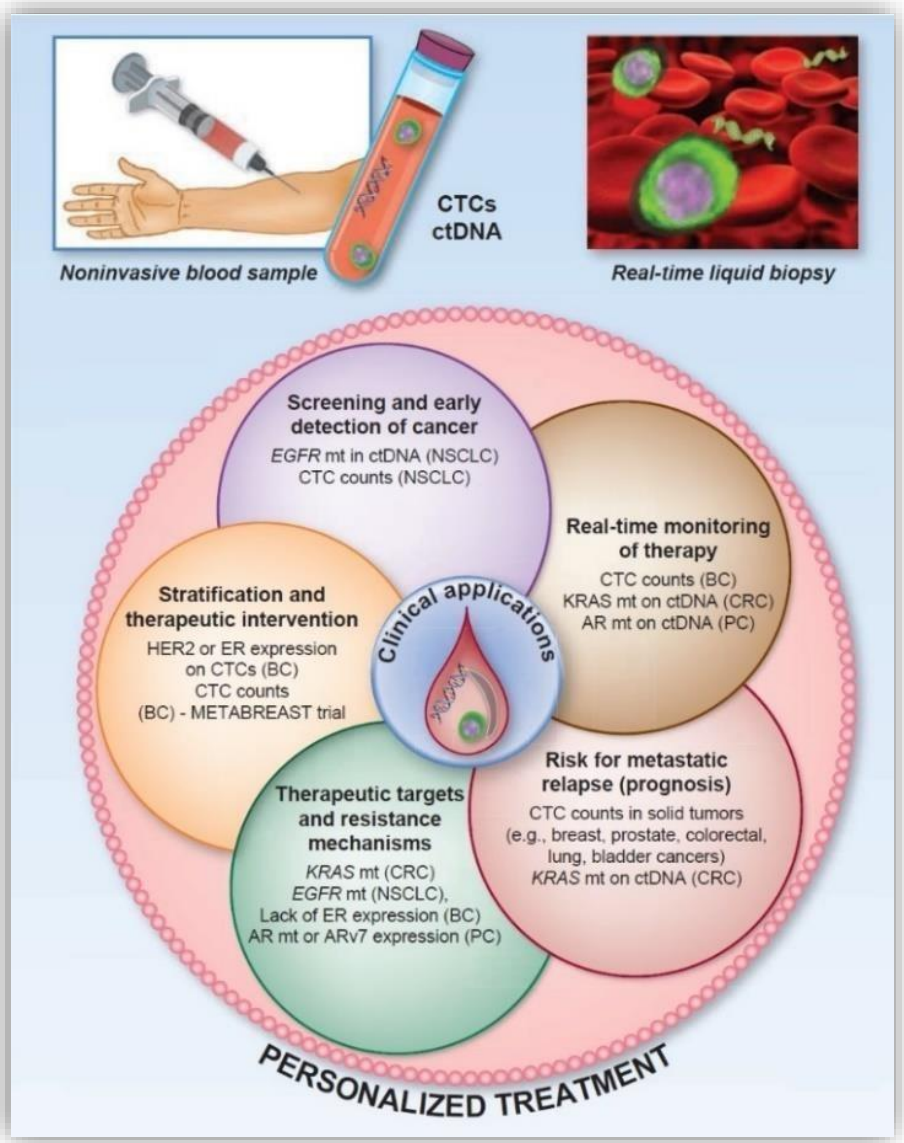

Alix-Panabières et al., Cancer Discov. **2016**; 6(5), 479

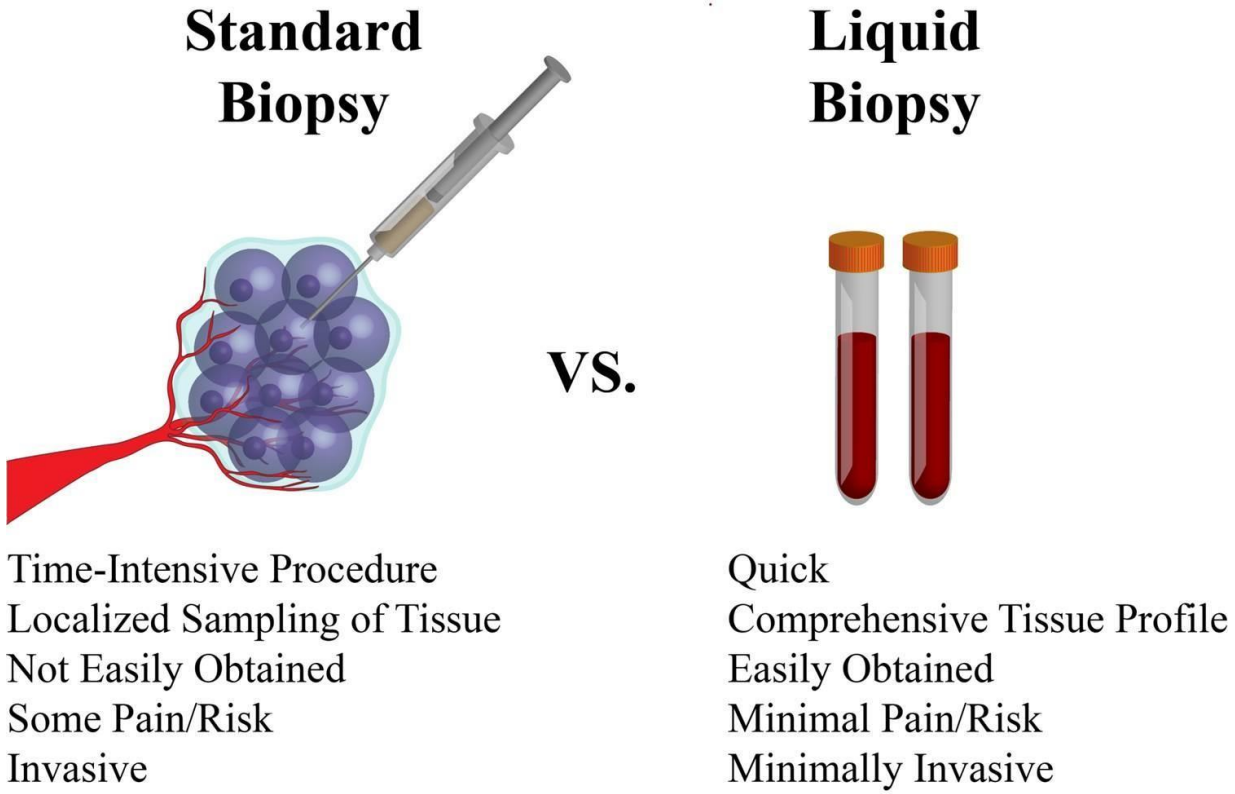

Lovly et al. **2016**. Circulating Tumor DNA. My Cancer Genome (Updated February 8).

Sosa et al., Nat. Rev. Cancer. **2014**; 14:611-622

Liquid biopsy for early diagnosis disease

The opportunity

Circulating tumour DNA (ctDNA) is easy accessible and can be detected in most metastatic cancers

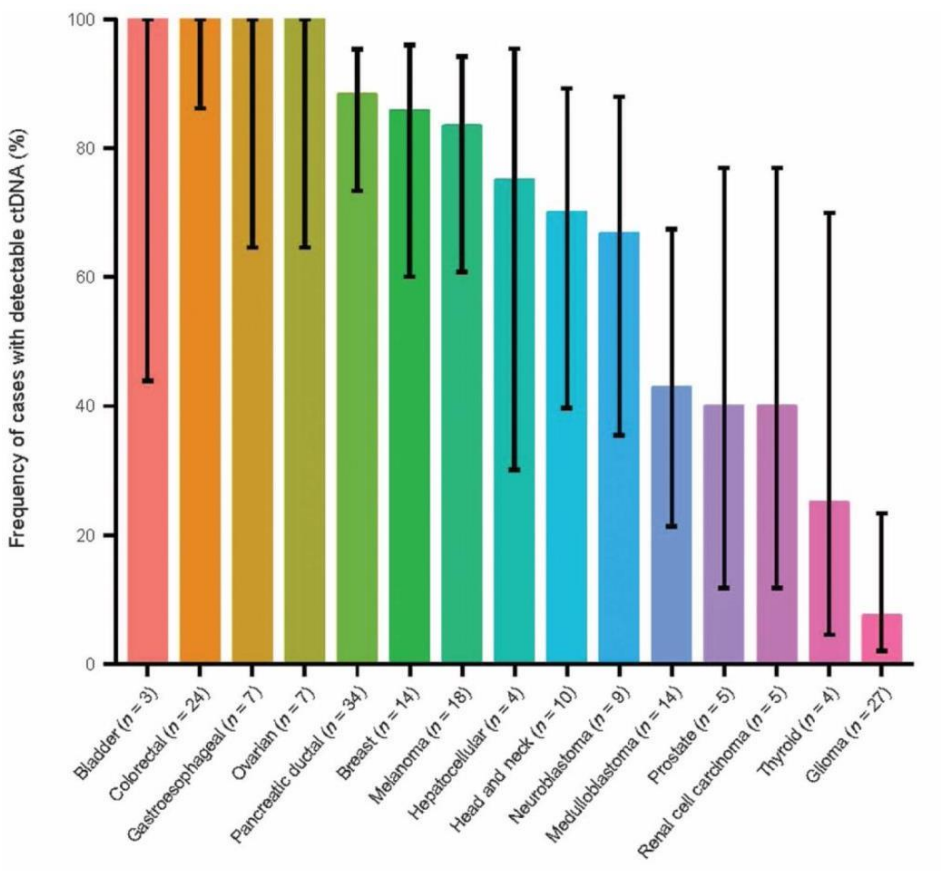

The challenge

ctDNA is often only present at low levels

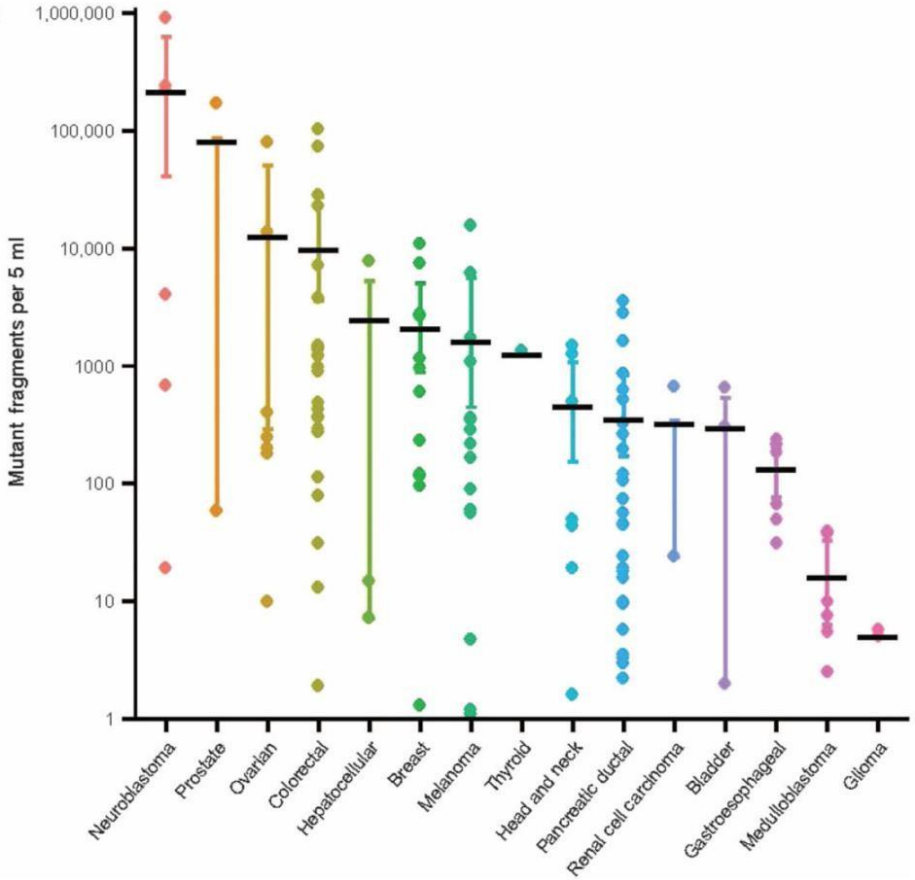

Bettegowda et al., *Sci Transl Med.* **2014**, 19, 6(224)

Detection of nucleic acid biomarkers

Targeted
Detection of mutations in a set of predefined genes

- Few loci are investigated
- Less than 1% frequency
- High analytical sensitivity and specificity

Technologies:
digital PCR, BEAMing, …

Untargeted
To screen the genome by discovering changes

- Genome wide analysis
- Less than 1% frequency
- Low analytical sensitivity and specificity

Technologies:
NGS, Safe-SeqS, …

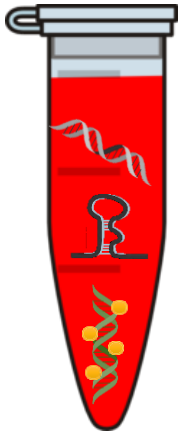

Liquid biopsy
Main technologies

ctDNA
Tumor mutational burden
Amplifications/deletions
Traslocations
Point mutations
Chromosomal abnormalities
Tumor heterogeneity

ctDNA/methylation
Epigenetic alterations
DNA methylation
Tumor heterogeneity

Circulating miRNAs

ctDNA
- ARMS-PCR
- Methylation specific PCR
- ddPCR
- NGS

miRNAs
- RT-qPCR
- ddPCR
- NGS

Diaz et al., J. Clin. Oncol. **2014**; 32(6):579–586

Lianidou et al., Genes Chromosom. Cancer **2019**; 58:219–232

Target Amplification Methods

- Polymerase chain reaction (PCR)
  - PCR using specific probes
  - RT PCR
  - Nested PCR-increases sensitivity, uses two sets of amplification primers, one internal to the other
  - Multiplex PCR-two or more sets of primers specific for different targets
  - Arbitrarily Primed PCR/Random Primer PCR
- Isothermal methods

Polymerase chain reaction (PCR) Inventor

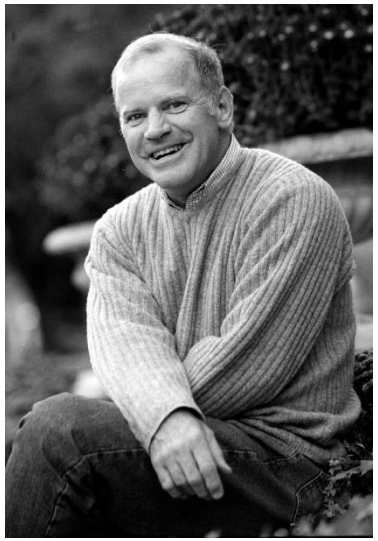

Kary Banks Mullis
(1944-2019)

Nobel Prize in Chemistry 1993

Beyond PCR … Isothermal amplification

Nucleic acids amplification operated at a constant temperature

- ❑ **Implementation in point-of-care devices is simplified**
- ❑ **Can be performed under simple conditions (e.g., water bath)**
- ❑ **Many isothermal amplification methods are available providing exponential or linear amplification**
- ❑ **Enzymatic and enzyme-free isothermal amplification methods are available**

Giuffrida M.C. et al., *Biosens Bioelectron*, **2017**, 90, 174-186.

Method	Temp (°C)	Reaction time (min)	Amplification	Target	Primers	Main applications
LAMP	60-65	30-60	10^9	dsDNA hundred base-pair long	4-6	Bacteria, Viruses
RPA	25-42	5-20	10^9 - 10^{11}	dsDNA ssDNA RNA	2	Pathogens, Viruses
NASBA	~41	90-120	10^9	RNA	2	Bacteria, Pathogens
RCA	30-65	60-120	10^3 linear 10^9 expon.	ssDNA	1	Plasmid, Viruses
NEEA	54-58	15-30	10^9	dsDNA RNA	2	Viruses, RNA DNA
HDA	37-60	60-120	10^6	dsDNA	2	Biomarkers, Viruses

Loop mediated isothermal amplification (LAMP)

- Amplification takes place at a single temperature (65°C)
  (No need of thermal cycler)
- Uses polymerase with high strand displacement activity
  (Bacillus stearothermophilus Bst DNA Polymerase instead of *Taq* Poly)
- Amplification efficiency is high (up to 10^9)
- Can be also used for RNA templates by addition of reverse transcriptase

Loop mediated isothermal amplification (LAMP)

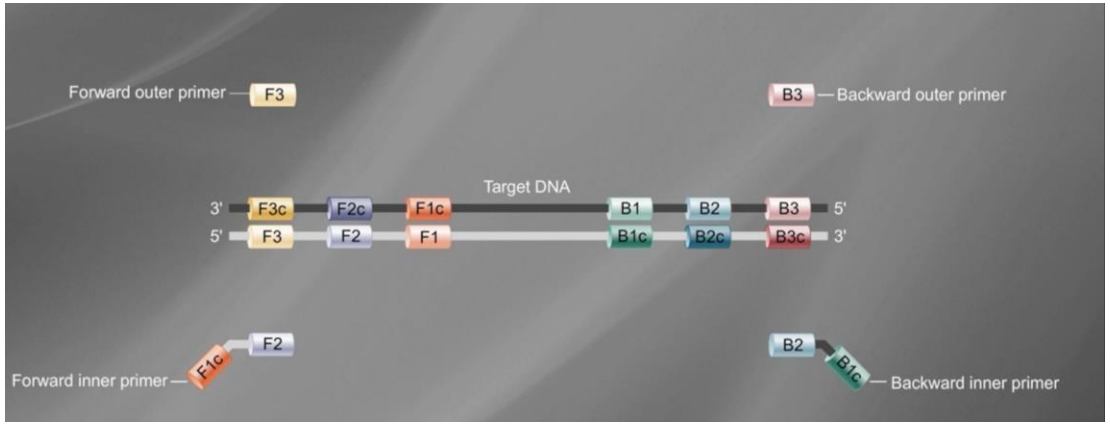

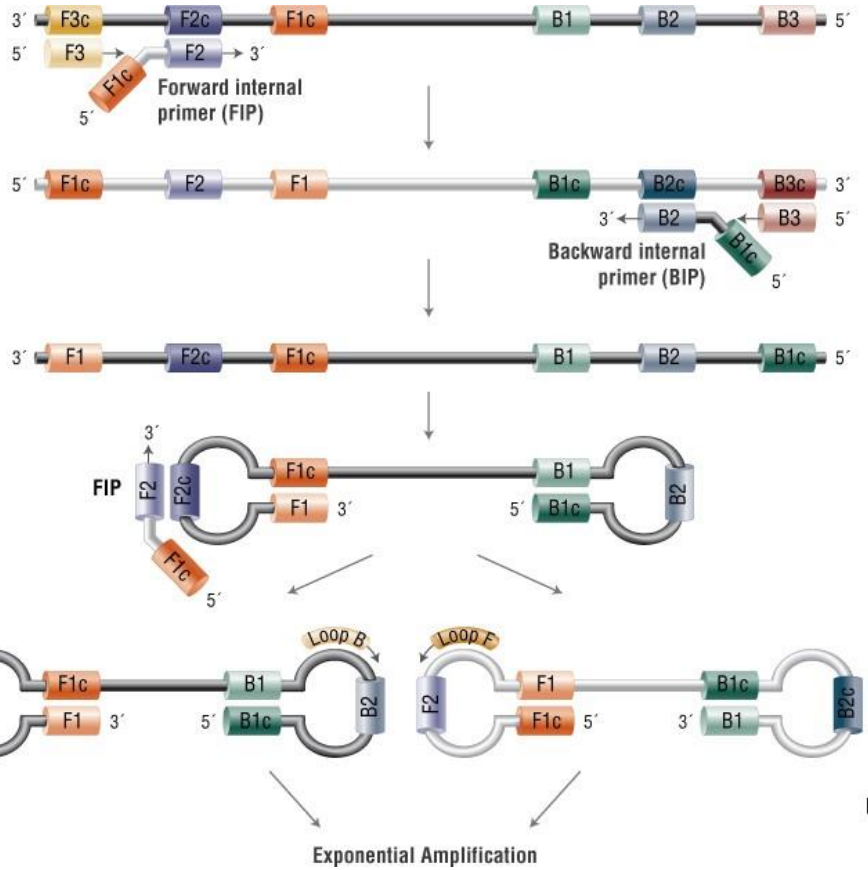

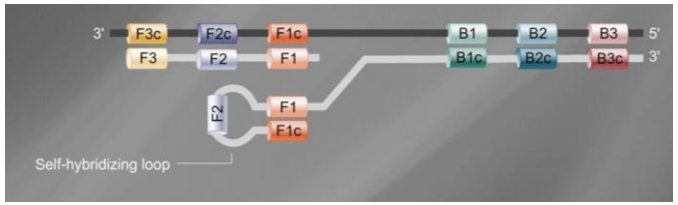

Loop-mediated isothermal amplification (LAMP) uses 4-6 primers recognizing 6-8 distinct regions of target DNA.

A strand-displacing DNA polymerase initiates synthesis and 2 of the primers form loop structures to facilitate subsequent rounds of amplification.

https://www.youtube.com/watch?v=L5zi2P4lggw

LAMP-Based SARS-CoV-2 Testing Methods

SARS-CoV-2 Rapid Colorimetric LAMP Assay Kit

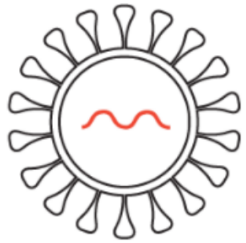

SARS-CoV-2

SARS-CoV-2 (+) ssRNA (30 kb)

target region

RT - 1st strand

cDNA - 2nd strand

dumbbell DNA structure

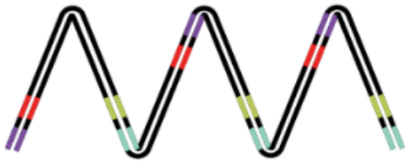

high molecular weight amplicons

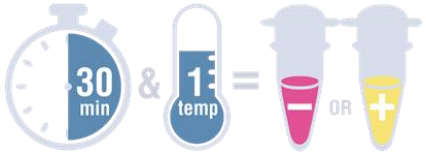

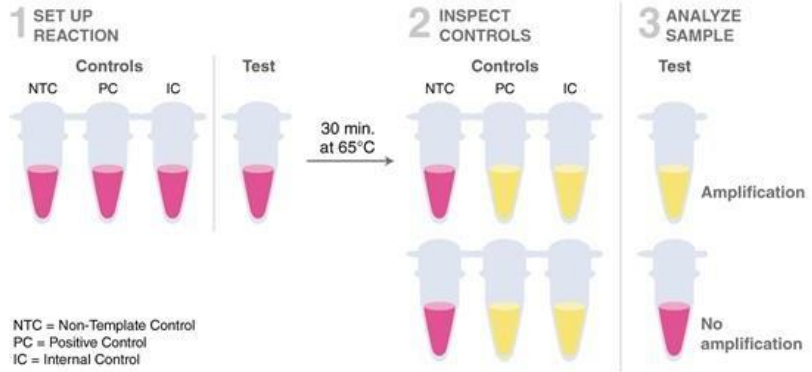

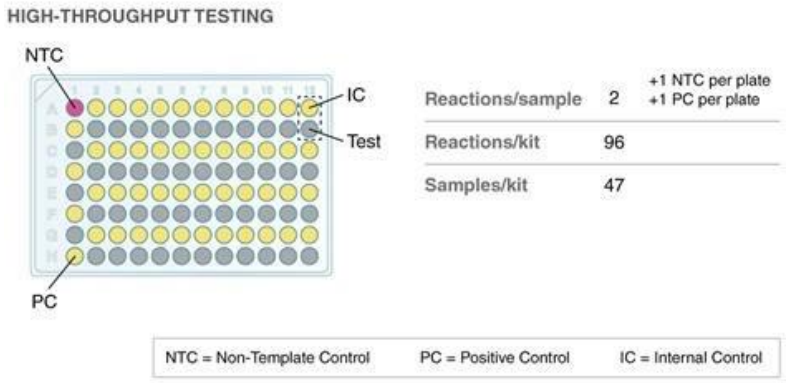

Molecular beacon-assisted isothermal circular strand displacement polymerization (ICSDP)

Isothermal amplification

Isothermal circular strand displacement polymerization. Displaced target available for a new cycle.

Linear amplification

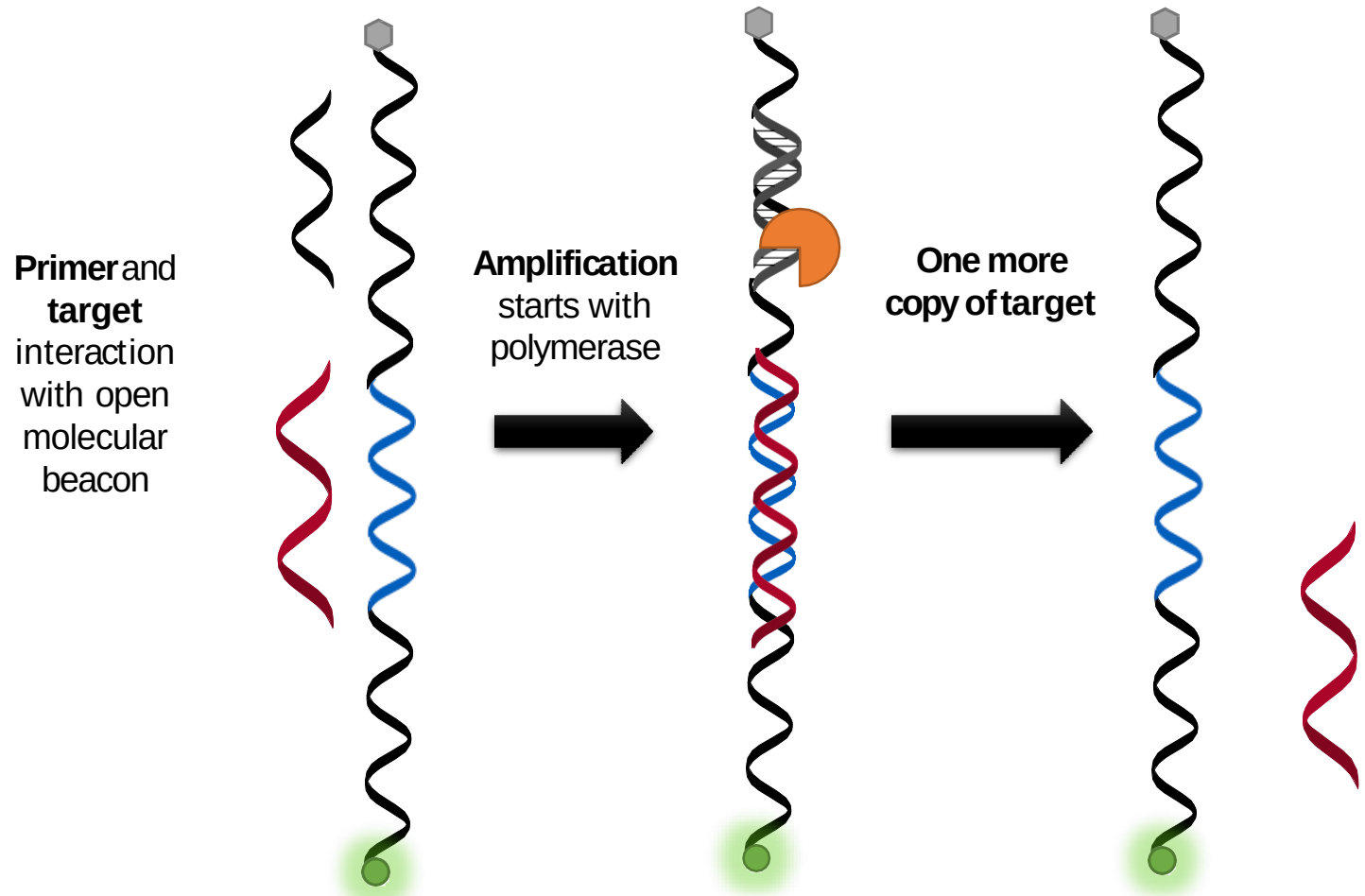

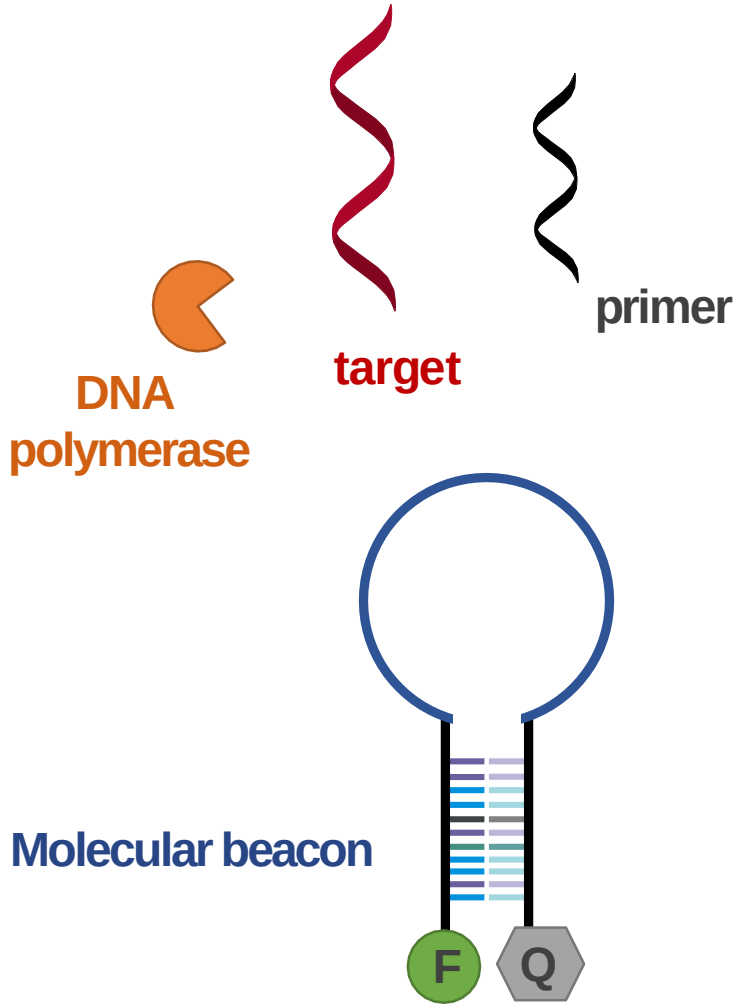

Guo Q. et al., *Nucleic Acids Res.* **2009**, 37, e20

Giuffrida M.C. et al., *Anal. Bioanal. Chem.* **2015**, 407, 6, 1533-1543

MICROFLUIDICS

It is the science and technology of systems that process or manipulate small (10^{-9} to 10^{-18} litres) amounts of fluids, using channels with dimensions of tens to hundreds of micrometres.

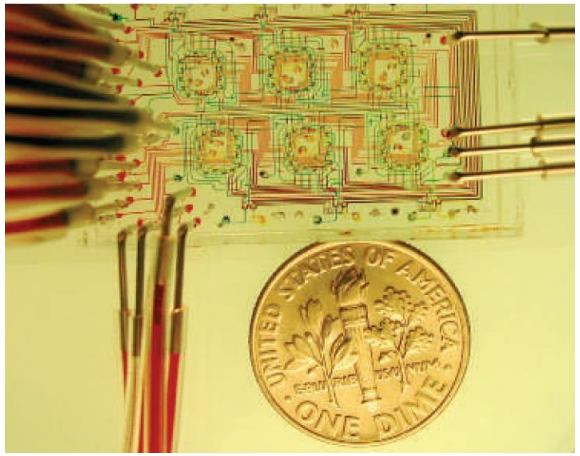

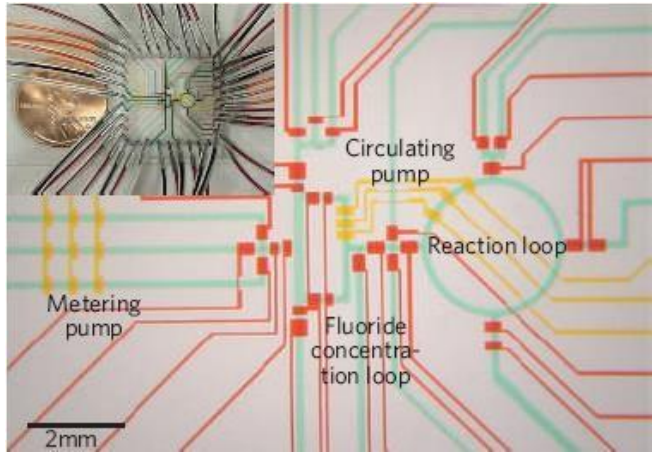

$1l = 1dm^3$

$1\mu l = 1mm^3$

$1nl = 100\mu m^3$

$1pl = 10\mu m^3$

$1fl = 1\mu m^3$

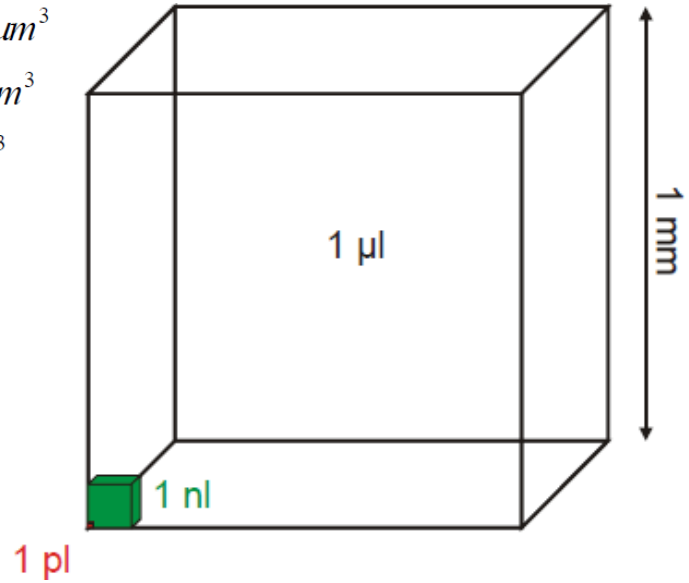

Typical size of a cell 1-30 µm

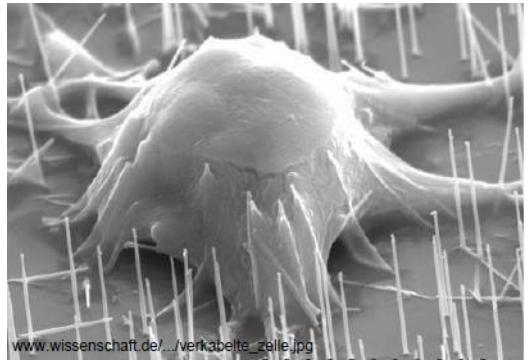

Drug inhaler, Droplet diameter ~ 5 µm

Whitesides, G. *Nature* **2006**, 442, 368–373

MICROFLUIDICS

Model for the description of the motion of fluids

Newtonian fluid → laminar flow

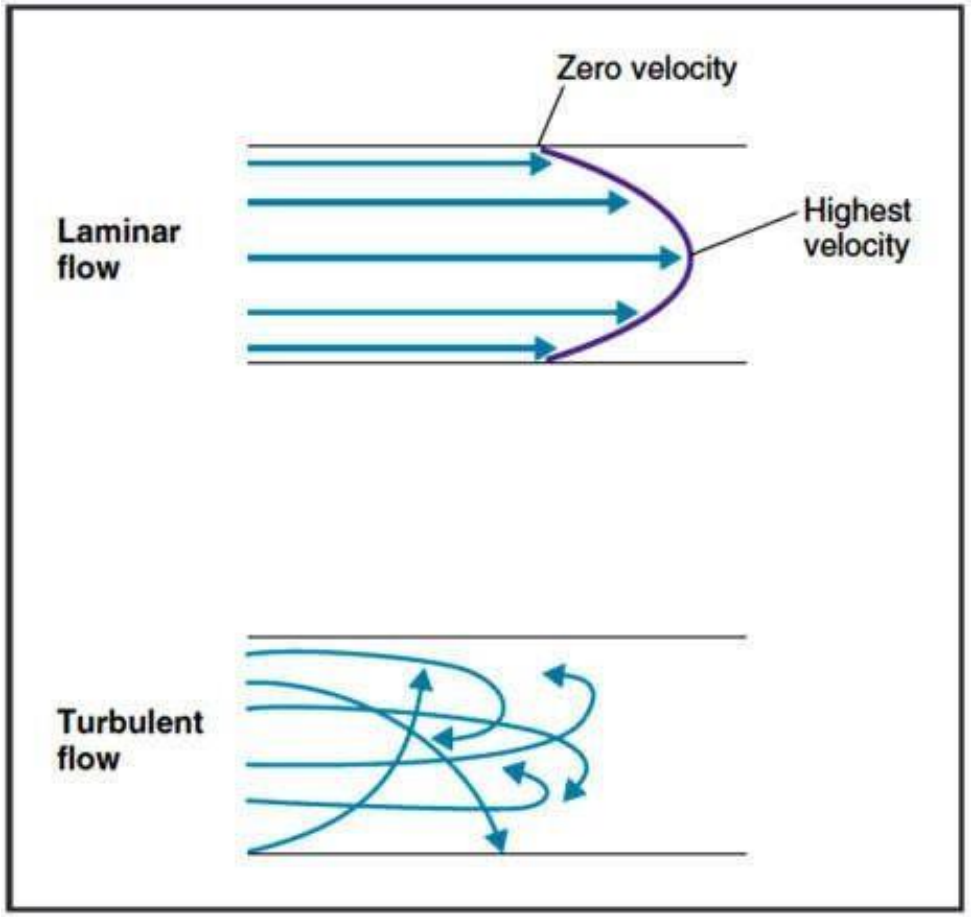

- **Non-dimensional Navier-Stokes equation**

$$\frac{\rho UL}{\mu}\left(\frac{\partial \mathbf{u}'}{\partial t'}+\mathbf{u}'\nabla\mathbf{u}'\right)=-\nabla p'+\eta\nabla^2\mathbf{u}'+\mathbf{f}'$$

Reynolds number

$$\mathrm{Re}=\frac{\rho UL}{\mu}\approx\frac{\text{Inertial forces}}{\text{Viscous forces}}$$

Re>2000
Turbulent

Re<2000
Laminar

MICROFLUIDICS: devices fabrication

Fabrication of microfluidic device by PDMS replica molding

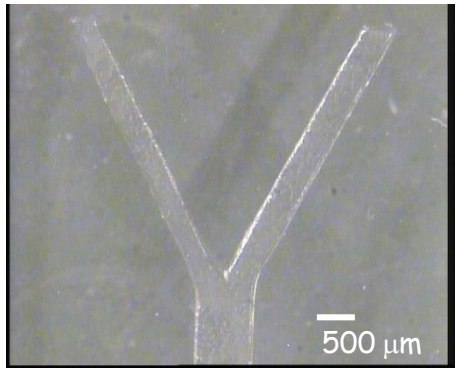

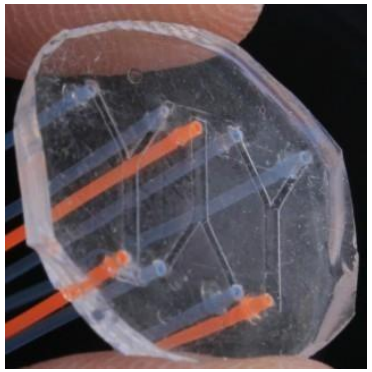

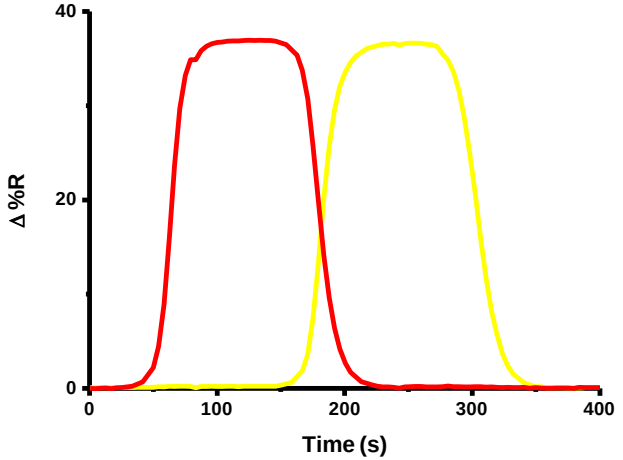

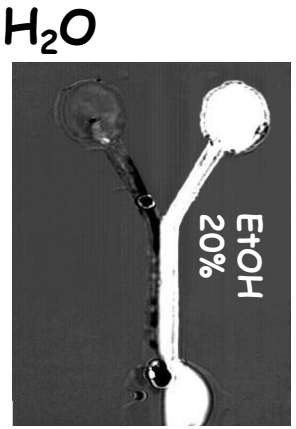

Re≈100

Laminar flow

Immiscible liquids

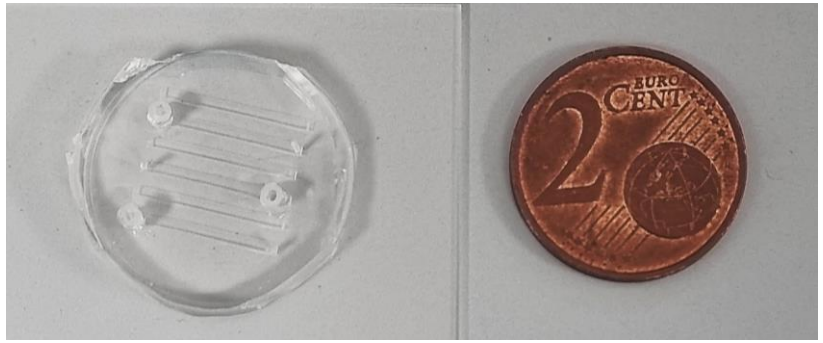

microfluidic channels (14×0.4×0.8mm)

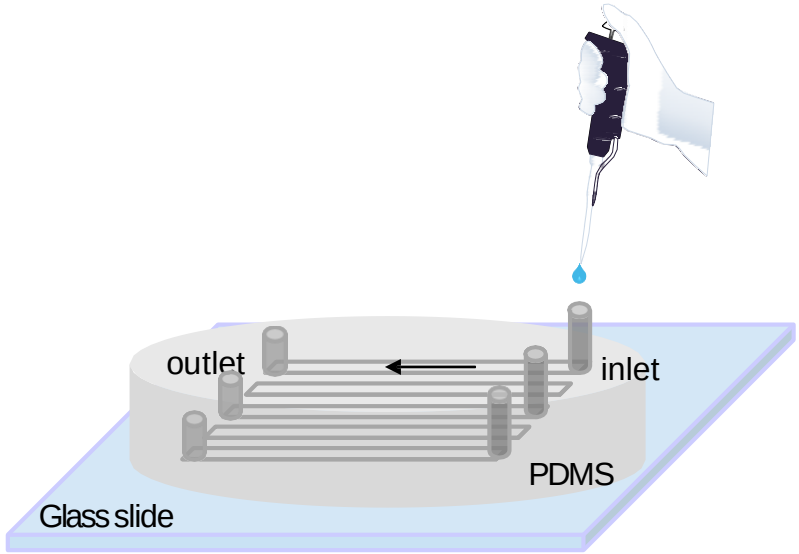

< 1 µL of sample volume

Parallel microchannels for multiple detection

D'Agata R. et al., *Biosens. Bioelectron.* **2010**, 25(9):2095-2100.

MICROFLUIDICS: devices fabrication

Fabrication of microfluidic device by PDMS replica molding

Master with different design
in plastic or silicon wafer

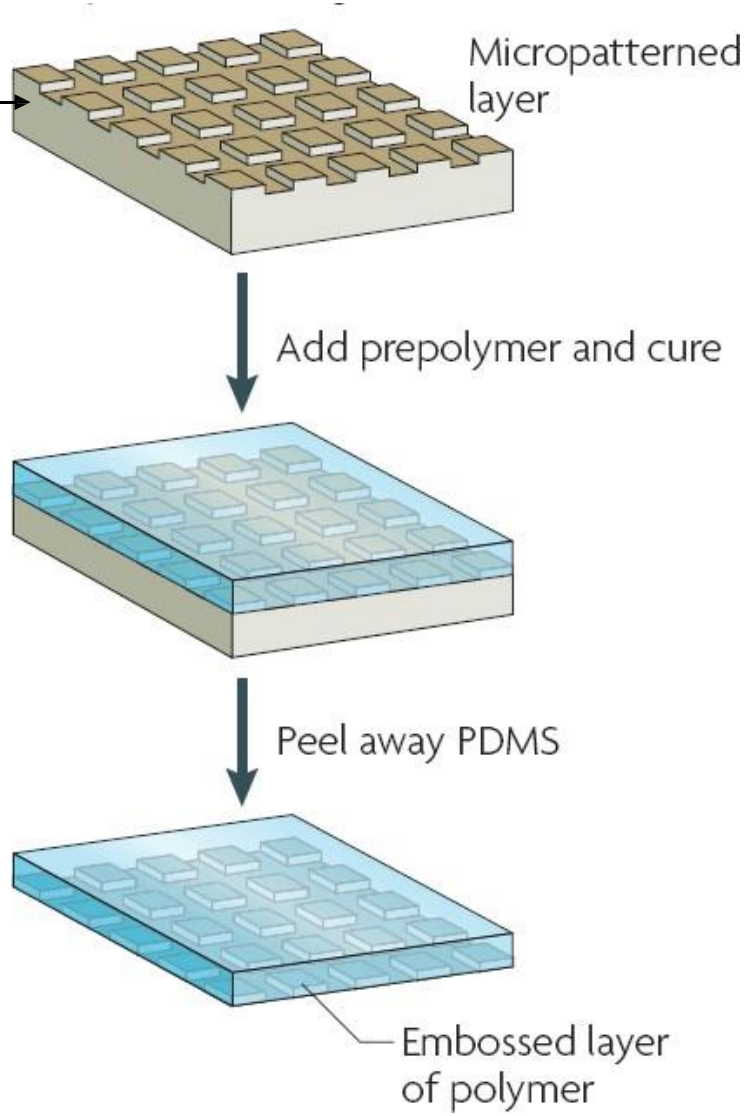

PDMS device with
microfluidic pattern

Weibel et al. *Nature Reviews: Microbiology* **2007**, 5, 209.

MICROFLUIDICS: Why?

- Small sample volume
- Miniaturization
- Reduction of analysis time
- Parallel devices and faster processes
- High-throughput
- Integration and portable devices
  (lab-on-a-chip, micro Total Analysis Systems μTAS)

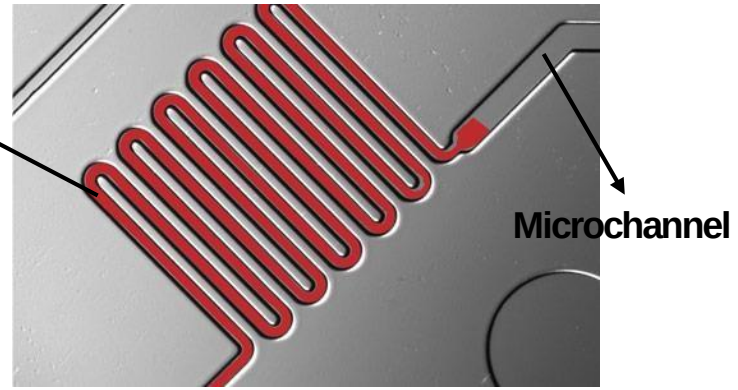

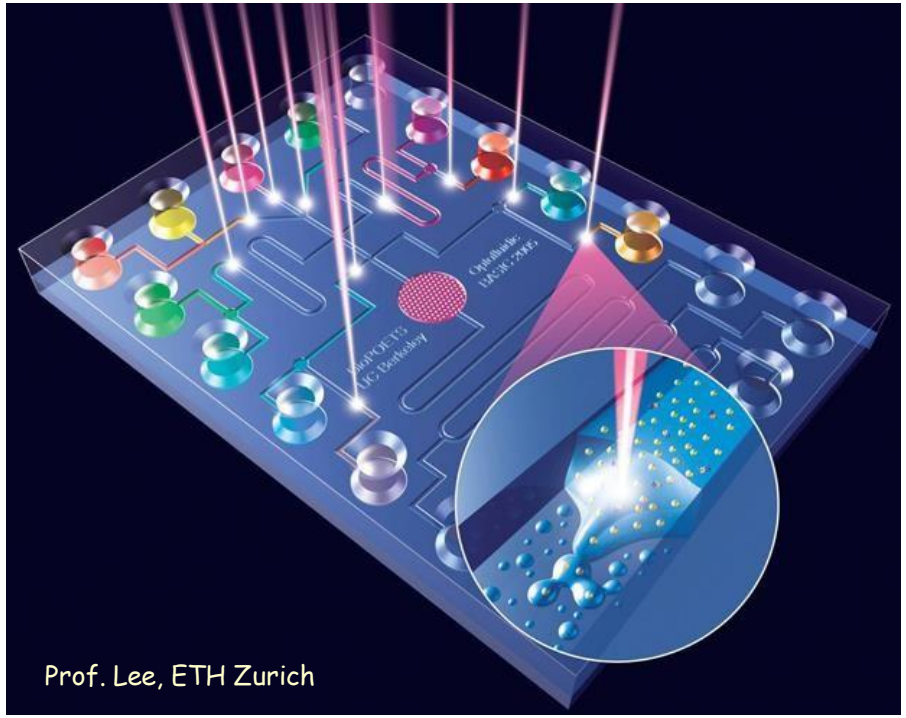

Zhang Y. et a., *Anal. Chim. Acta* **2009**, 638, 115-125

microRNA (miRNA)

- **Single-stranded, non-coding RNA molecules**
- **Key-role in protein expression**
- **mRNA silencing**
- **Remarkable stability when released into biofluids**

Challenges for miRNA detection

- Analytes are present at low concentrations

  Biomarker levels: fg mL^{-1} - ng mL^{-1}

- Short length sequence

  Length: 19-23 nt

- High sequence homology

Mendell J.T. et al., *Cell* **2012**, 148, 1172-1187

Tu M. et al., *Sci. Rep.* **2016**, 6, 25032

D'Agata R. et al., *Anal. Bioanal. Chem.* **2019**, 411: 4425

Microfluidic lab-on-a-chip platform for liquid biopsy: microRNA

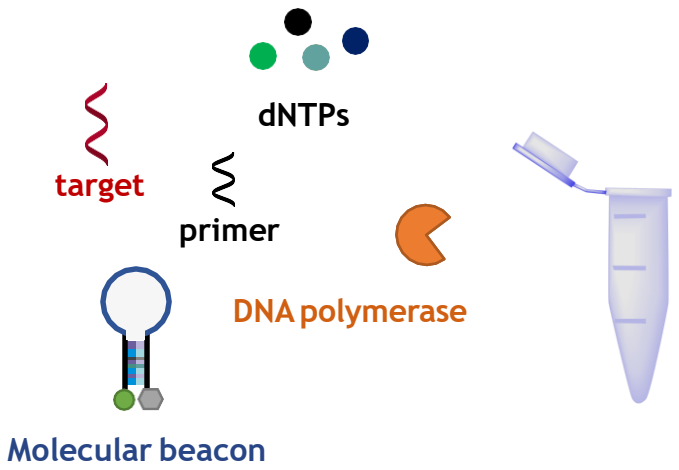

ICSDP amplification

30 °C 2 hr
constant temperature

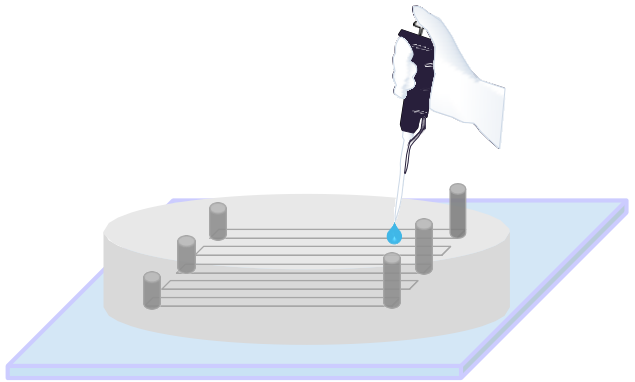

Fluorescence detection

microRNA-127
biomarker for chronic joint disease

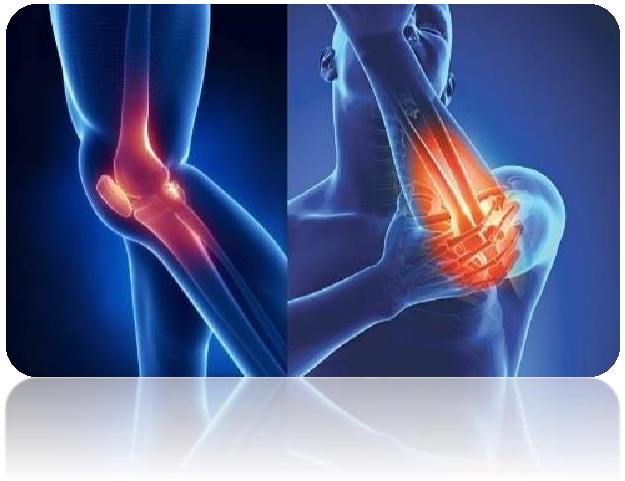

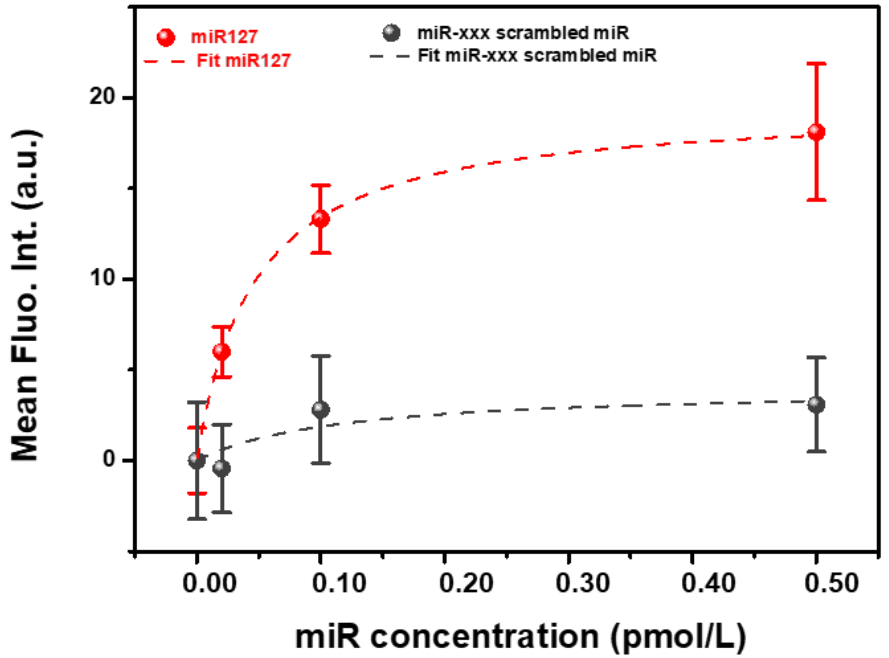

- Low sample volume
- No time consuming
- High selectivity in buffer
- Discrimination in synovial fluid
- Low detection

Optical biosensors: Surface Plasmon Resonance

Electromagnetic radiation in resonance with surface plasmon oscillation.

Surface plasmon polaritons : quasi-particles resulting from the coupling of surface plasmons and photons

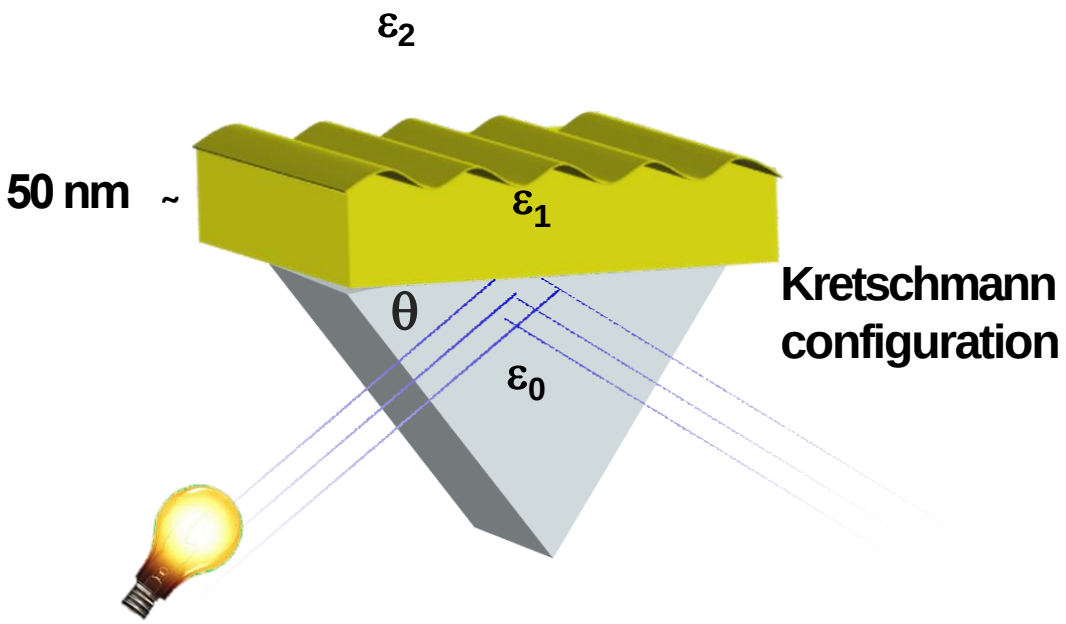

Kretschmann configuration

Plasmon wave vector = radiation wave vector

$$K_{SPP} = \frac{\omega}{c}\sqrt{\frac{\varepsilon_1'\varepsilon_2}{\varepsilon_1'+\varepsilon_2}} = \frac{\omega}{c}\sqrt{\varepsilon_0}\,sen\,\vartheta = K_{Light}$$

Radiation wave vector

$$k_{Light} = \frac{\omega}{c}\sqrt{\varepsilon_0}sen\theta$$

Snell's Law

$$\sin\theta = \frac{\varepsilon_1}{\varepsilon_0}$$

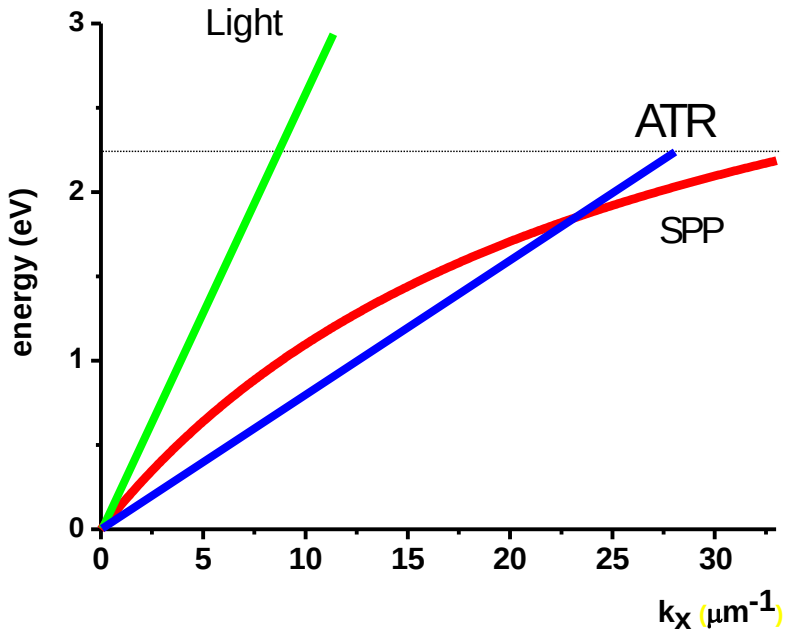

Optical biosensors: Surface Plasmon Resonance

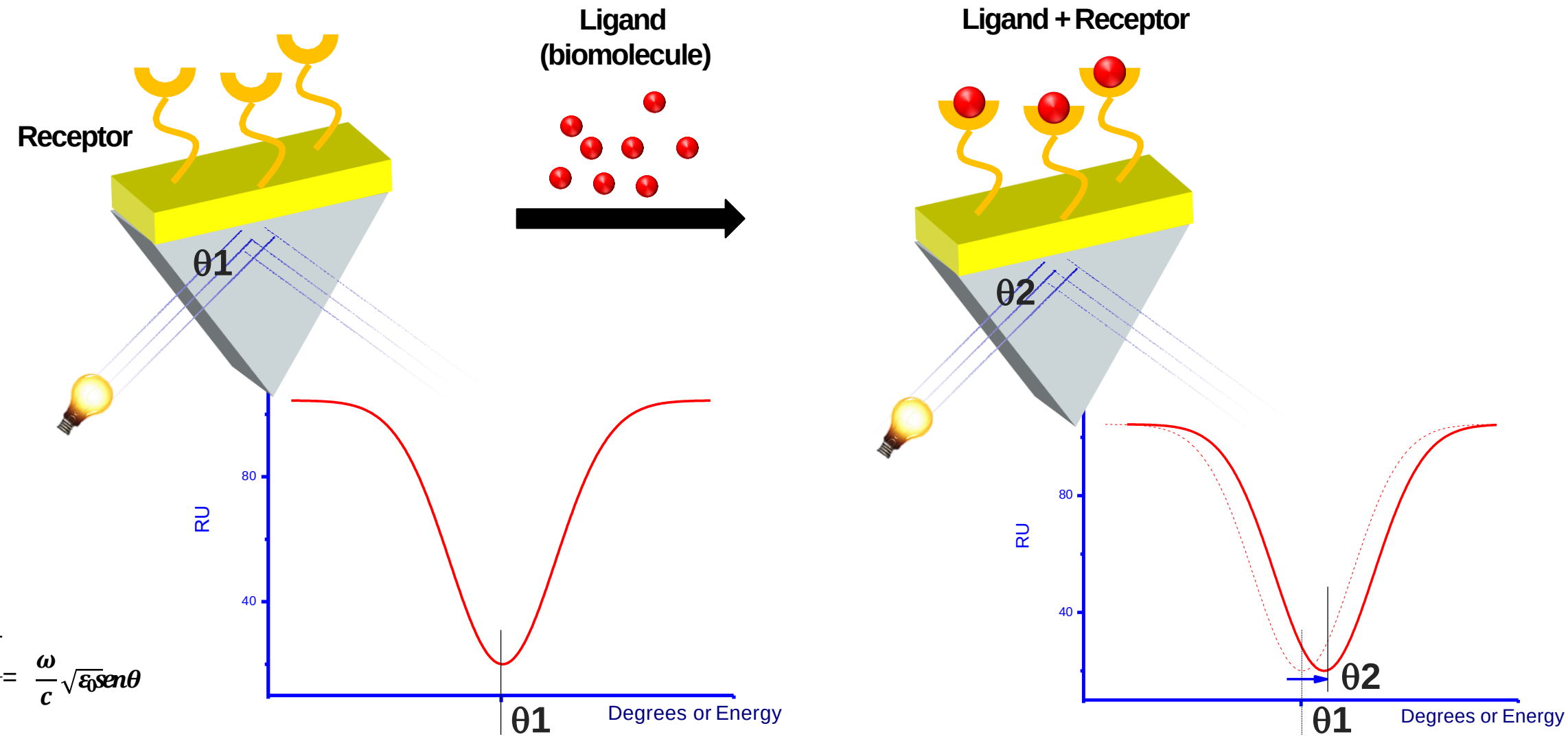

$$\frac{\omega}{c}\sqrt{\frac{\varepsilon_1'\varepsilon_2}{\varepsilon_1'+\varepsilon_2}} = \frac{\omega}{c}\sqrt{\varepsilon_0}\,sen\theta$$

$$n = \sqrt{\varepsilon}$$

Attenuated total reflection (ATR)

Optical biosensors: Surface Plasmon Resonance

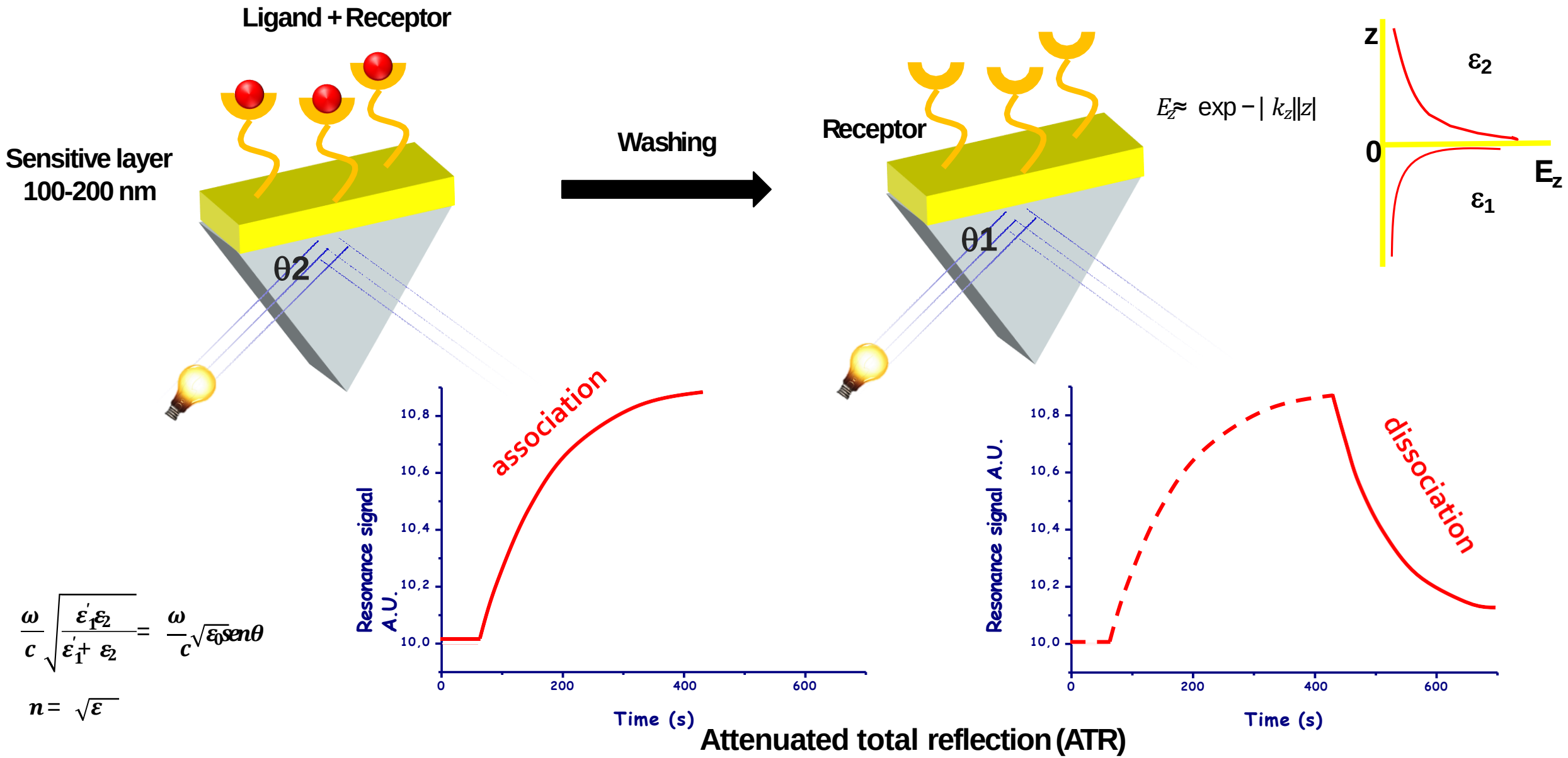

$$\frac{\omega}{c}\sqrt{\frac{\varepsilon_1'\varepsilon_2}{\varepsilon_1'+\varepsilon_2}} = \frac{\omega}{c}\sqrt{\varepsilon_0}\,sen\theta$$

$$n = \sqrt{\varepsilon}$$

Attenuated total reflection (ATR)

Surface Plasmon Resonance Imaging (SPRI)

- Real-time analysis
- Label-free
- High sensitivity
- Multi-analyte monitoring

Sensitivity can be improved up to nM-fM

PCR-free method!

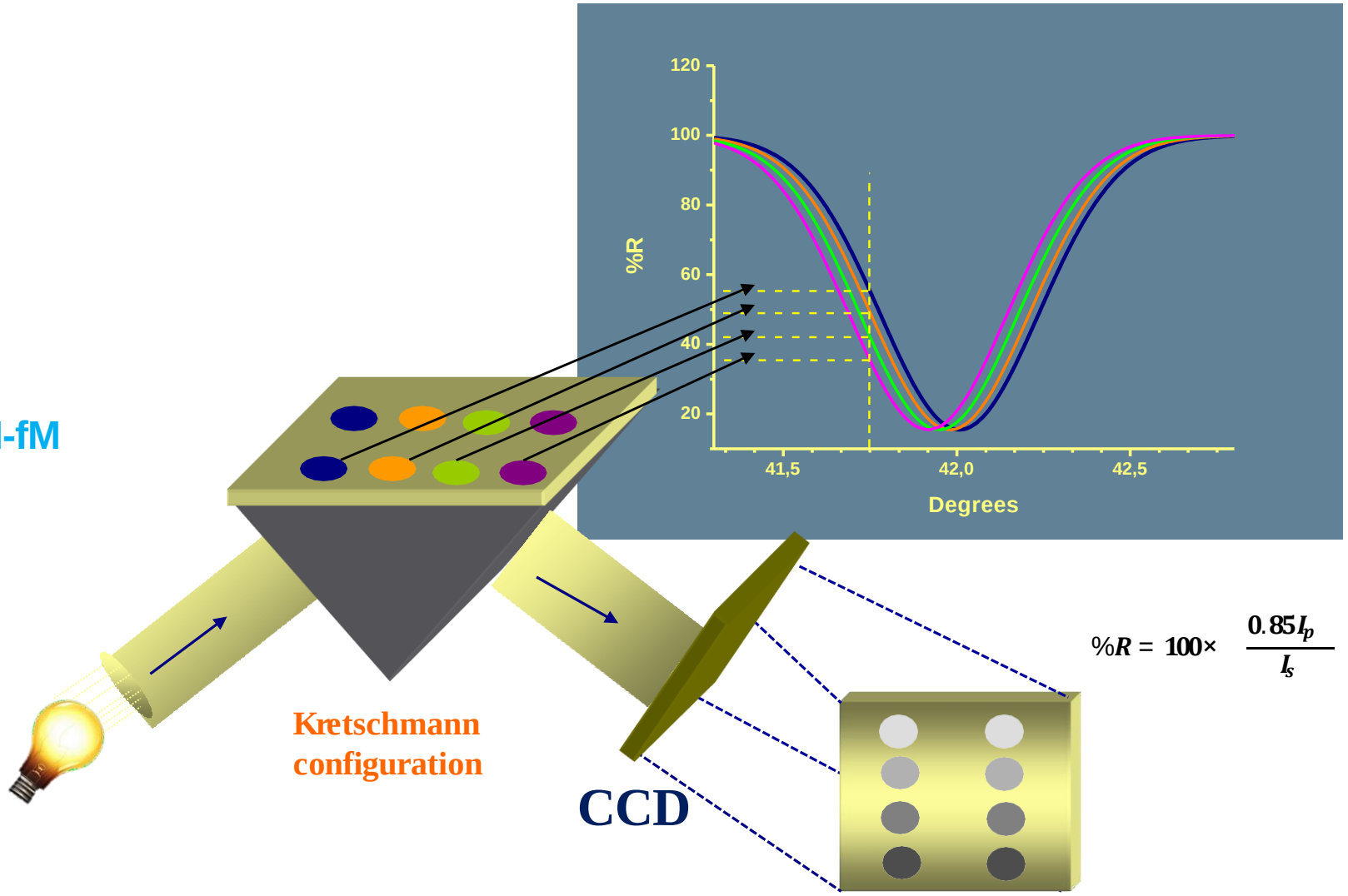

Rothenhäusler et al. Surface–plasmon microscopy. **1988**, Nature 332, 615–617

D'Agata at al. Anal Bioanal Chem. **2013**; 405(2-3):573-84.

Surface Plasmon Resonance Imaging (SPRI)

The lateral resolution of a SPR image is limited by the surface plasmon decay distance L_x that is the distance on the surface by which the intensity of the field associated to plasmons decreases by a 1/e factor.

$$L_x = \frac{1}{2k \; k''_x}$$

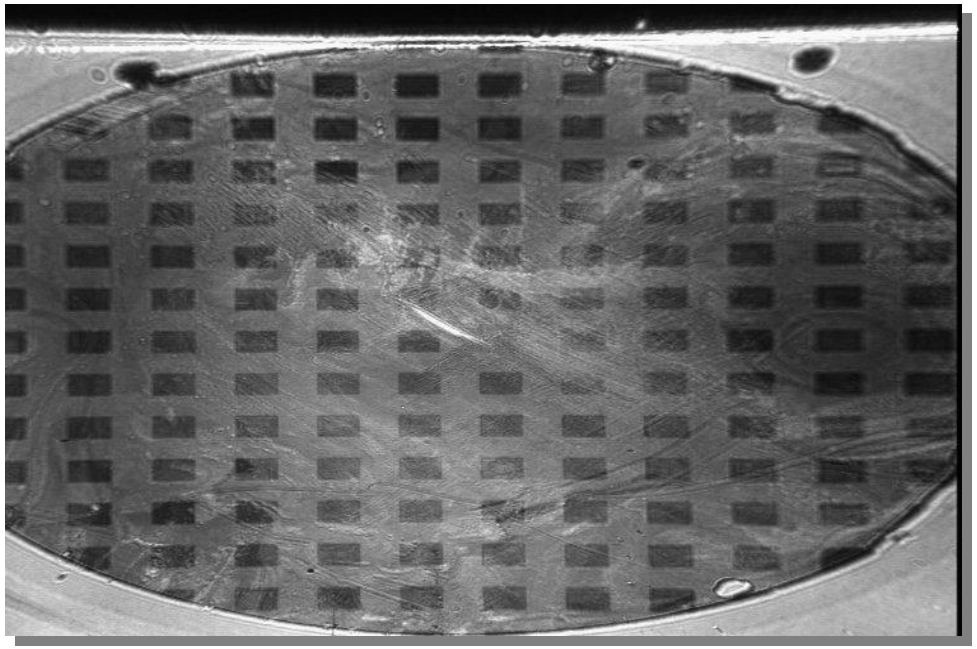

k''_x is the immaginary part of the x component of the wave-vector

For gold:

L_x=0.1 μm at λ=488 nm Å, L_x=10 μm at λ=647 nm

Surface Plasmon Resonance Imaging (SPRI)

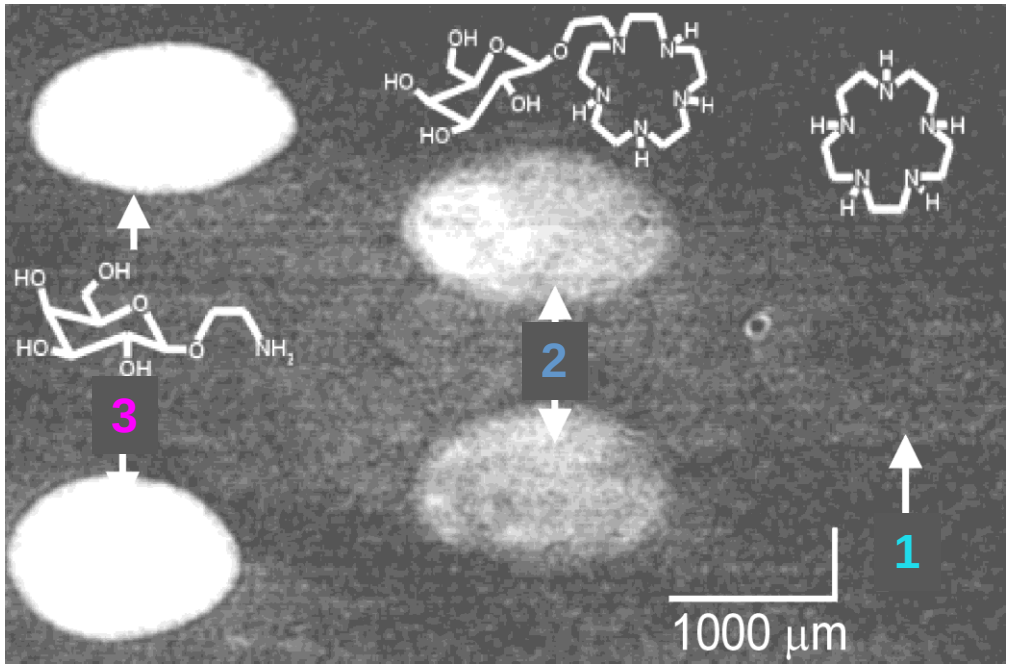

Example of SPRI image

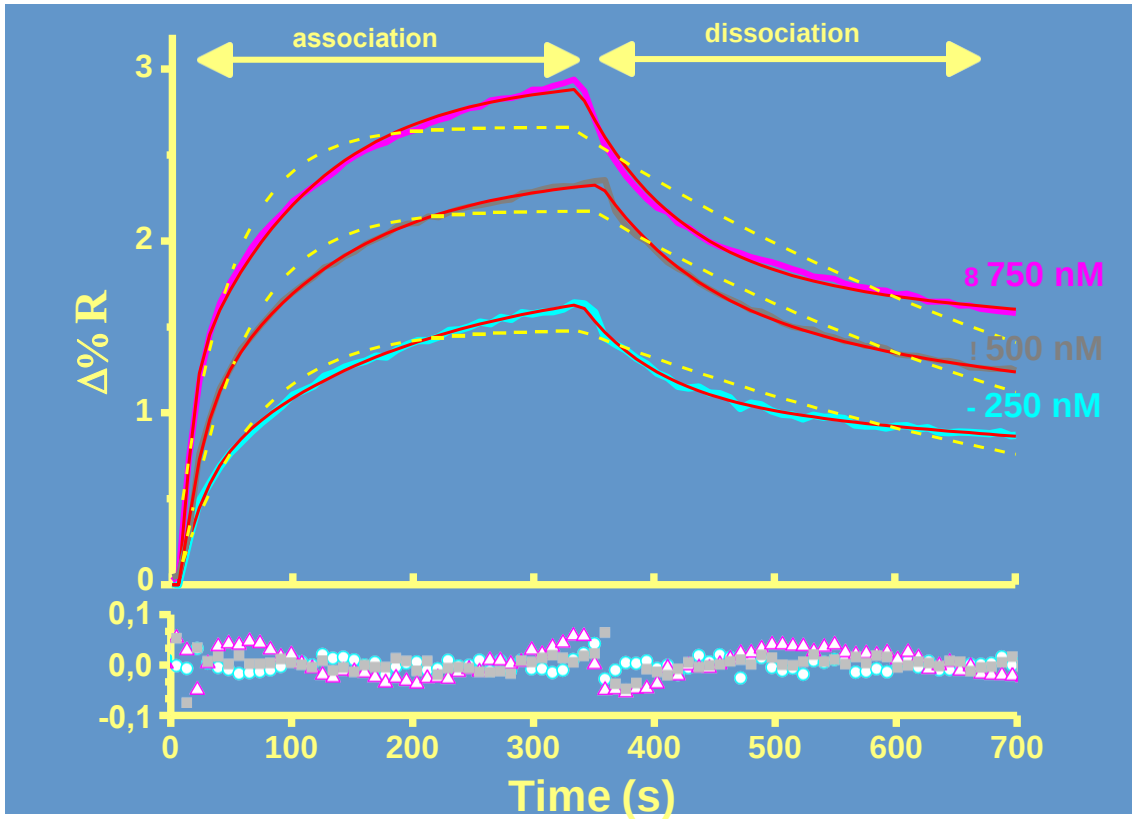

D'Agata at al. Organic & Biomolecular Chemistry, **2006**, 4; 610.

Microfluidic lab-on-a-chip plasmonic platform: detection of DNA

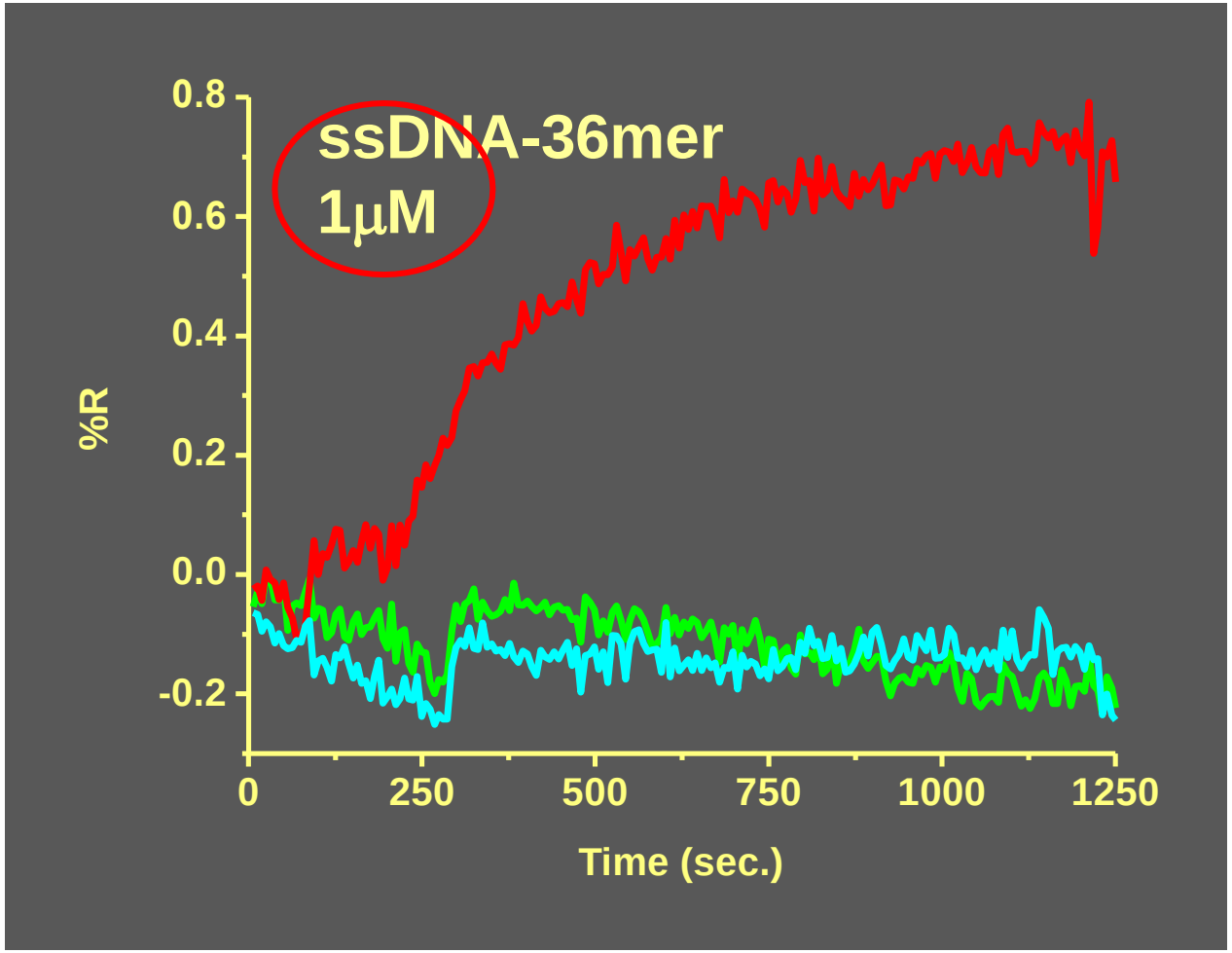

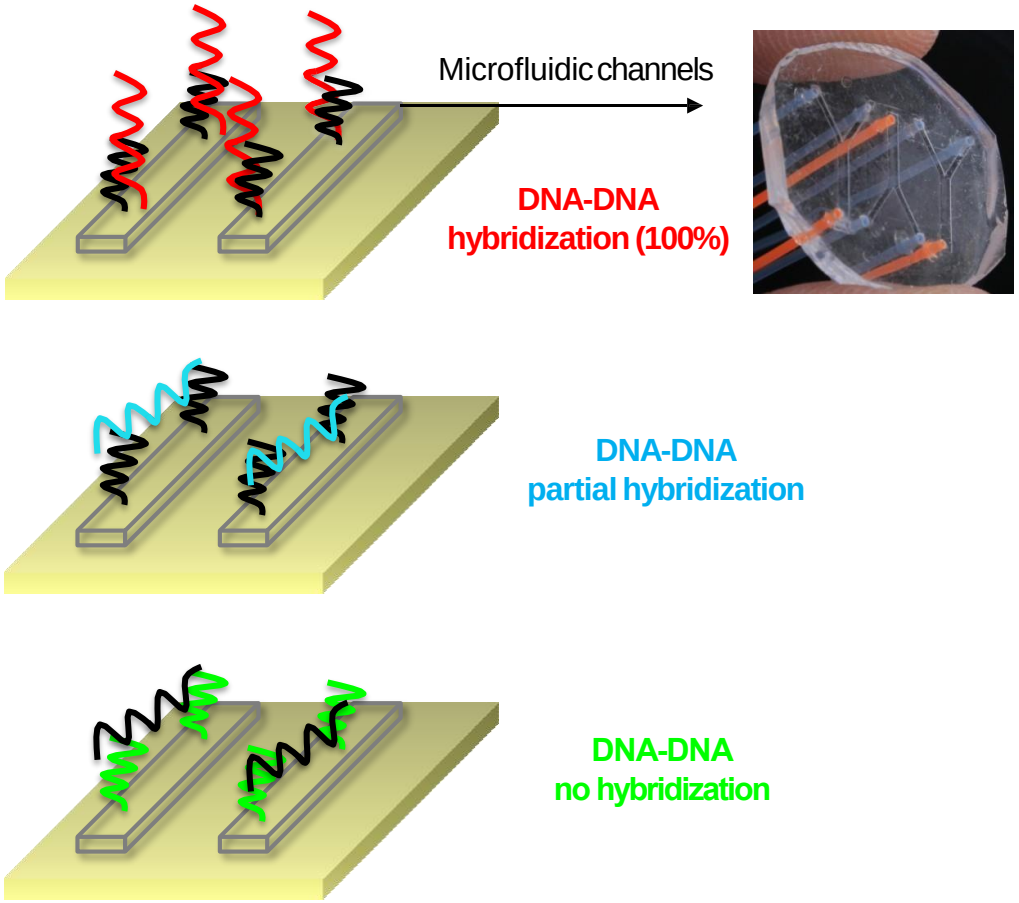

5'-LL-AAACCCTTAATCCCA-3' PROBE

3'-TTTGGGAATTAGGGTTTTTTTTTTTCGTCGAATAGCA-5'

ssDNA-36mer-match

Nanoparticle amplification-SPRI

Surface Plasmon resonance
Gold nanoparticles (NPs) + gold surface

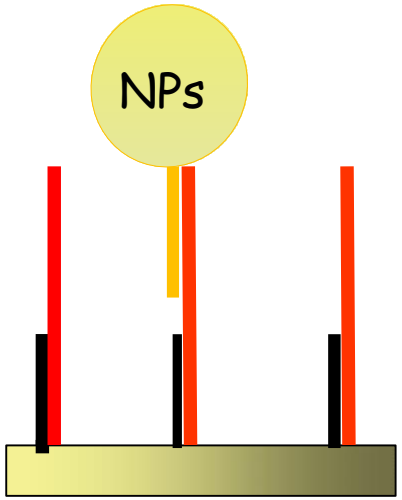

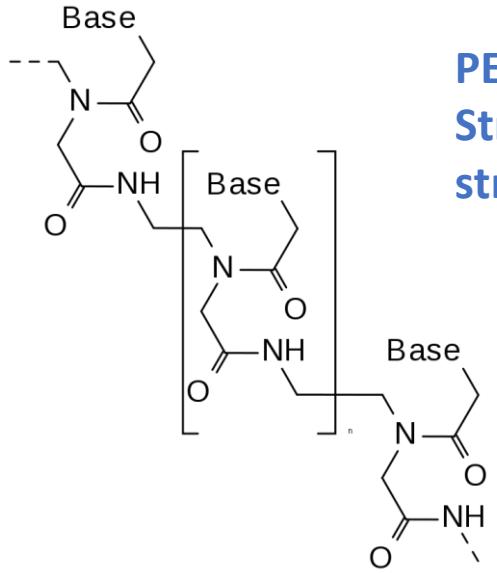

PEPTIDE NUCLEIC ACID –PNA
Stronger affinity for complementary strands of DNA

By Mixtures - Own work, CC BY-SA 3.0, https://commons.wikimedia.org/w/index.php?curid=1737834

5′-GCAGCTTATCGT-3′-Biotin
ssDNA-12merC_6Biotin

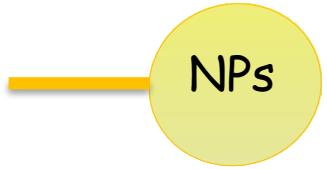

5′-LL-AAACCCTTAATCCCA-3′ PNA-15mer

3′-TTTGGGAATTAGGGTTTTTTTTTTTCGTCGAATAGCA-5′
ssDNA-36mer-match

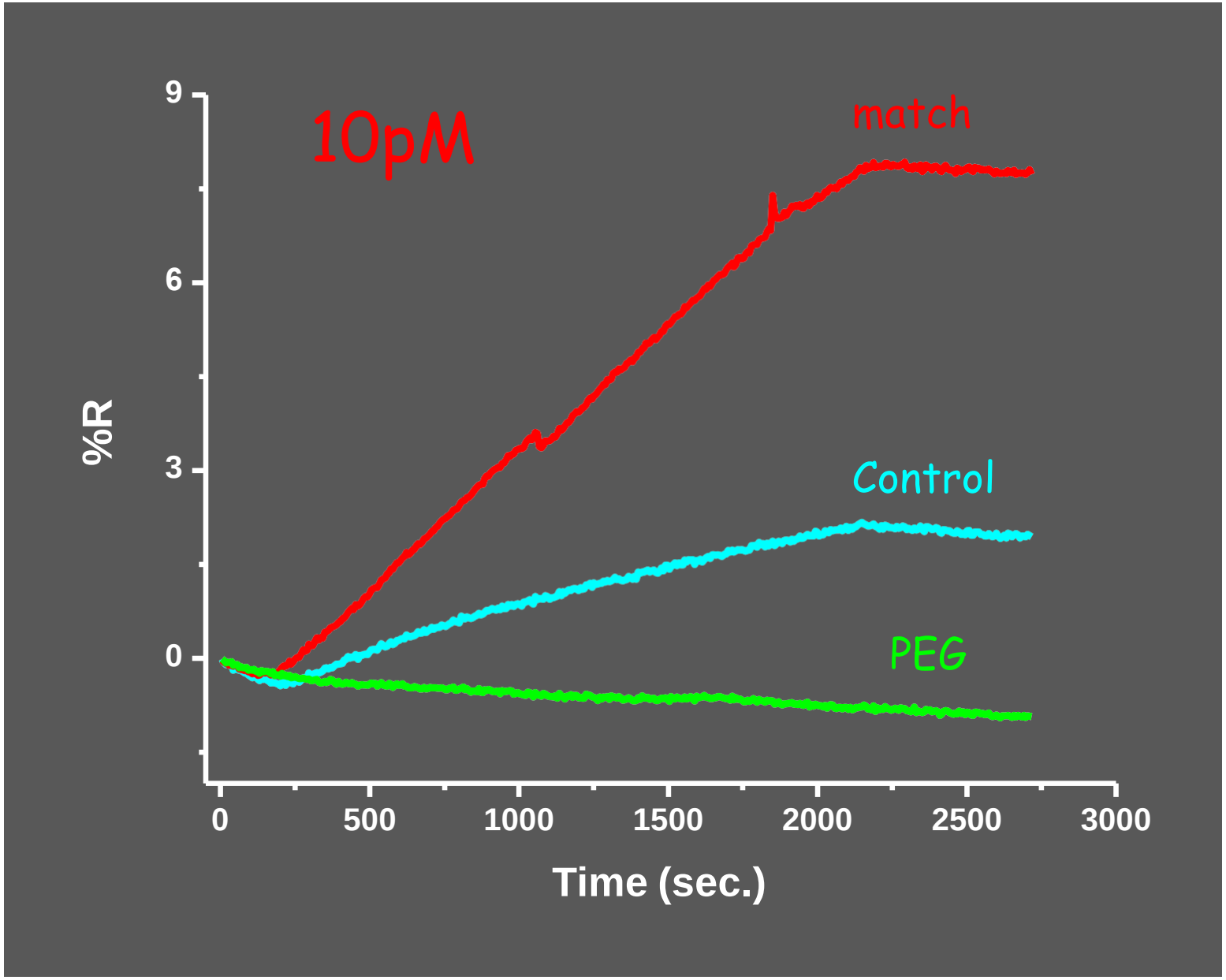

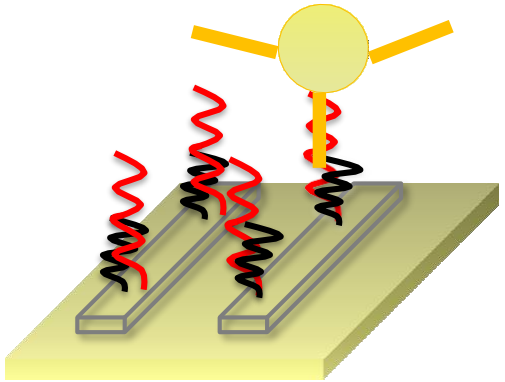

DNA-DNA
hybridization (100%)

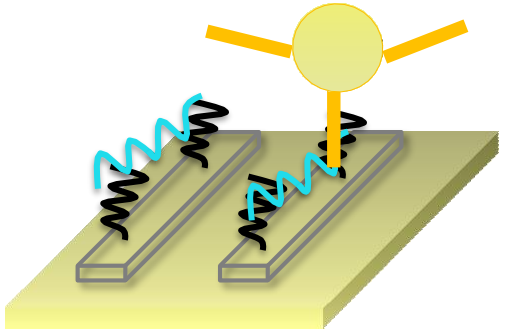

DNA-DNA
partial hybridization

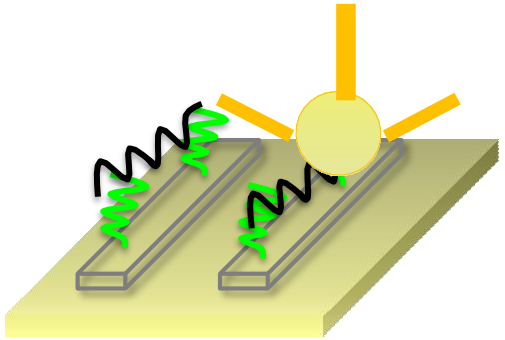

DNA-DNA
no hybridization

D'Agata et al., *ChemBioChem* **2008**, 9, 2067

Nanoparticle amplification-SPRI: SNPs detection

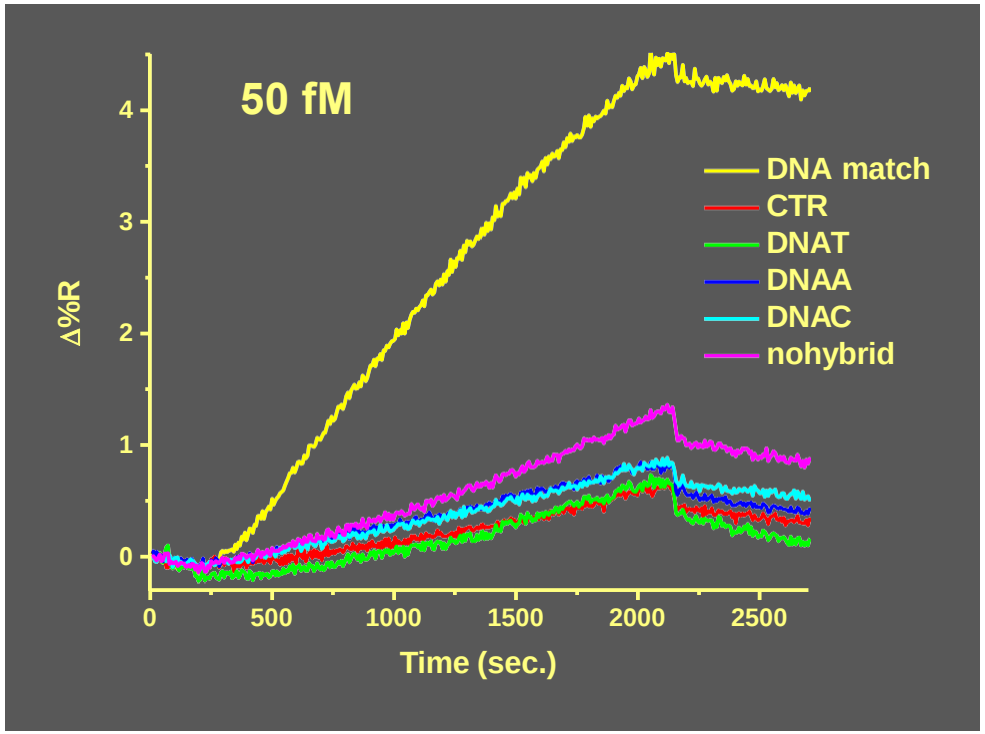

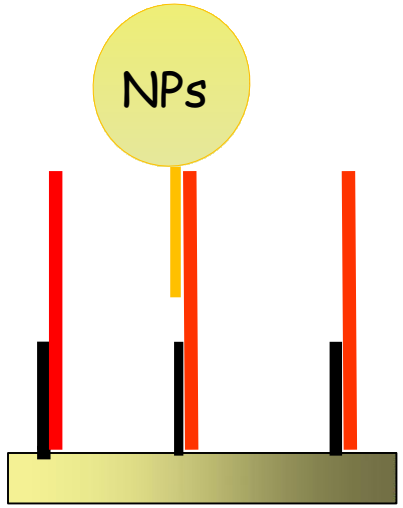

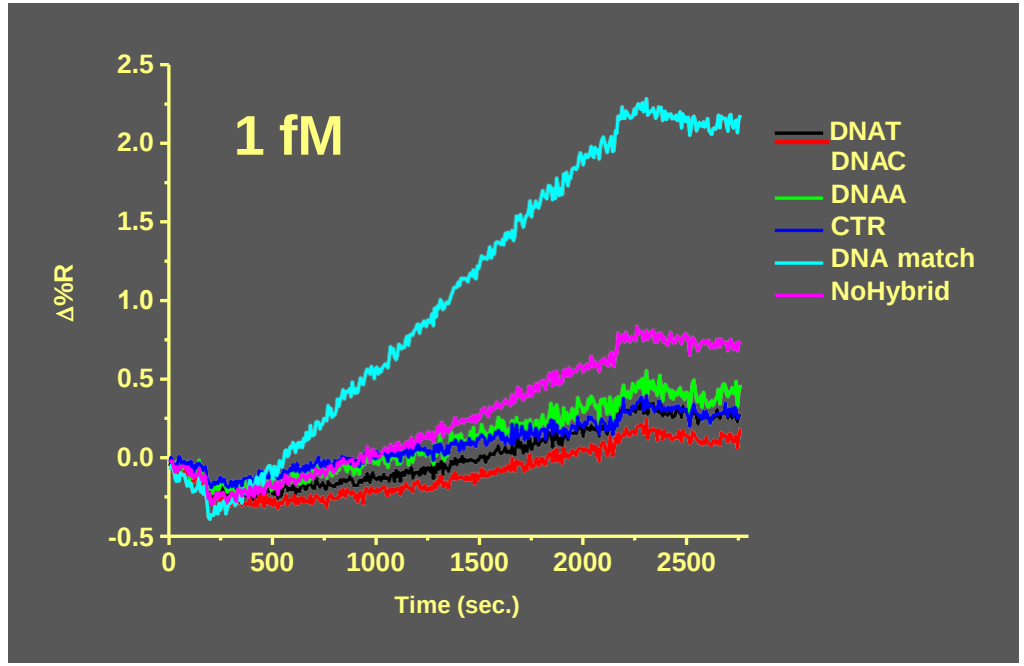

PCR-free detection of KRAS mutations (Plasma from colorectal cancer patients)

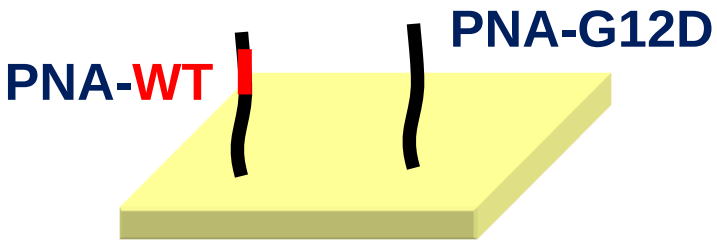

YouTube https://youtu.be/88n3IRsWTm8

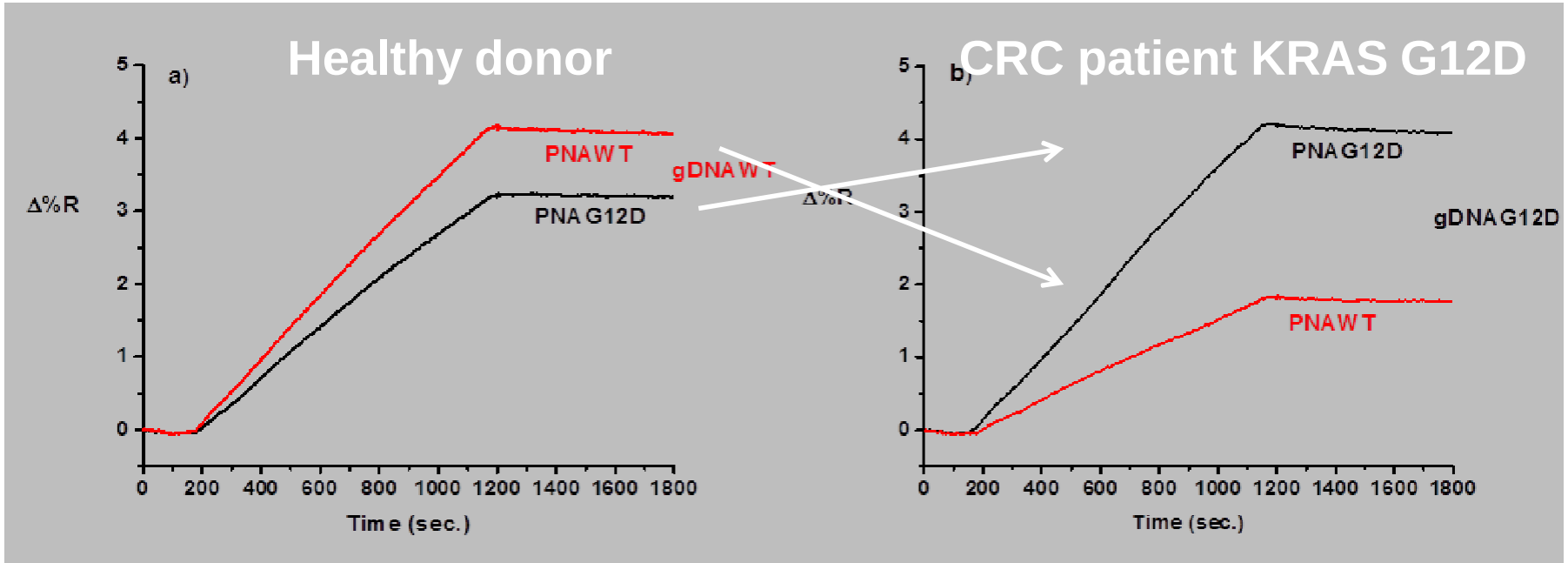

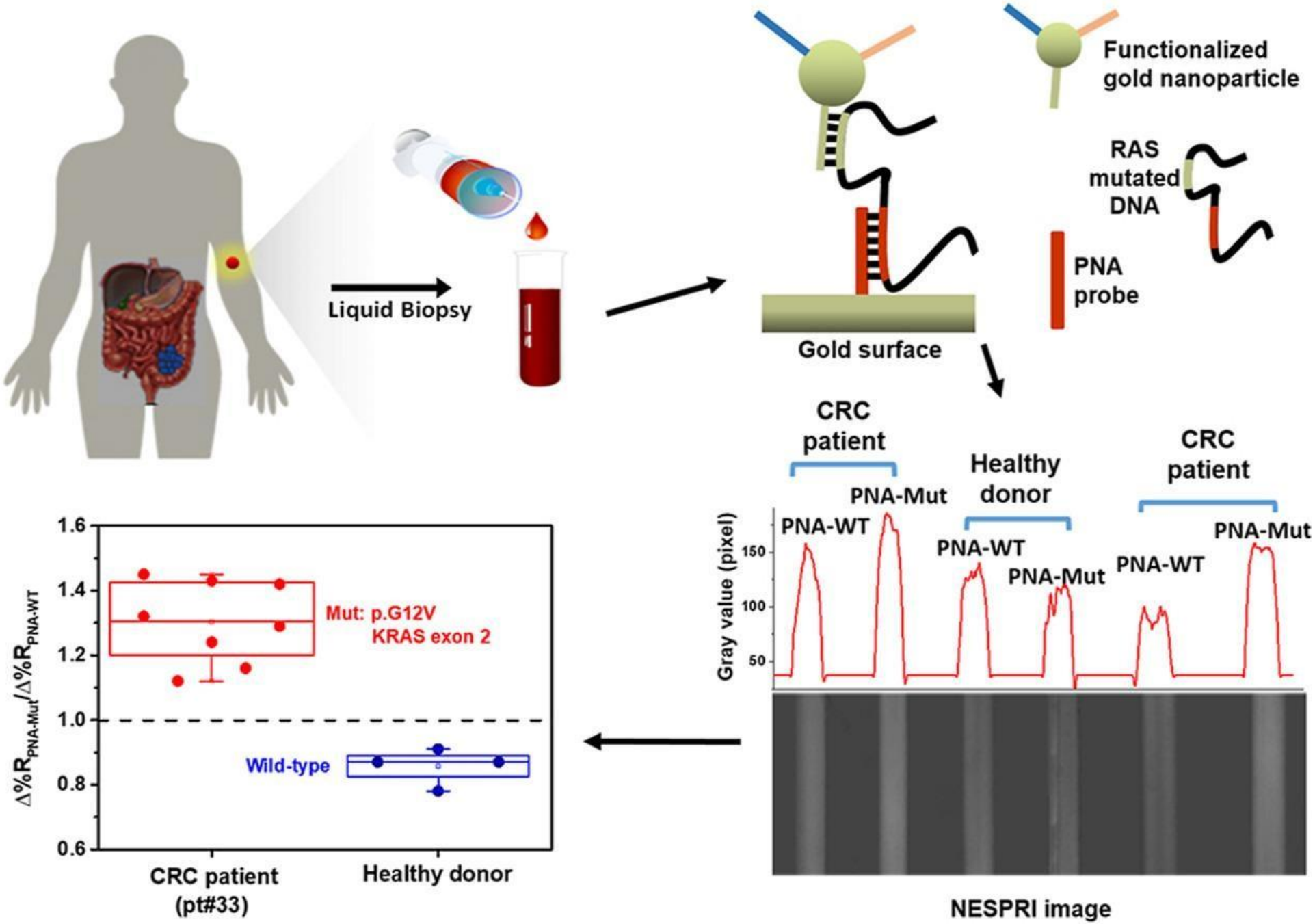

D'Agata et al., Biosens. Bioelectron., **2020**, 170, 112648

Biomimetic receptors

Used for biosensors or for sample preparation/purification

Obtained via combinatorial chemistry and/or molecular modelling

- Peptides
- Aptamers
- MIP (Molecularly Imprinted Polymers)

Combinatorial chemistry approach: Synthesys of aminocids via split and mix

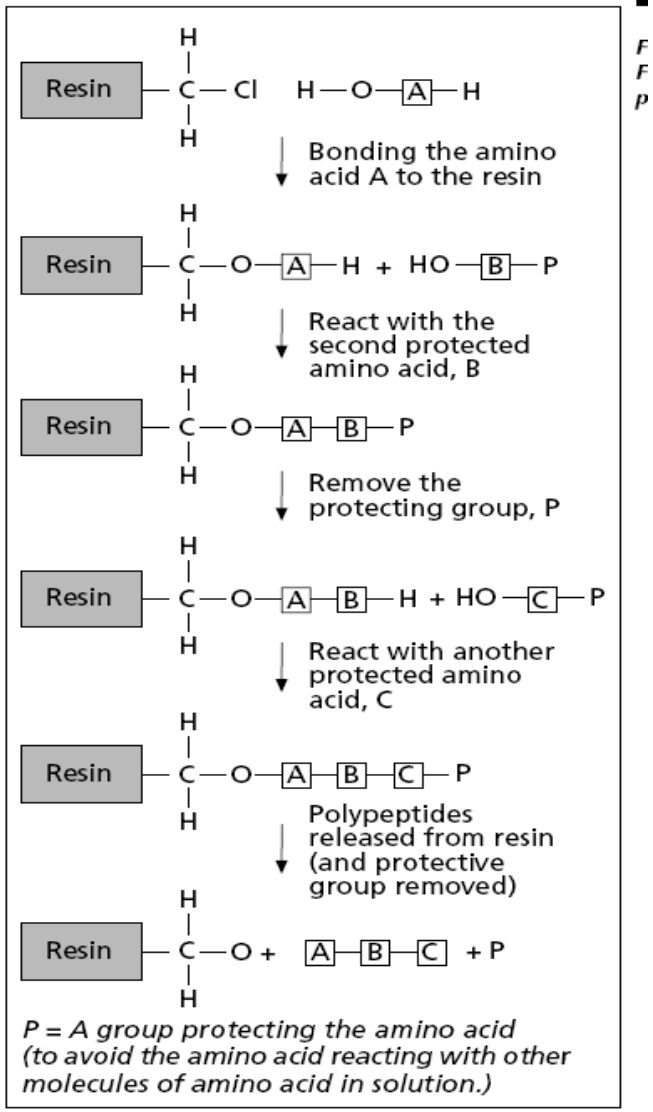

Split synthesis

Stage	Reaction vessel 1 (A)	Reaction vessel 1 (B)	Reaction vessel 1 (C)	
1	Resin + A	Resin + B	Resin + C	3 compounds
		MIX		
2	Resin-A+A Resin-B+A Resin-C+A	Resin-A+B Resin-B+B Resin-C+B	?	9 compounds
		MIX		
3	Resin-A-A+A Resin-B-A+A Resin-C-A+A Resin-A-B+A Resin-B-B+A Resin-C-B+A Resin-A-C+A Resin-B-C+A Resin-C-C+A	Resin-A-A+B Resin-B-A+B Resin-C-A+B Resin-A-B+B Resin-B-B+B Resin-C-B+B Resin-A-C+B Resin-B-C+B Resin-C-C+B	Resin-A-A+C Resin-B-A+C Resin-C-A+C Resin-A-B+C Resin-B-B+C Resin-C-B+C Resin-A-C+C Resin-B-C+C Resin-C-C+C	27 compounds
		MIX		

Biomimetic Approach

- Starting from the biological structure it is possible to reproduce with natural amino acids the proper shape of binding dock

- The biomimetic approach relies on the design and development of artificial oligopeptides as a mimic of the biological binding site by using molecular modeling

✓Why oligopeptides?

- Nature exploited aminoacids structures to obtain the most of receptors

- Oligopeptides have the advantage of informatics help from the point of the crystallographic informations from native proteins

- Great number of combinations using 20 aminoacids which can do any binding traps

BIOMIMETIC RECEPTORS FOR PESTICIDES

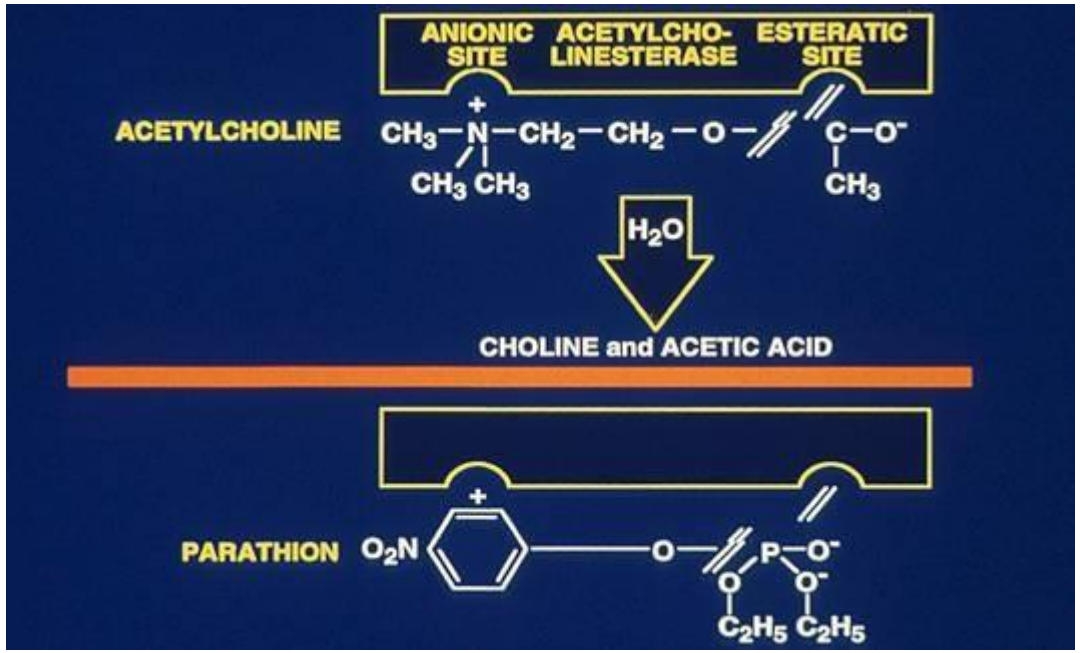

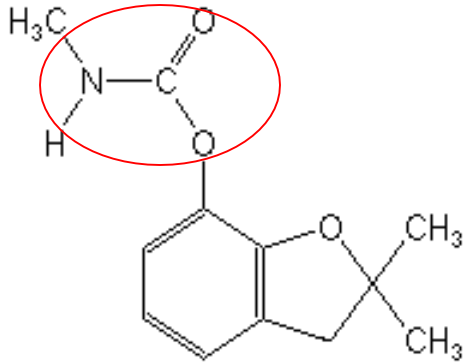

Carbamate

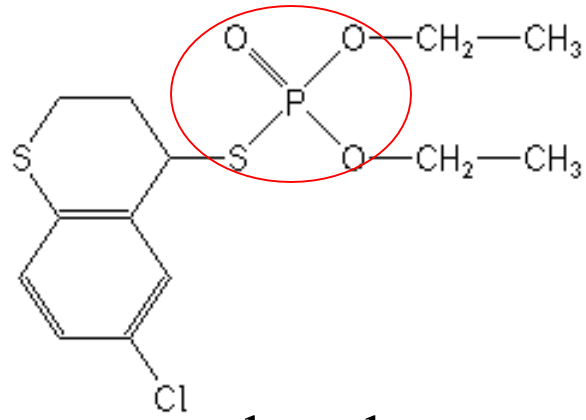

organophosphate

✓Mechanism of AChE inhibition

AChE, the target enzyme of pesticides, **is an efficient serine hydrolase** that catalyzes the breakdown of acetylcholine (ACh)

Acetylcholine + H_2O → choline + acetic acid

How pesticides work

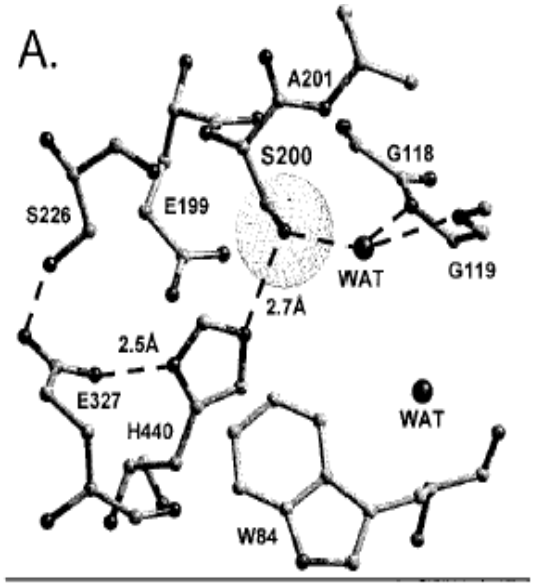

Native structure: the active site, including the catalytic triad (S200-H440-E327) and the oxyanion hole (-NH of G118, G119, and A201)

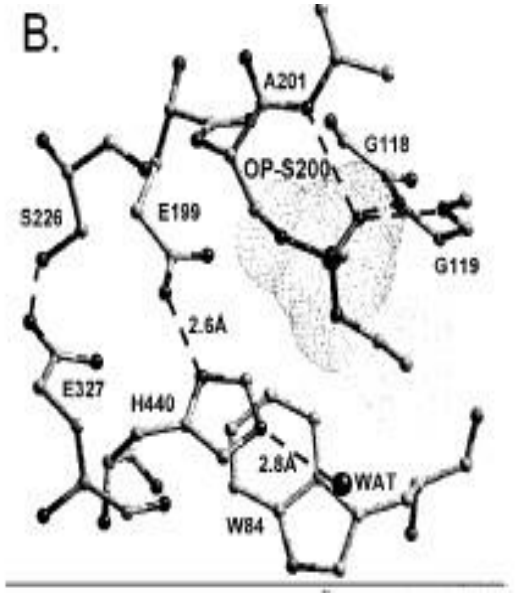

Pro-aged structure: Phosphonylation triggers a conformational change for H440 that disrupts the H-bond to E327

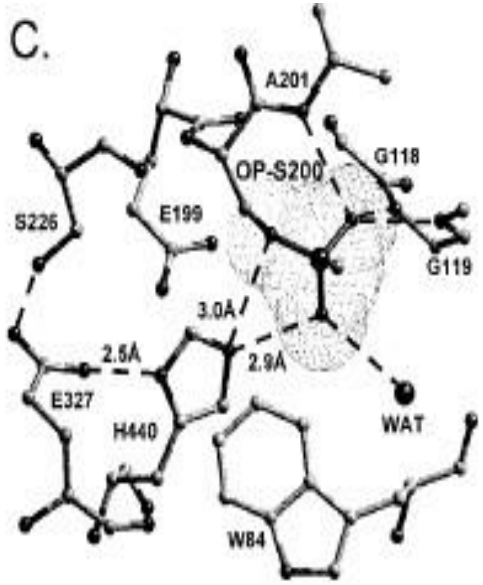

Aged structure: For reaction of AChE with VX and most phosphonates, aging predominates, and dealkylation results in movement of H440 to the negatively charged pocket formed by E327 Ox, S200 Ox, and one anionic oxygen of the dealkylated OP

From *Millard et al J.Am.Chem.Soc. 121, (1999)*

❖Computational screening

✓AChE-OP crystallographic structure (PDB ID: 1VXO)

Methylphosphonylated Acetylcholinesterase (Aged) Obtained By Reaction With O-Ethyl-S-[2-[Bis(1-Methylethyl) Amino]Ethyl] Methylphosphonothioate (Vx) conventional X-ray crystallography resolution [Å]: 2.40

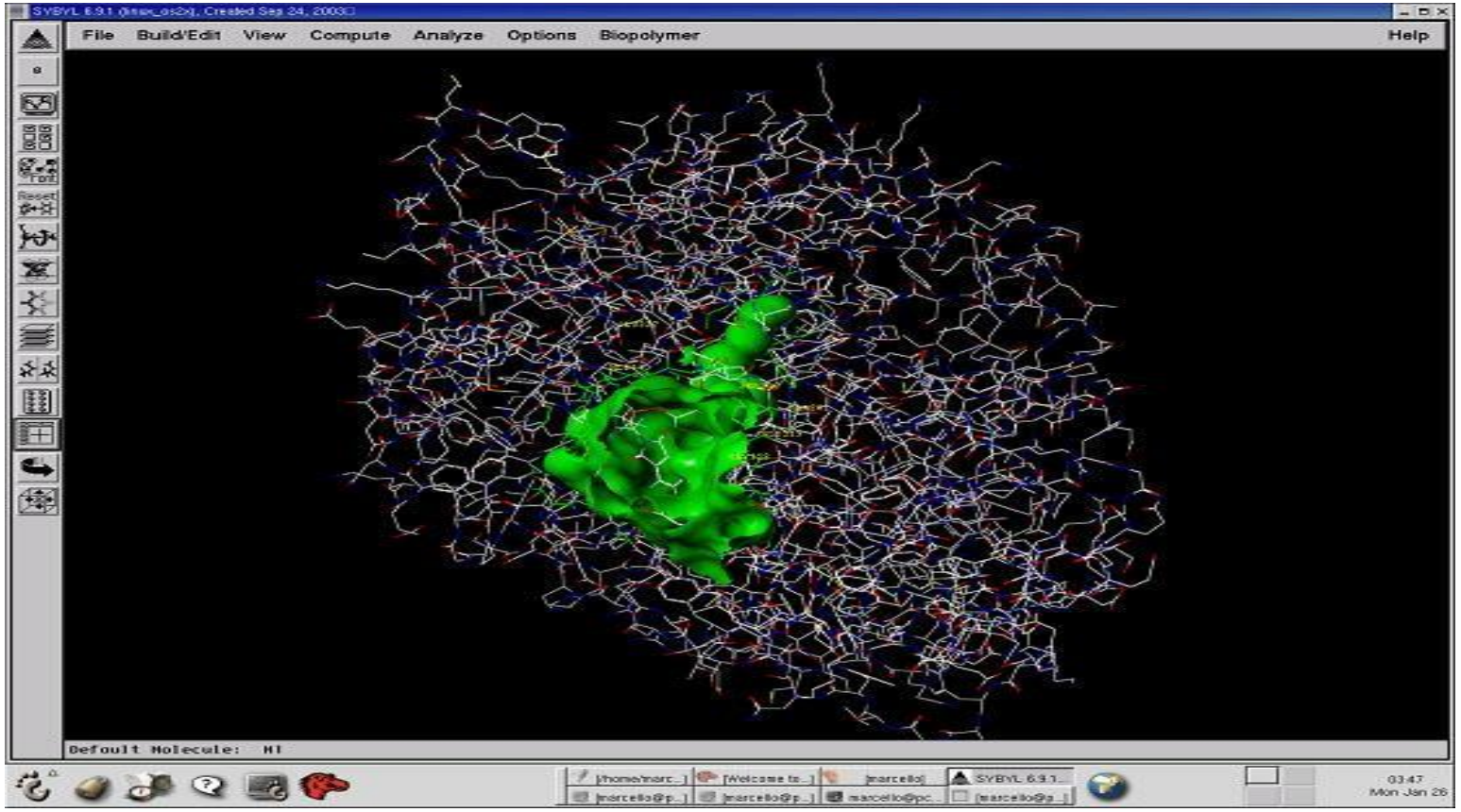

In green the molecular electrostatic potential distribution on the surface of the enzyme binding pocket

✓Design of the oligopeptides library as possible receptors

The geometry of the binding pocket was investigated to create oligopeptides library

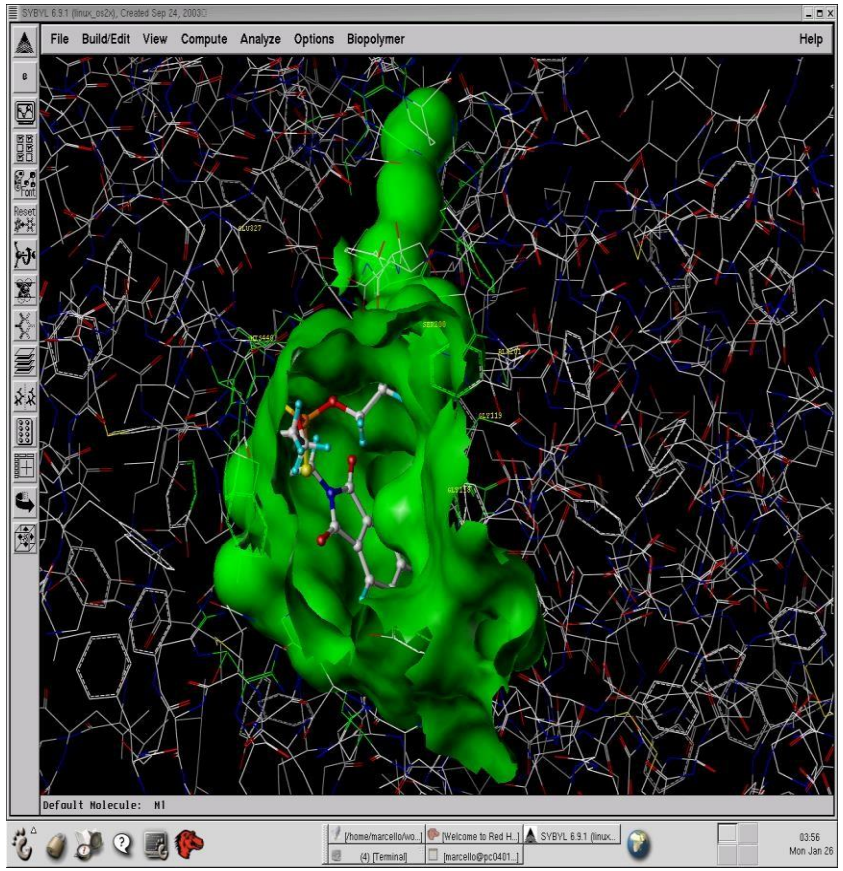

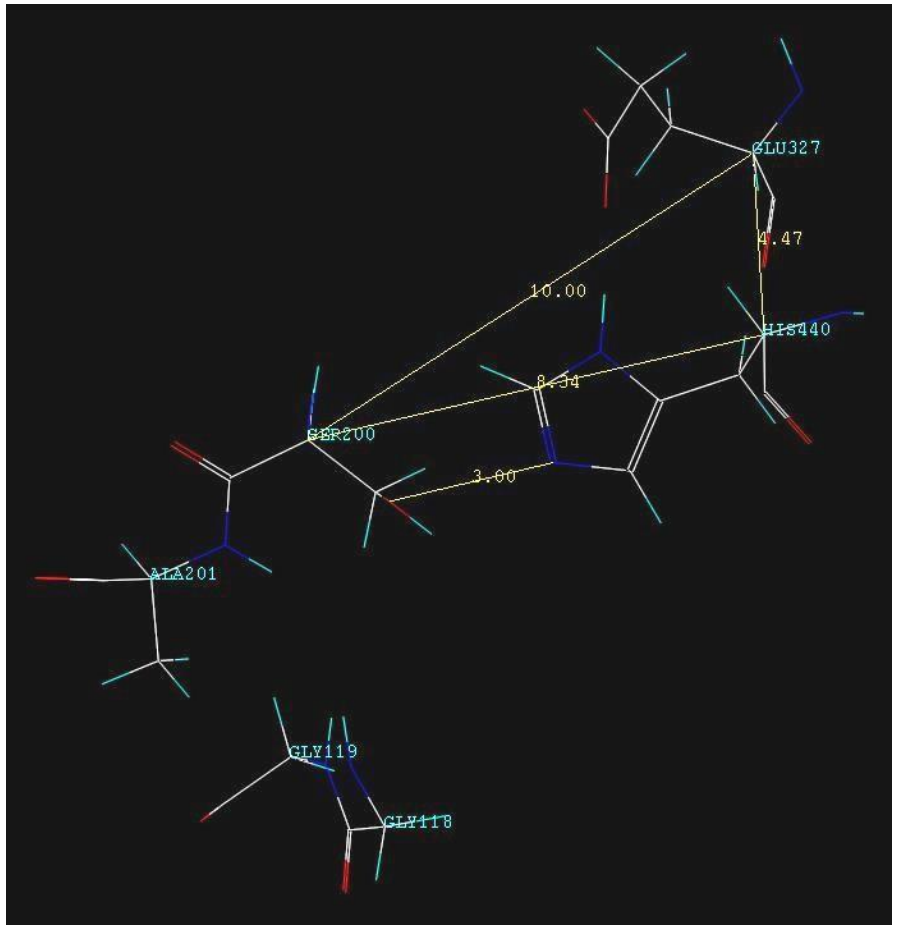

Three dimensional coordinates of the asymmetric carbon (Cα) of each aminoacid involved in the binding pocket were calculated in order to reproduce the geometry observed

✓Tetrapeptides library

- easy to synthesise
- more possibility to preserve in solution the secondary structure predicted

•A series of tetrapeptides, containing the possible combinations of the catalytic triad (SER 200, HIS 440, GLU 327) and the catalytic oxyanion hole (GLY 118 GLY 119 ALA 201) was drawn

•The proper geometry of binding pocket was achieved using alternatively a GLY or a PRO residue

Library

(24 tetrapeptides)

Ser-Gly-His-Glu	**Glu-Gly-Ser-Ala**
Ser-Gly-Glu-His	**His-Gly-Ser-Ala**
His-Glu-Gly-Ser	**Gly-Pro-Ser-Ala**
Glu-His-Gly-Ser	**Ser-Ala-Pro-Glu**
Ser-Pro-His-Glu	**Ser-Ala-Pro-His**
Ser-Pro-Glu-His	**Ser-Ala-Pro-Gly**
His-Glu-Pro-Ser	**Glu-Pro-Ser-Ala**
Glu-His-Pro-Ser	**His-Pro-Ser-Ala**
Gly-Gly-Ser-Ala	**Gly-Ser-Gly-Ala**
Ser-Ala-Gly-Glu	**Ala-Gly-Ser-Gly**
Ser-Ala-Gly-His	**Ser-Gly-Pro-Ala**
Ser-Ala-Gly-Gly	**Ala-Pro-Gly-Ser**

✓Simulated binding results vs paraoxon of the tetrapeptides selected for experimental screening

	A Ser-Ala-Gly-Glu	B His-Gly-Ser-Ala	C Glu-Pro-Ser-Ala	D His-Glu-Pro-Ser
Binding Score (KJ/mol)	38	73	21	93

Negative control (NC): **Glu-His-Ser-Gly**

Primary sequence of AChE catalytic triad

PARAOXON

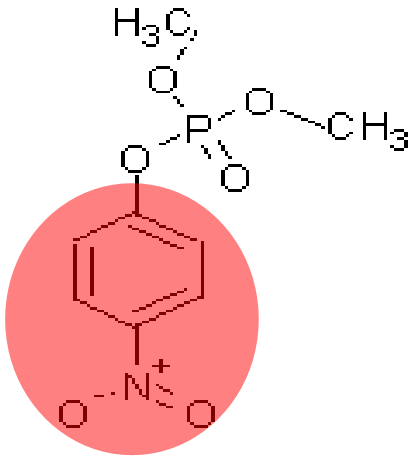

A **Ser-Ala-Gly-Glu**

B **His-Gly-Ser-Ala**

C **Glu-Pro-Ser-Ala**

D **His-Glu-Pro-Ser**

NC **Glu-His-Ser-Gly**

✓Pre-analytical applications: selective affinity columns (Extraction or purification)

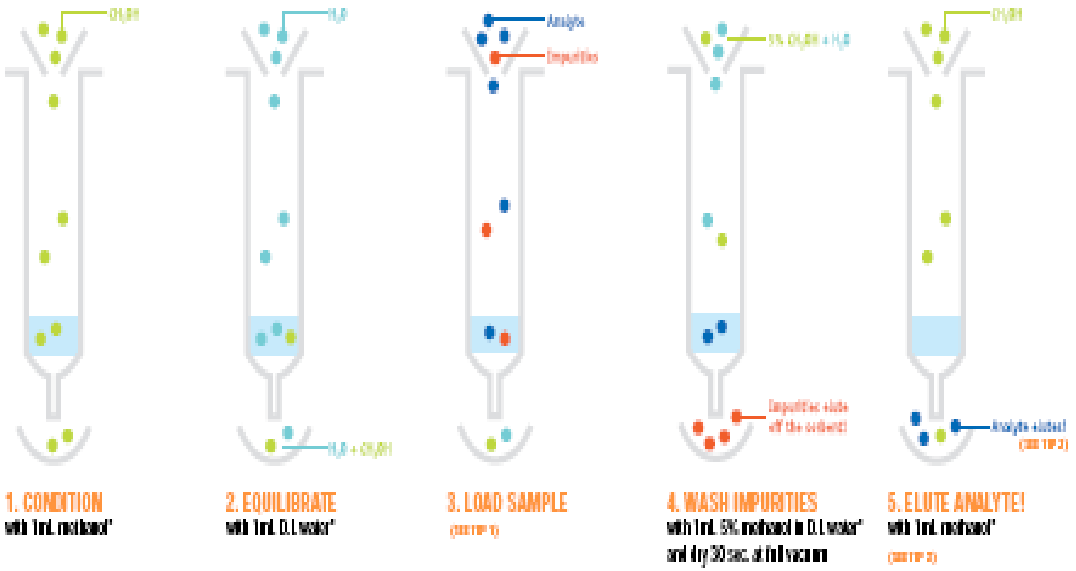

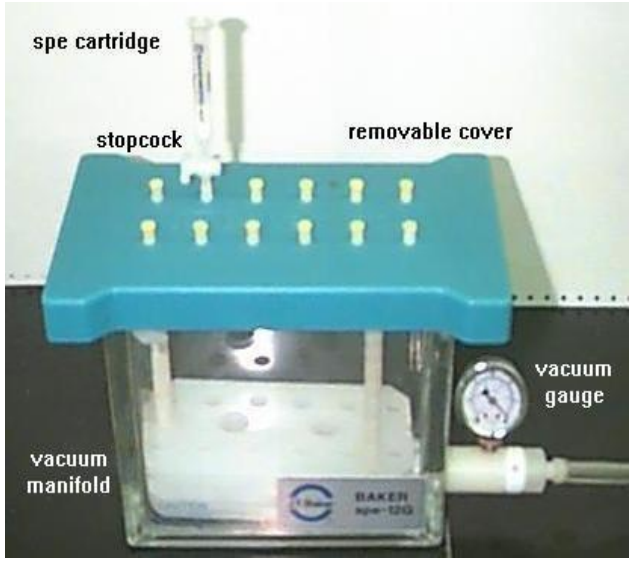

is a technique enabling purification of a biomolecule with respect to biological function or individual chemical structure. The substance to be purified is specifically and reversibly adsorbed to a ligand (binding substance), immobilized by a covalent bond to a chromatographic bed material (matrix). Samples are applied under favourable conditions for their specific binding to the ligand. Substances of interest are consequently bound to the ligand while unbound substances are washed away. Recovery of molecules of interest can be achieved by changing experimental conditions to favour desorption.

biomolecules

MDPI

Article

Computationally Designed Peptides for Zika Virus Detection: An Incremental Construction Approach

Marcello Mascini [1,2,*], Emre Dikici [3,4], Marta Robles Mañueco [3], Julio A. Perez-Erviti [5], Sapna K. Deo [3,4], Dario Compagnone [2], Joseph Wang [6], José M. Pingarrón [1] and Sylvia Daunert [3,4,7,*]

- Zika infection is known to cause neurological problems to pregnant women and potentially cause microcephaly and other congenital malformations and diseases to the unborn child. Zika affects, both male and females and it has been reported that the virus can be transmitted sexually through semen and vaginal fluids.
- The Zika virus is a mosquito-borne flavivirus, and due to the lack of specific antibodies/binders that can be used in immunoassays for diagnosis of the disease, these immunoassays present cross-reactivity with other flaviviruses and arboviruses. It is well established that ZIKV has many common genetic sequences and protein structures with other flaviviruses, like DENV, West Nile virus or Chikungunya. This limits the use of immunoassays for the detection of human pathogens within the flavivirus genus.
- The flavivirus envelope protein is responsible for virus entry and represents a major target for neutralizing antibodies. The Zika virus structure is similar to other known flaviviruses structures except for the ~10 amino acids that surround the Asn-154 glycosylation site found in each of the 180 envelope glycoproteins that make up the icosahedral shell

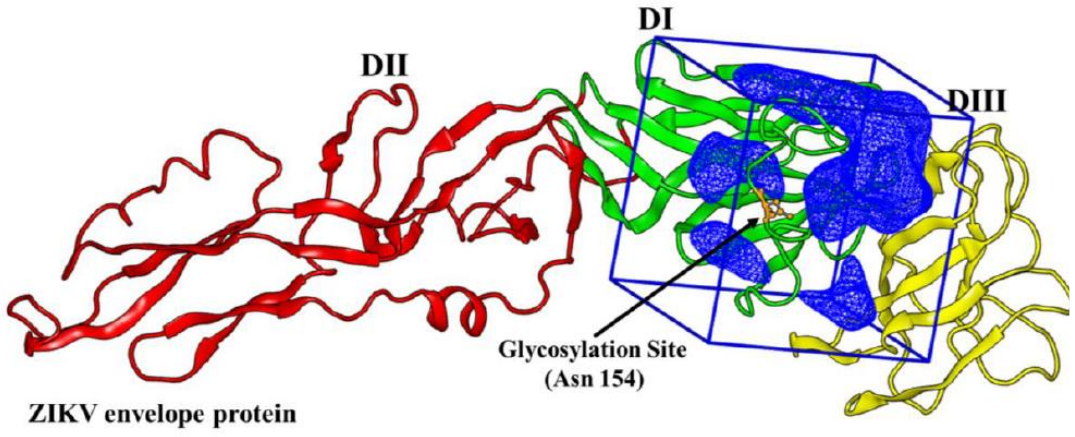

(a)

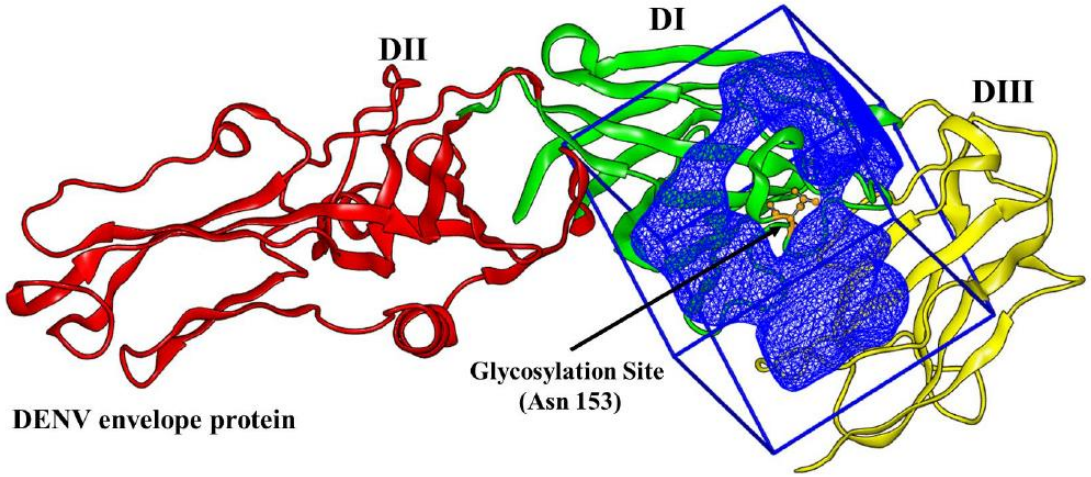

(b)

Glycosylation site

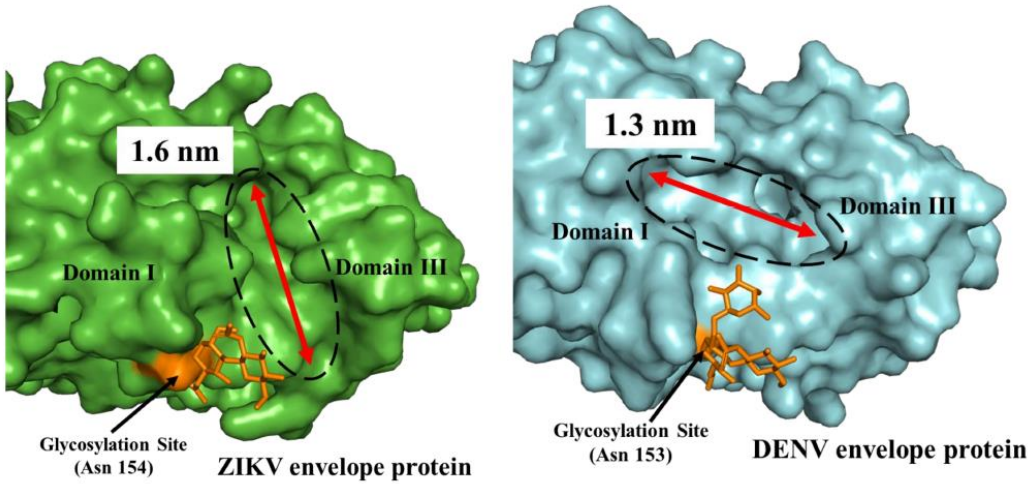

(a) (b)

Figure 4. *Cont.*

Molecular docking

(a) (b)

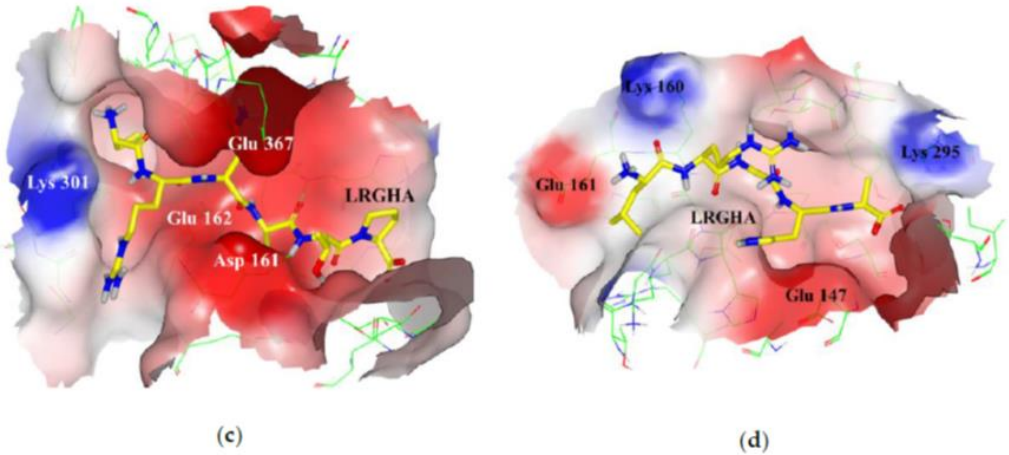

(c) (d)

Figure 5. *Cont.*

8 different peptides selected, sinthesyzed, biotynilated and tested with direct ELISA test using Avidin-HRP

i.e. inactivated virus onto ELISA microwells , reaction with peptides, incubation with Avidin-HRP

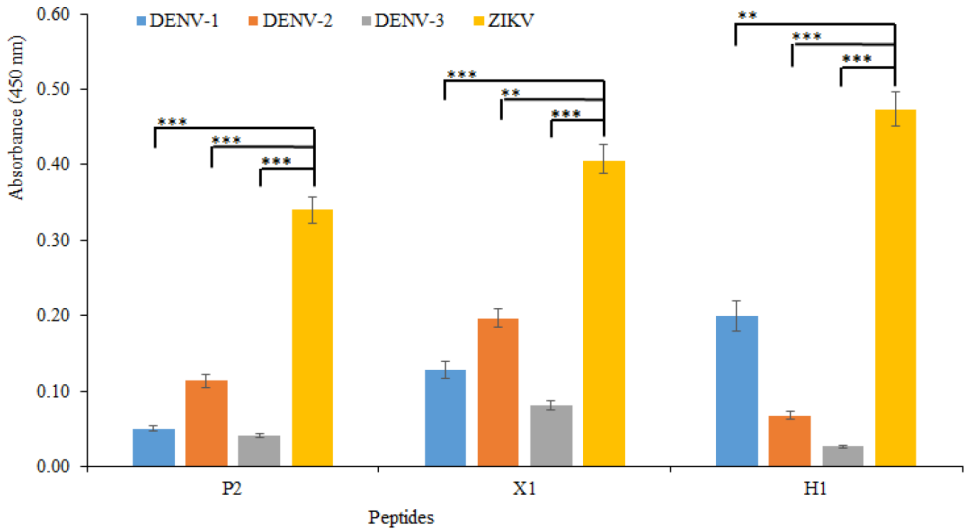

Figure 7. Cross-reactivity study. In the ELISA direct assay, the spectrophotometric absorbance signals were obtained by using the best three peptides (P2, X1, and H1) binding the ZIKV and three serotypes of DENV (DENV-1, -2, and -3) at the concentration of 10^6 copies/mL. Statistical significance between ZIKV and DENV serotypes (1–3) was calculated using two-way analysis of variance. Different p values were indicated by **($p < 10^{-3}$) or ***($p < 10^{-4}$).

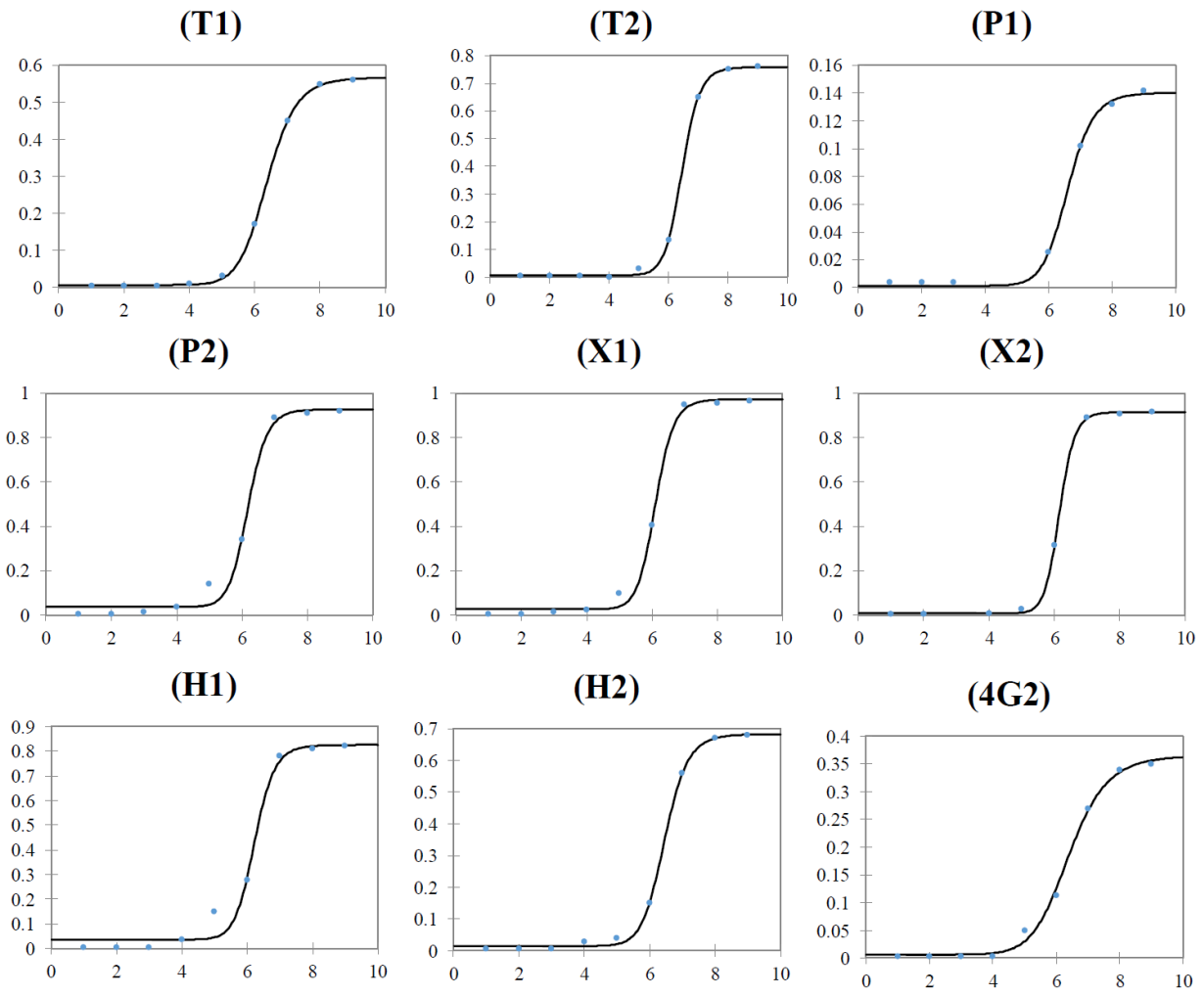

Figure 6. Sigmoidal ZIKV particles concentration response trend of the ELISA assay obtained using the eight peptides and antibody 4G2. *Y*-axis = absorbance (450nm); *X*-axis = log [ZIKV], copies/mL.

Aptamers are oligonucleotides (DNA or RNA molecules) that can bind with high affinity and specificity to a wide range of target molecules (proteins, peptides, drugs, vitamins and other organic or inorganic compounds).

They were "discovered" in 1990 by the development of an in vitro selection and amplification technique, known as SELEX (Systematic Evolution of Ligands by Exponential enrichment).
(Ellington et al., **Nature** 346, 818; Tuerk and Gold, **Science** 249, 505)

Their name is derived from the Latin word "**aptus**" which means "to fit".

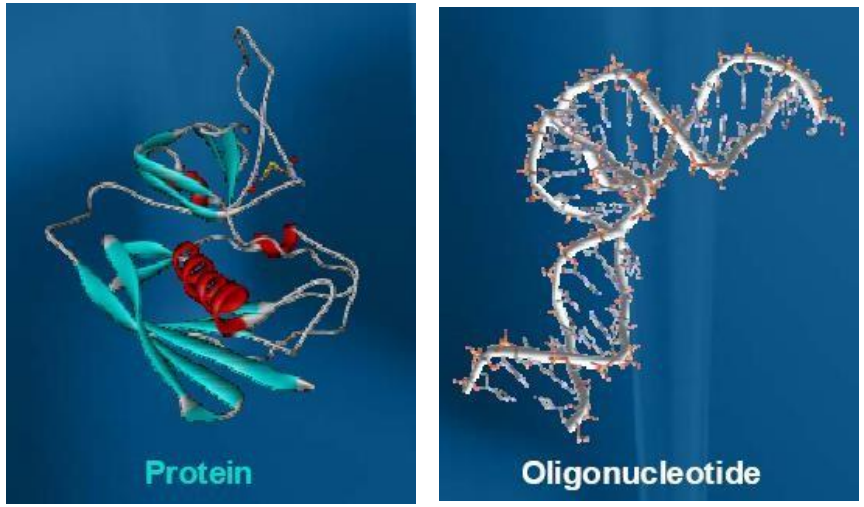

Similar to proteins short oligonucleotides can adopt complex three-dimensional structures

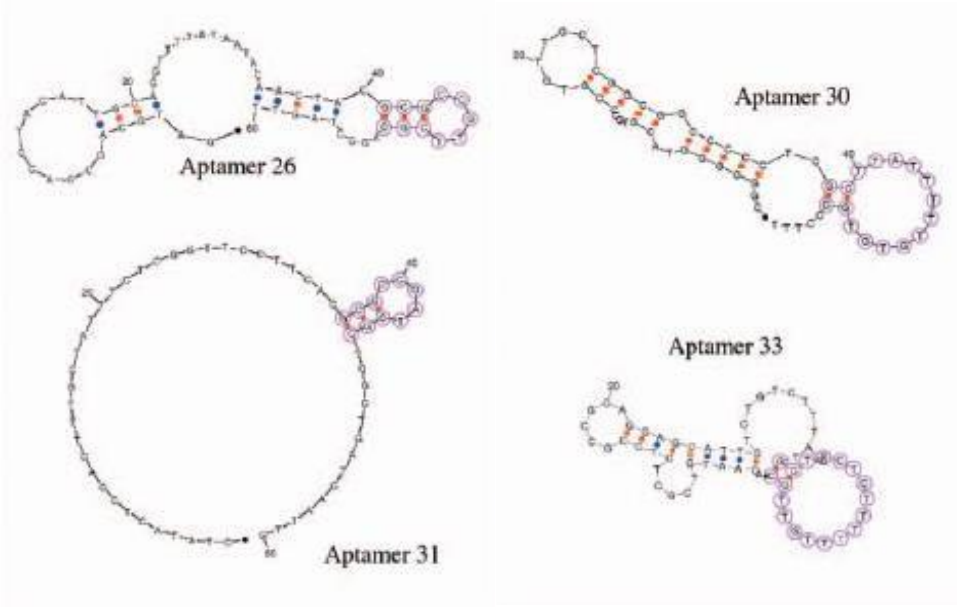

Starting point: Combinatorial oligonucleotide library

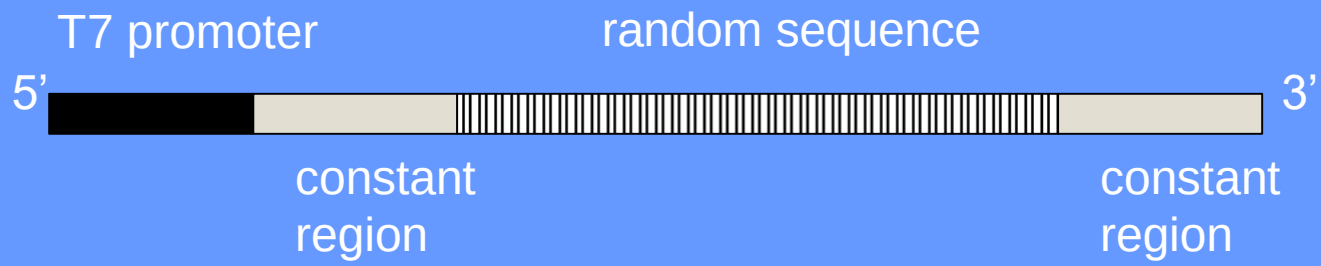

A library containing a 25-nucleotide random region is represented by 4^{25} (~10^{15}) individual sequences available for partitioning.
Normally, the starting round contains **10^{14}-10^{15} individual sequences**.

A, **G**, **C**, **U**(**T**)

$4^1 = 4$
$4^2 = 16$
$4^3 = 64$
$4^4 = 256$
$4^5 = 1024$
……
……
……
$4^{25} = 1125899906842624$

Pool of randomized DNA or RNA

10^{15} different sequences!!!!

Biomedicine & Pharmacotherapy 132 (2020) 110902

Contents lists available at ScienceDirect

Biomedicine & Pharmacotherapy

journal homepage: www.elsevier.com/locate/biopha

Review

Aptamers used for biosensors and targeted therapy

Yi Ning, Jue Hu, Fangguo Lu *

Department of Microbiology, The Medicine School of Hunan University of Chinese Medicine, Changsha, Hunan, 410208, PR China

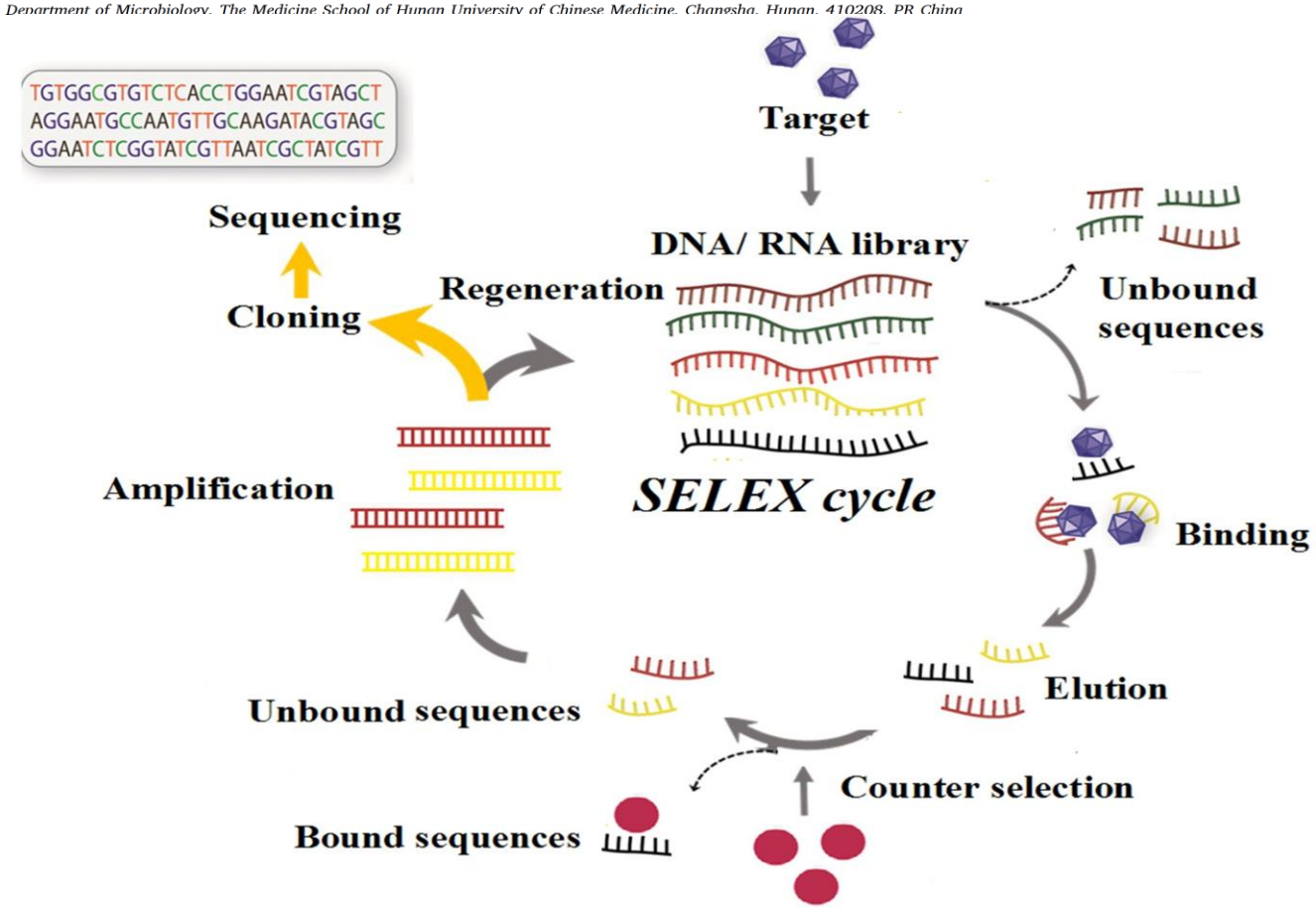

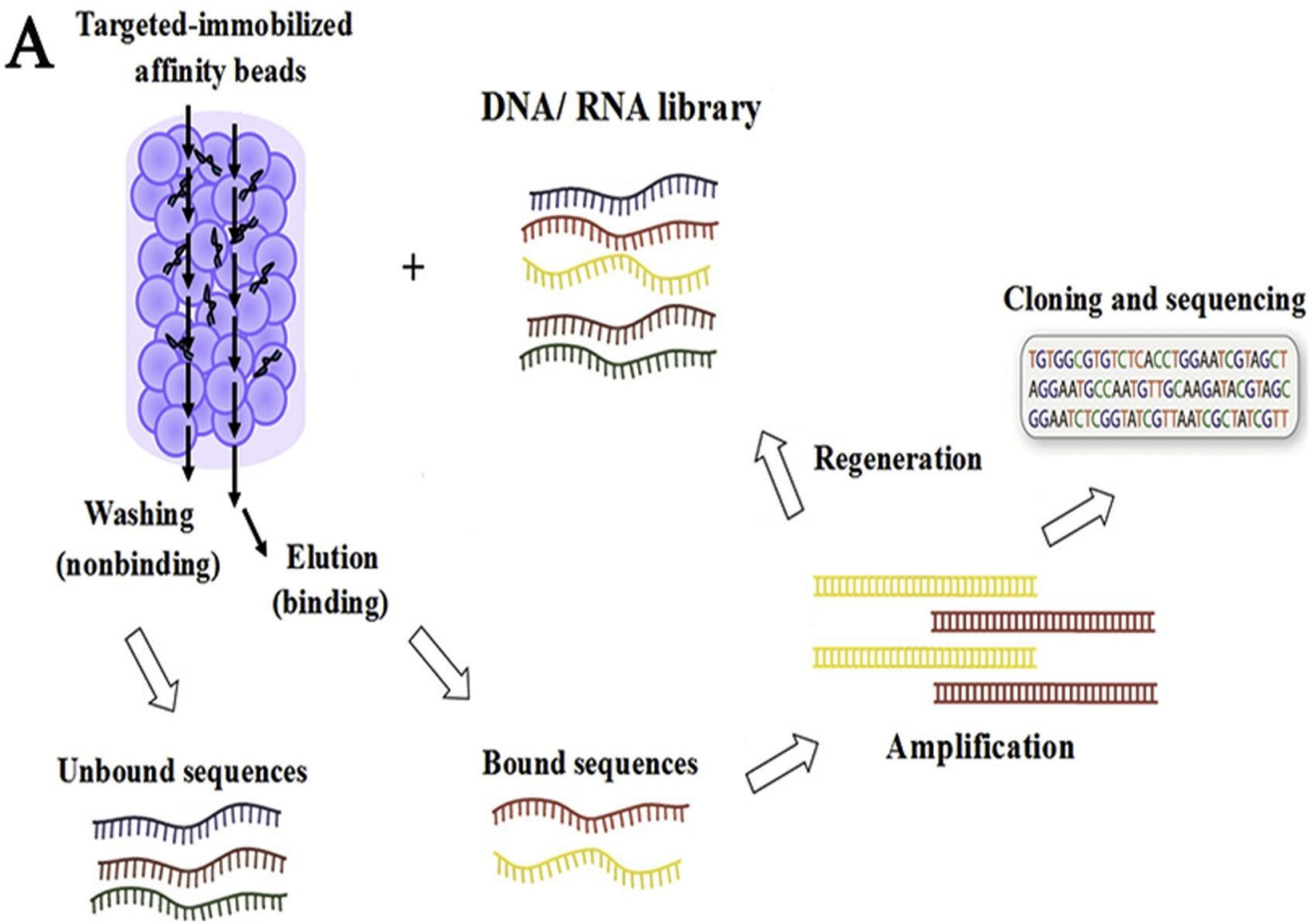
A
Targeted-immobilized affinity beads
DNA/ RNA library
+
Cloning and sequencing
TGTGGCGTGTCTCACCTGGAATCGTAGCT
AGGAATGCCAATGTTGCAAGATACGTAGC
GGAATCTCGGTATCGTTAATCGCTATCGTT
Regeneration
Washing (nonbinding)
Elution (binding)
Unbound sequences
Bound sequences
Amplification

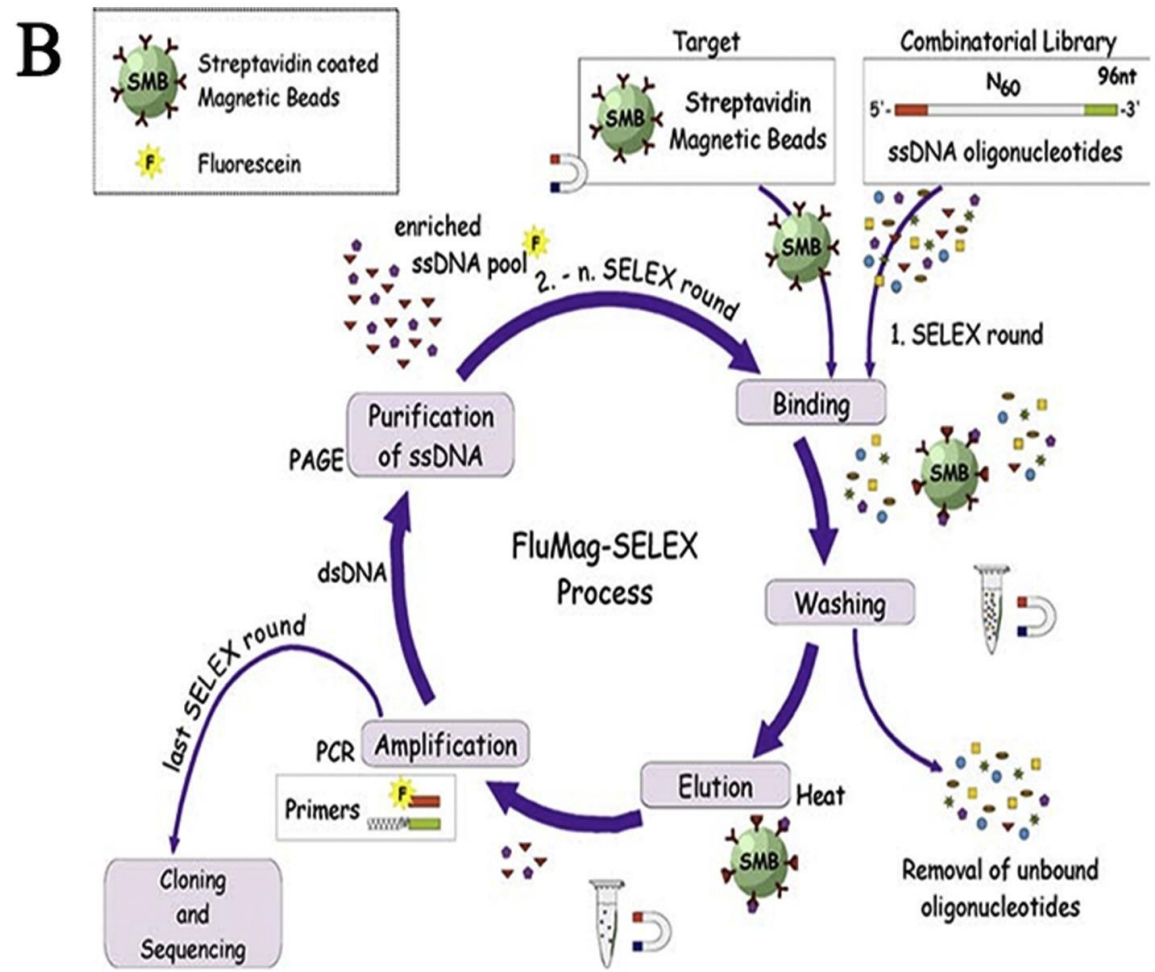
B
Streptavidin coated Magnetic Beads
Fluorescein
Target
Streptavidin Magnetic Beads
Combinatorial Library
N60
96nt
5'-
-3'
ssDNA oligonucleotides
enriched ssDNA pool
2. - n. SELEX round
1. SELEX round
Binding
Purification of ssDNA
PAGE
FluMag-SELEX Process
Washing
dsDNA
last SELEX round
PCR Amplification
Primers
Elution
Heat
Cloning and Sequencing
Removal of unbound oligonucleotides

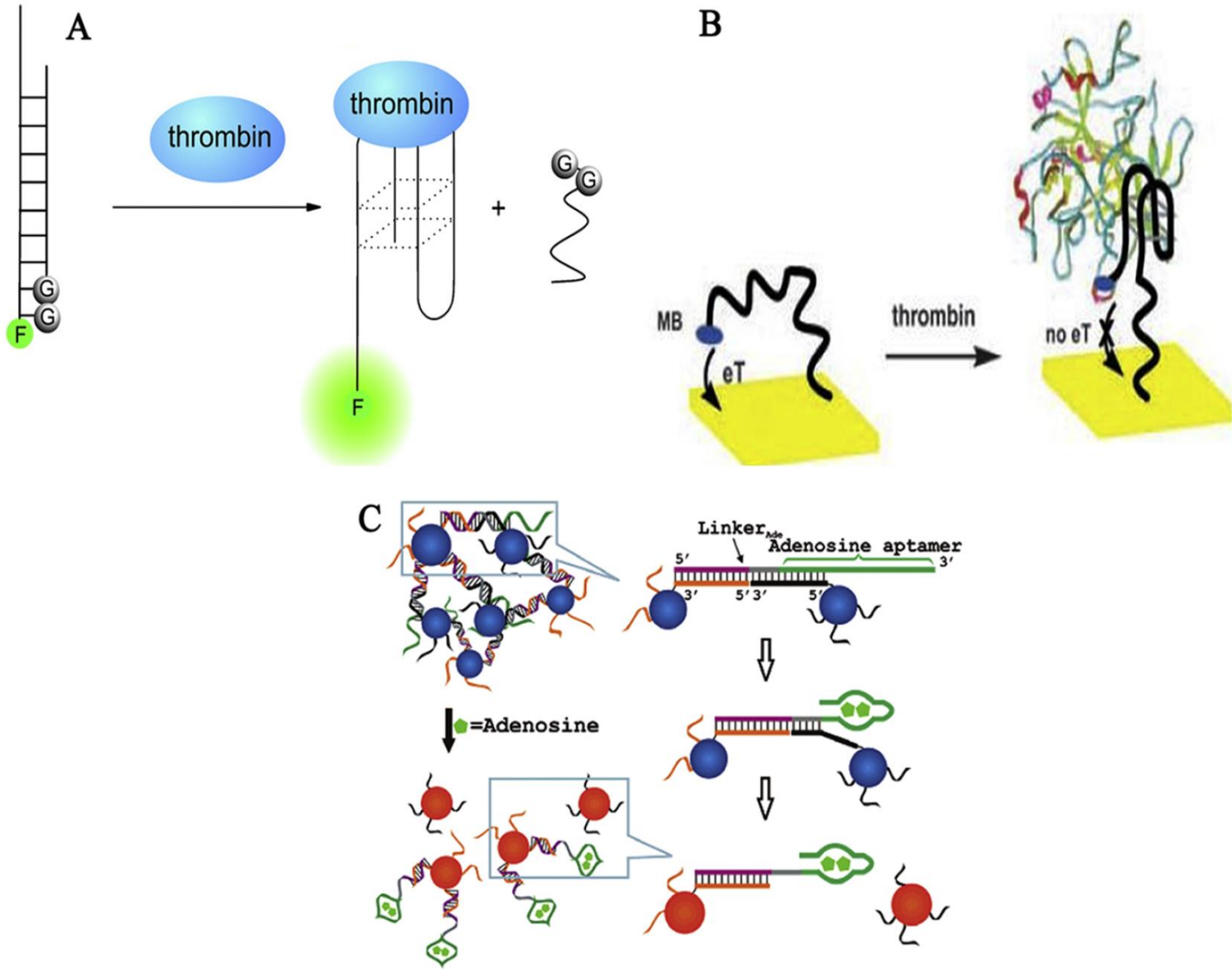

Fig. 5. Various signals generated by aptasensor based on structure-switching designs. (A) A schematic representation of the fluorescent aptasensor for thrombin assay. Thrombin-induced structure change of the aptamer from quenching-state into G-quartet structure could lead to fluorescence enhancement. Fig. 5A adapted from ref. [100]; (B) A schematic representation of the electrochemical aptasensor for thrombin assay. Before adding the thrombin, MB covalently labeled onto aptamer could transfer electron with the electrode surface due to the flexible conformation of the aptamer. Upon adding the thrombin A, G-quaduplex structure was formed and the MB moiety was far away from the electrode surface, resulting in the electrochemical signal-off. Fig. 5B adapted from ref. [105]; (C) A schematic representation of the colorimetric aptasensor for adenosine assay. Gold nanoparticles are functionalized with aptamer. Addition of the adenosine results in nanoparticles linking together and aggregating, thus causing the change in color. Fig. 5C adapted from ref. [107]. Copyright (2007) American Chemical Society.

Molecularly imprinted polymers (MIPs) are synthetic receptors for a targeted molecule. As such, they are analogues of the natural antibody−antigen systems

DOI: 10.1021/acs.chemrev.8b00171 Chem. Rev. 2019, 119, 94−119

Plastic Antibody

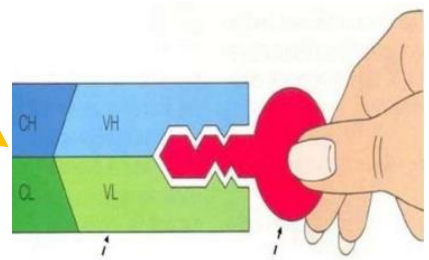

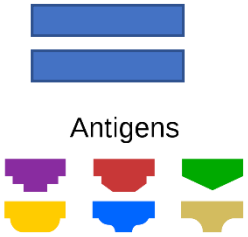

Natural Antibody

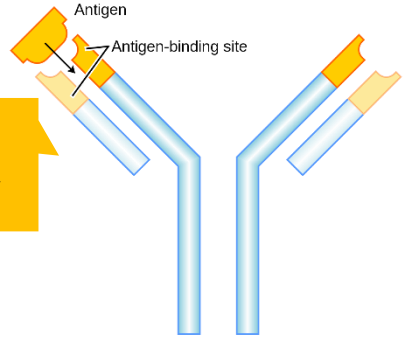

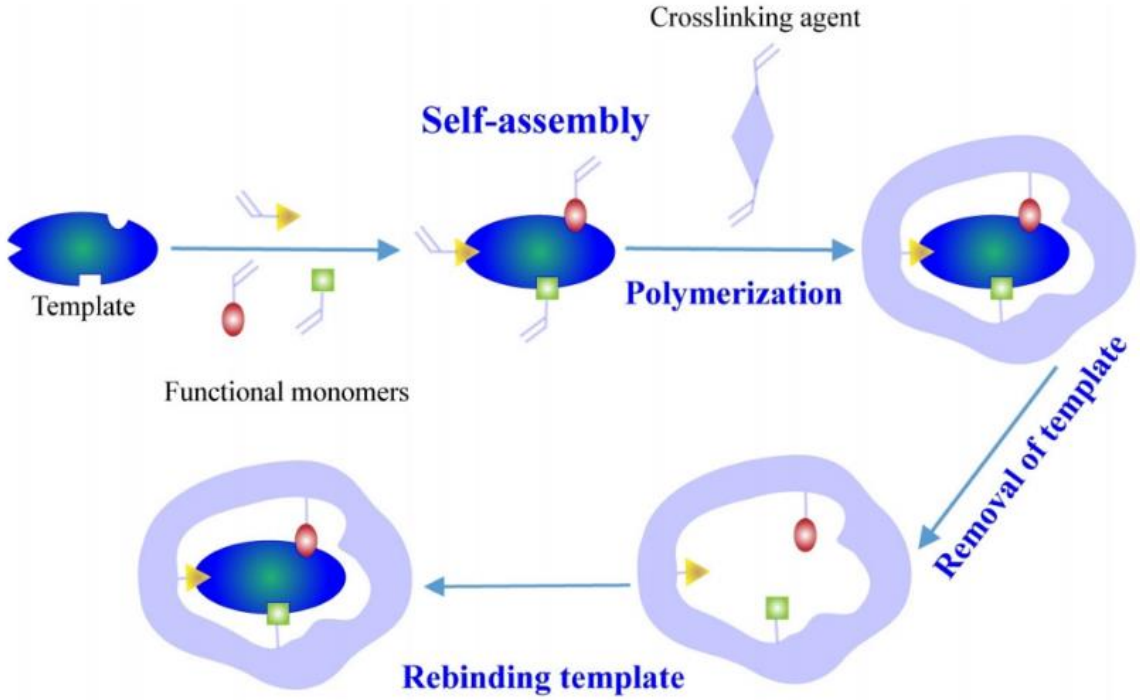

Scheme 1. Schematic representation of the synthesis of molecu-larly Imprinted Polymers (MIPs).

Abdellatif Ait Lahcen[a] and Aziz Amine*[a],2018

MIP-State of the art

MIPs Applications

MIPs are excellent materials with high selectivity and are widely used for:

Sample preparation in bio analytical methods

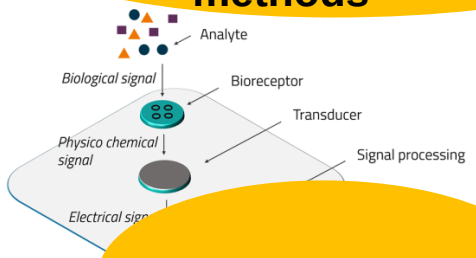

Sensors applications

Chromatography

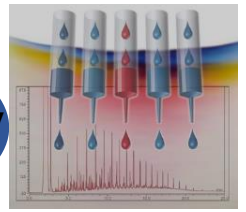

Drug delivery

Catalysis

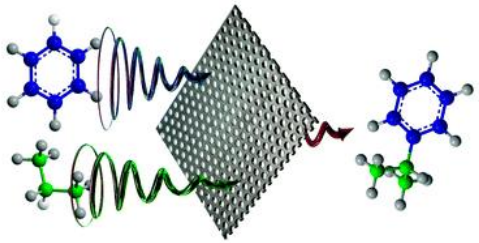

Solid phase extraction

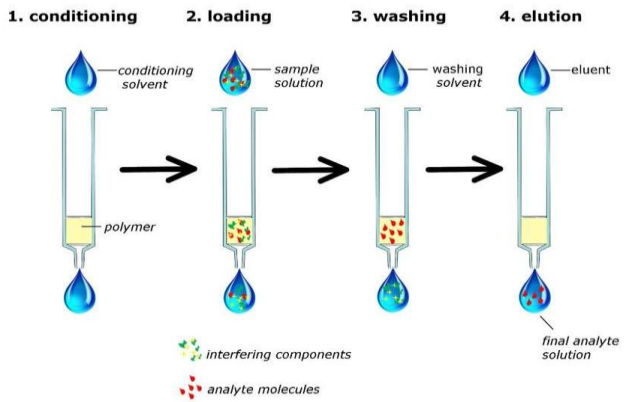

Advantages of MIPs

❖ High **selectivity** and **affinity** for the **target molecule** used in the imprinting procedure.

Compared to biological systems such as proteins and nucleic acids MIP has:

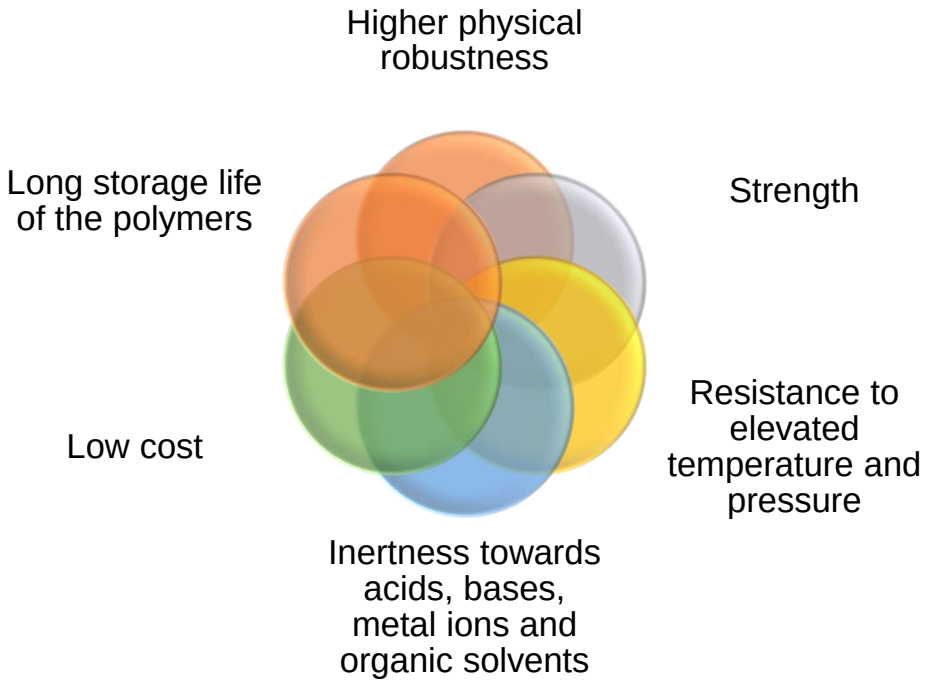

Int J Mol Sci. 2011; 12(9): 5908–5945
***Chem. Rev.* 2000, *100,* 2495-2504**

02 MIP-State of the art

MIPs Synthesis

Components of MIP Mixture

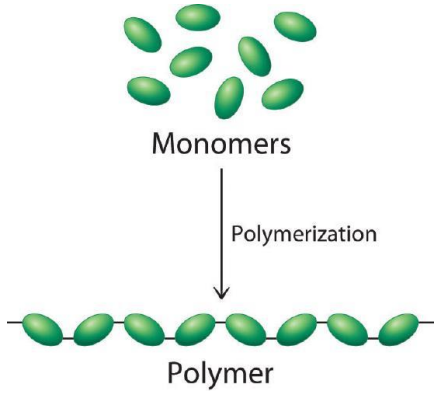

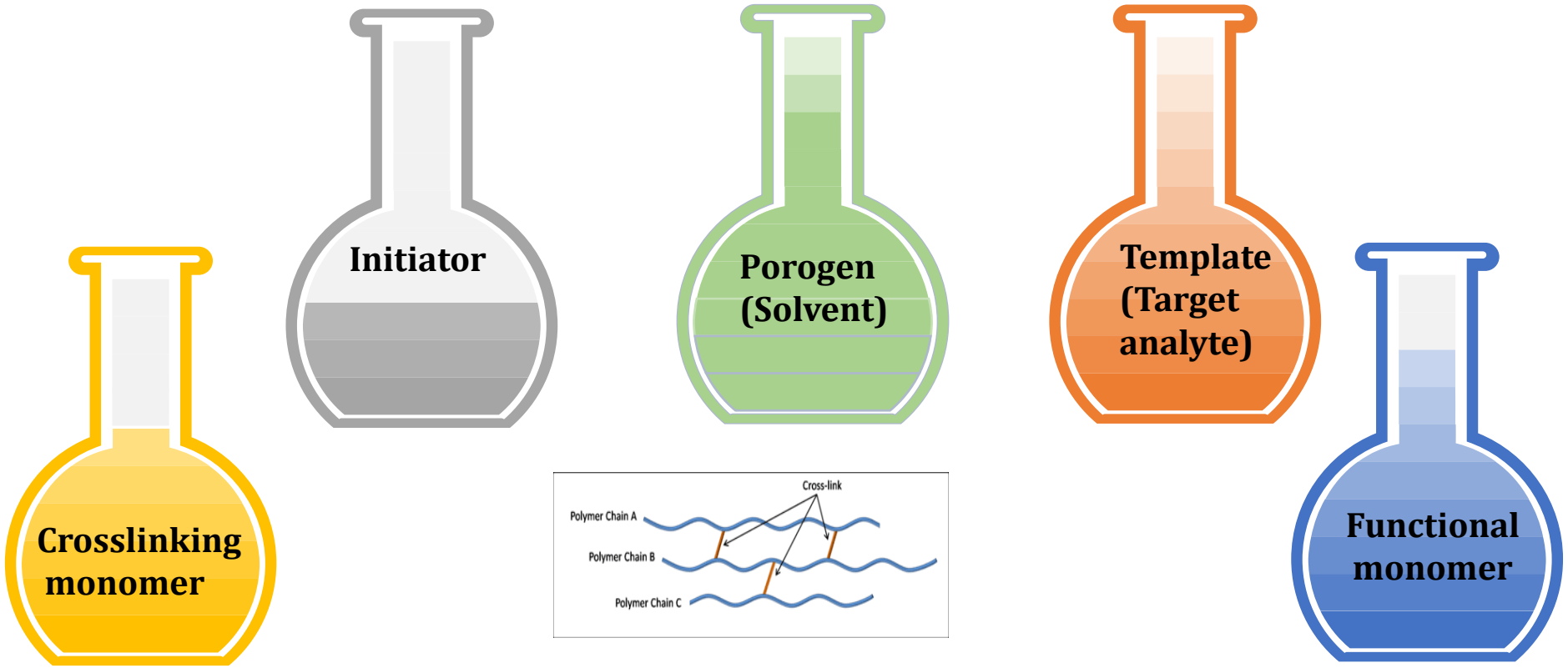

MIPs Synthesis

General procedure

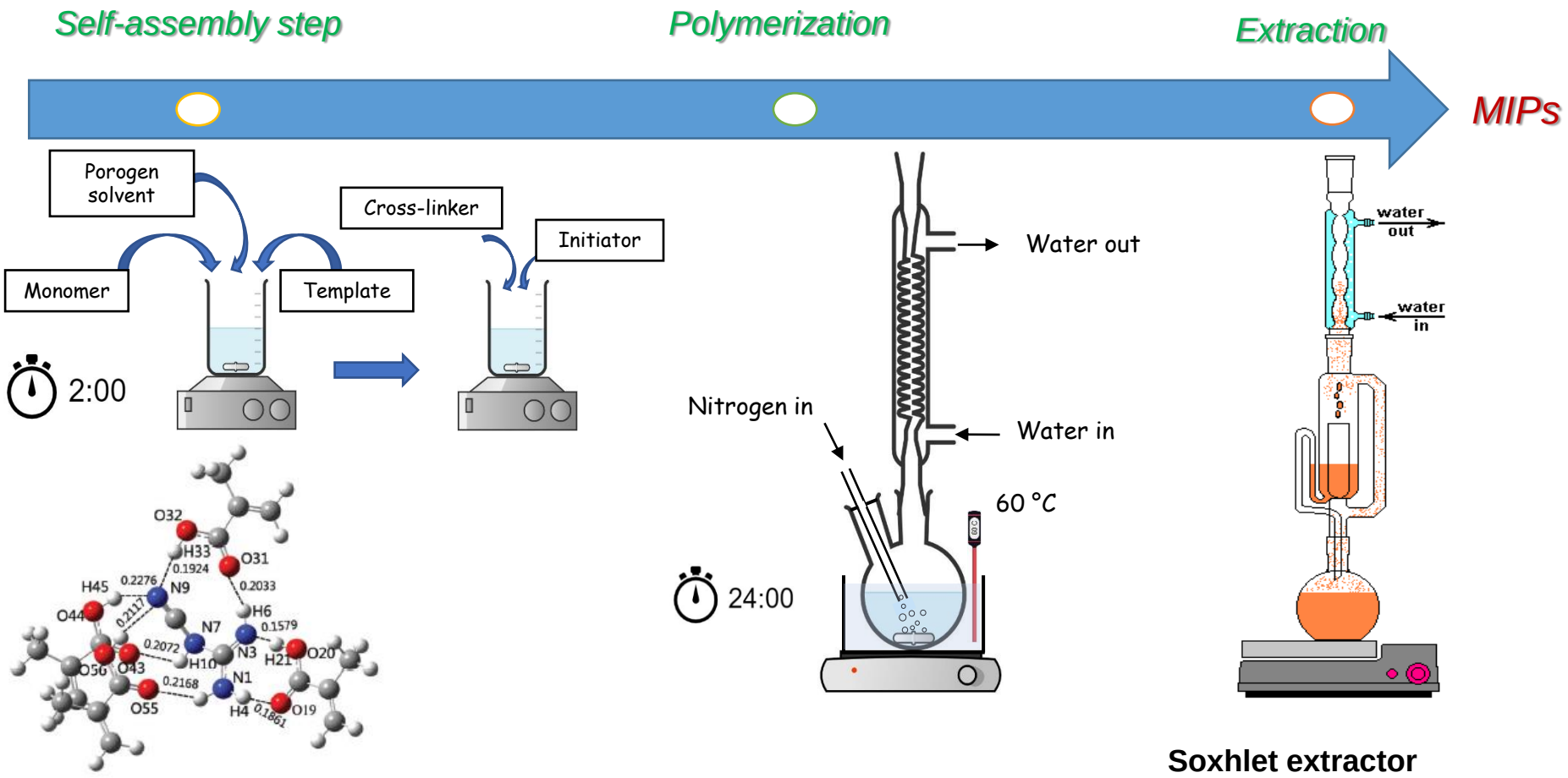

Soxhlet extractor

MIP synthesis

Sulfamethoxazole MIPs Synthesis

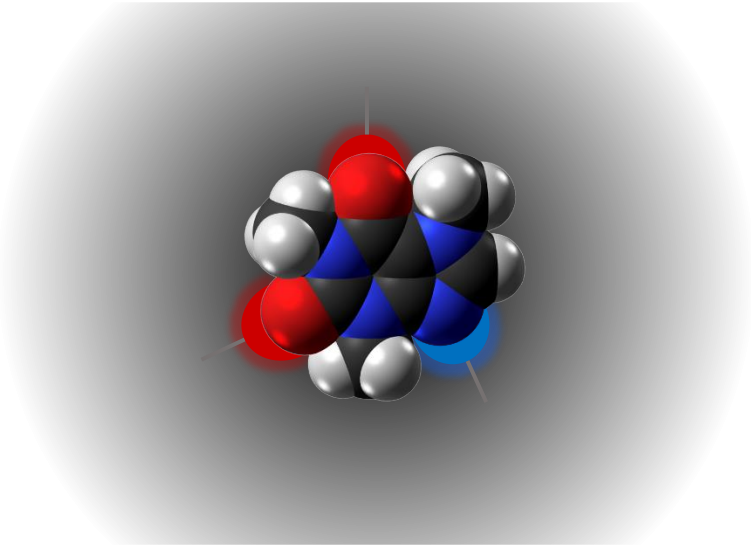

Selective rebinding

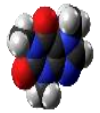

Template (Sulfamethoxasole)

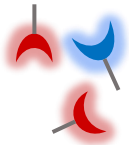

Monomer (Methacrylamide MMA)

MIP-Synthesis

MIPs Synthesis

Synthesis of MIPs

- Thermal heating :24h
- Ultrasound bath :2h
- Ultrasonic probe :Few min

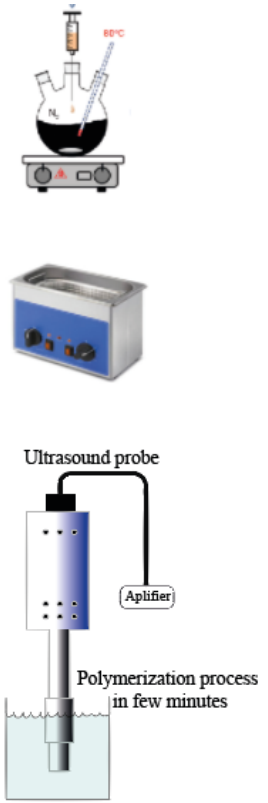

Figure : Synthesis of magnetic molecularly imprinted polymer

03 MIP-Synthesis

Theoretical optimizations prior to MIP s synthesis

Selection of the functional monomer

Prepolymer	$E_{Monomer}$ (Hartree)	$E_{Complex}$	ΔE (kcal/mol)
Sulfamethoxasole:SMX	-1169.32	-	
SMX-Acrylamide	-245.92	-1415.29	-31.37
SMX- 4-vinyl pyridine	-323.88	-1493.25	-31.37
SMX-Methacrylic acid	-304.788	-1474.13	-13.80
SMX-Methacrylamide	-285.03	-1454.41	-37.65

Selection of the solvent

Complexes monomer-template-solvent	$E_{complex}$ (Hartree)
SMX- Methacrylamide-ETOH	-1608.60
SMX- Methacrylamide-DMSO	-2004.76
SMX- Methacrylamide-DMF	-1701.53
SMX- Methacrylamide-ACETONE	-1646.392
SMX- Methacrylamide-ACETONITRILE	-1586.45
SMX- Methacrylamide-TOLUENE	-1724.49
SMX- Methacrylamide-WATER	-1530.38
SMX- Methacrylamide-METHANOL	-1569.47

Methacrylamide -SMX have highest interaction energy in DMSO solvent due to the formation of a more stable complex.

MIPs synthesis optimizations

Optimization of time and amplitude of synthesis was done to select the best parameters for MIP-Ultrasound probe synthesis

	Parameters	Comment	Polymer quality
MMA -MIP 22-07-2020	10 MIN /20A	Polymer was formed	++
MMA -NIP 22-07-2020	10 MIN /20A	Polymer was formed	++
MMA -MIP 23-07-2020	7. 5MIN /30A	Polymer was formed	+++
MAA-NIP 23-07-2020	7. 5MIN /30A	Polymer was formed	+++
MMA-MIP 23-07-2020	5 MIN /20A	Polymer was formed	++++
MMA-NIP 23-07-2020	5 MIN /20A	Polymer was formed	++++

5 min as time of synthesis and 20 as pulse amplitude was selected

Graph of the un-retained template

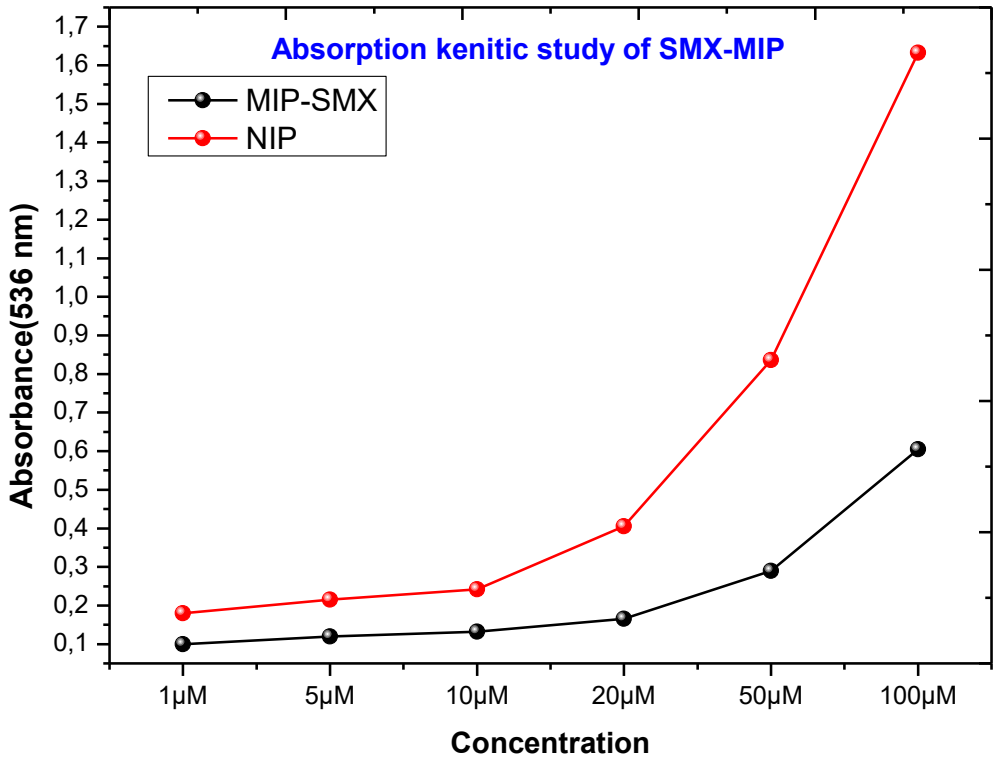

MIP has higher capacity to capture the template compared to non imprinted polymer

02 MIP-State of the art

MIP based electrochemical sensors and nanomaterials

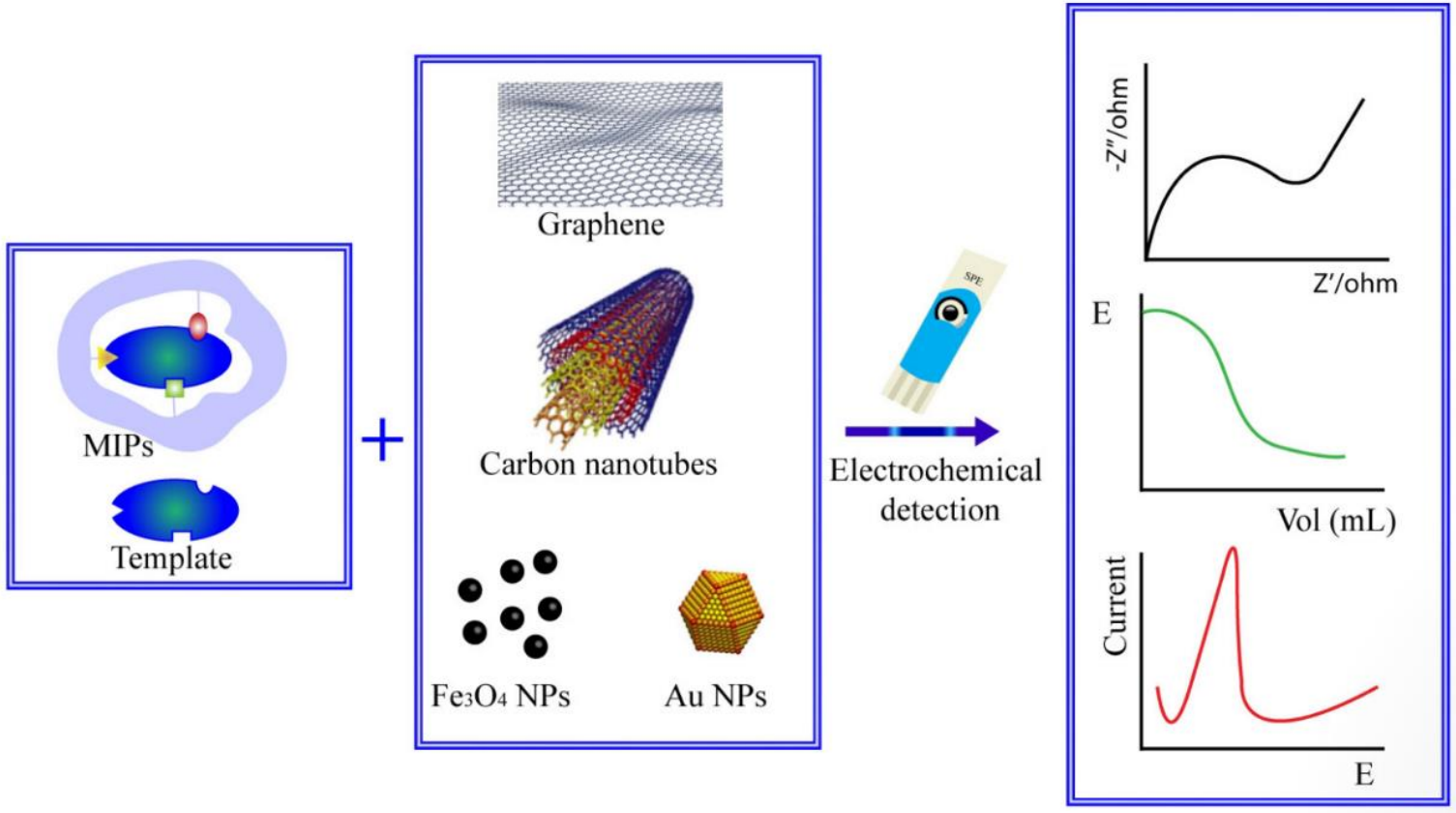

Scheme of MIP based electrochemical sensors and nanomaterials.

Abdellatif Ait Lahcen[a] and Aziz Amine[a],2018*

02 MIP-State of the art

MIP based electrochemical sensors and nanomaterials

Electrosynthesis of MIPs

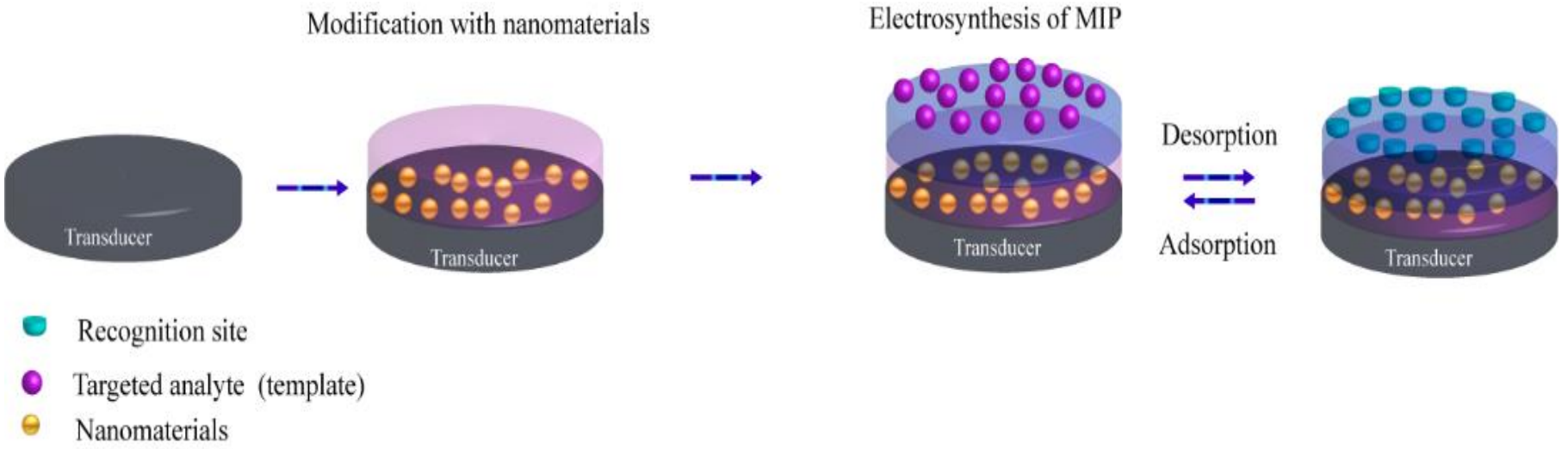

~~Initiator~~

~~Crosslinking monomer~~

Template (Target analyte)

Porogen (Solvent) Buffer

Functional monomer

MIP-State of the art

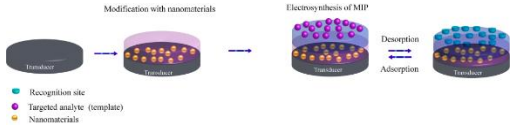

MIP based electrochemical sensors and nanomaterials

Target

- Template

Electrochemical behaviour

- Non-electroactive
- Electroactive

Detection

- Voltametric measurement of redox marker ferricyanide
- Impedance spectroscopy
- Direct electrochemical detection

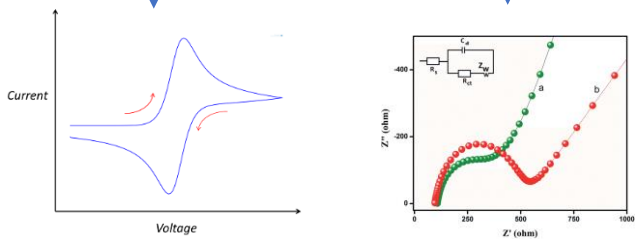

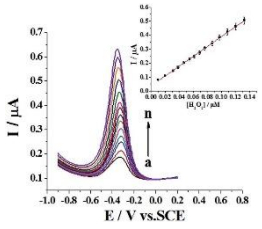

MIP-MEPS based sensing strategy for the selective assay of dimethoate. Application to wheat flour samples

UNIVERSITÀ DEGLI STUDI DI TERAMO

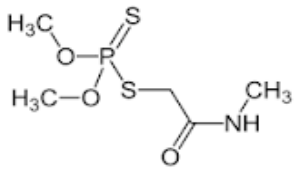

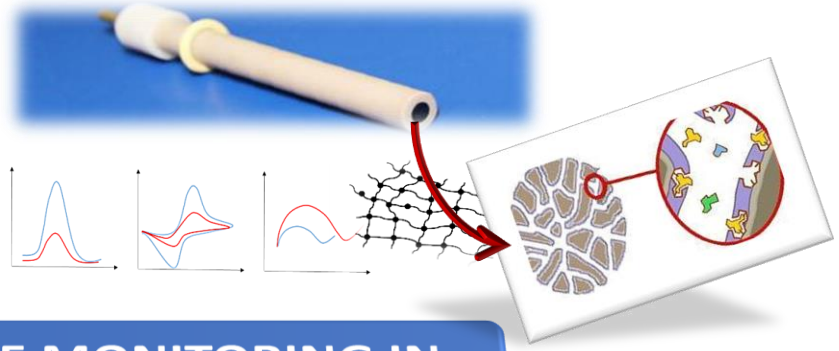

DIMETHOATE MONITORING IN WHEAT FLOUR

SAMPLE PREPARATION

ANALYTE DETECTION

MICROEXTRACTION BY PACKED SORBENT (MEPS)

MIP-GLASSY CARBON ELECTRODE

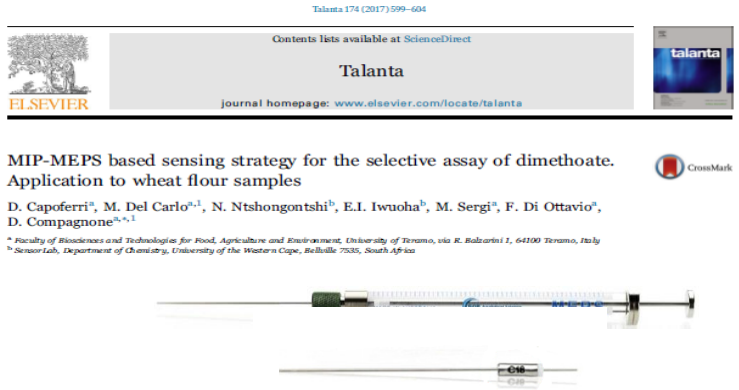

Talanta 174 (2017) 599–604

Contents lists available at ScienceDirect

Talanta

journal homepage: www.elsevier.com/locate/talanta

MIP-MEPS based sensing strategy for the selective assay of dimethoate. Application to wheat flour samples

D. Capoferri[a], M. Del Carlo[a,1], N. Ntshongontshi[b], E.I. Iwuoha[b], M. Sergi[a], F. Di Ottavio[a], D. Compagnone[a,*,1]

[a] Faculty of Biosciences and Technologies for Food, Agriculture and Environment, University of Teramo, via R. Balzarini 1, 64100 Teramo, Italy
[b] SensorLab, Department of Chemistry, University of the Western Cape, Bellville 7535, South Africa

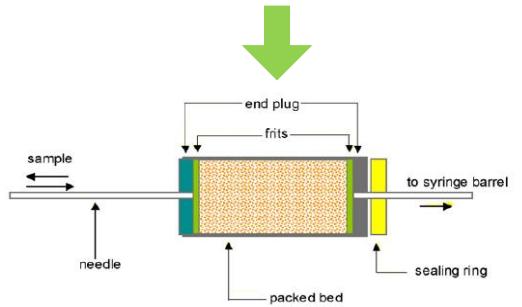

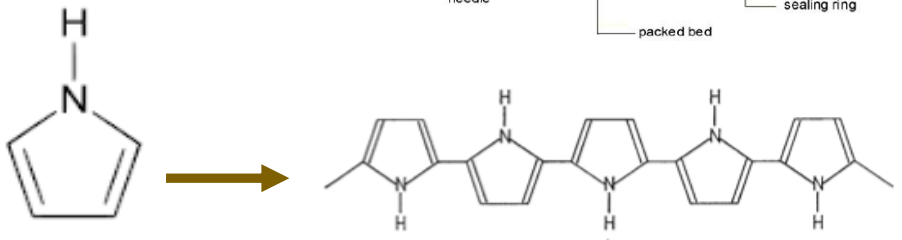

MIP-MEPS based sensing strategy for the selective assay of dimethoate. Application to wheat flour samples

UNIVERSITÀ DEGLI STUDI DI TERAMO

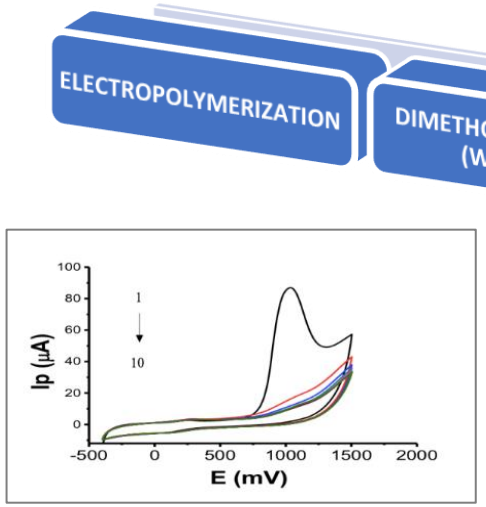

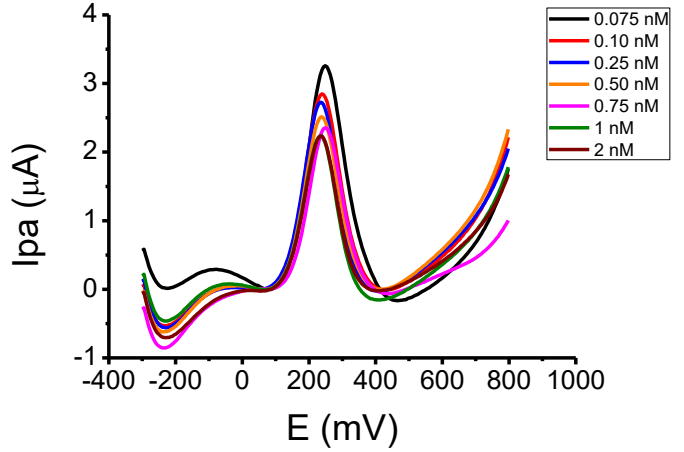

Dose-response curve

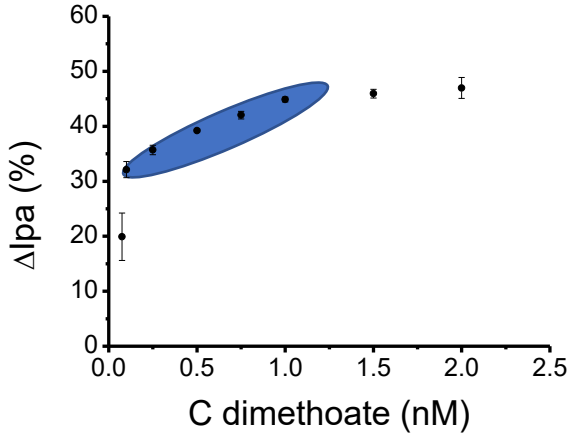

MIP-MEPS based sensing strategy for the selective assay of dimethoate. Application to wheat flour samples

UNIVERSITÀ DEGLI STUDI DI TERAMO

ΔIpa (%)	Repeatability (RSD %)	Reproducibility (RSD %)
0.5 nM dimethoate (n=3)	0.68	2.72
1 nM dimethoate (n=3)	0.95	5.51

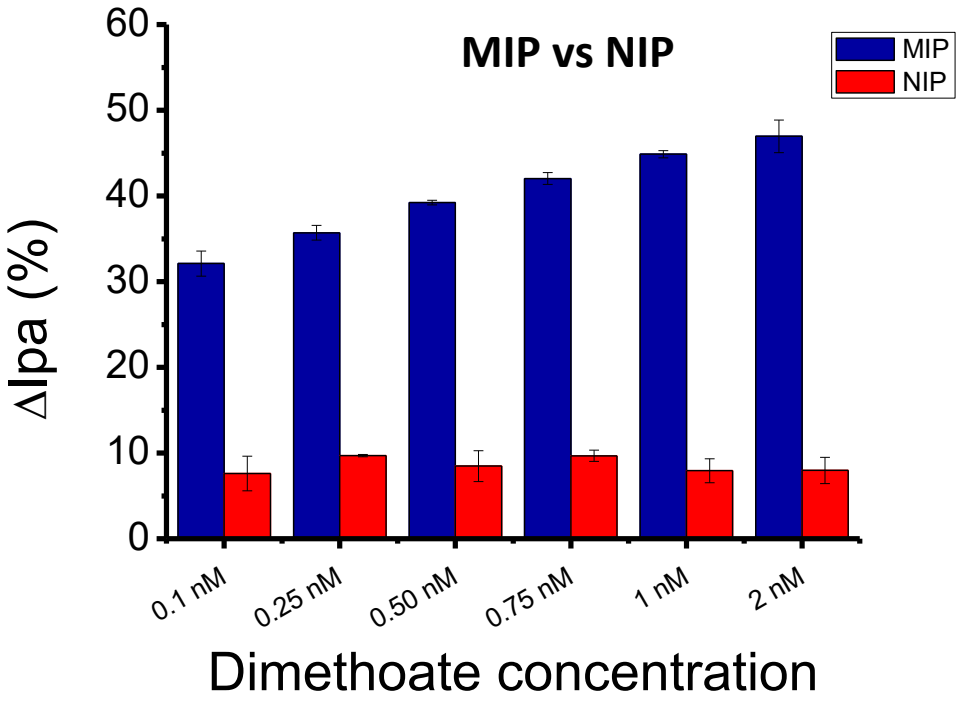

ΔIpa (%) for malathion, parathion and paraoxon after the rebinding step was negligible; **omethoate** gave a response of **23%**.

Dimethoate

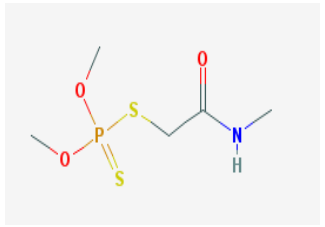

Omethoate

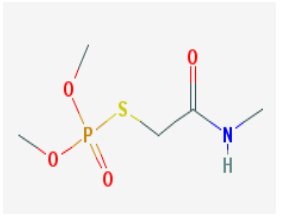

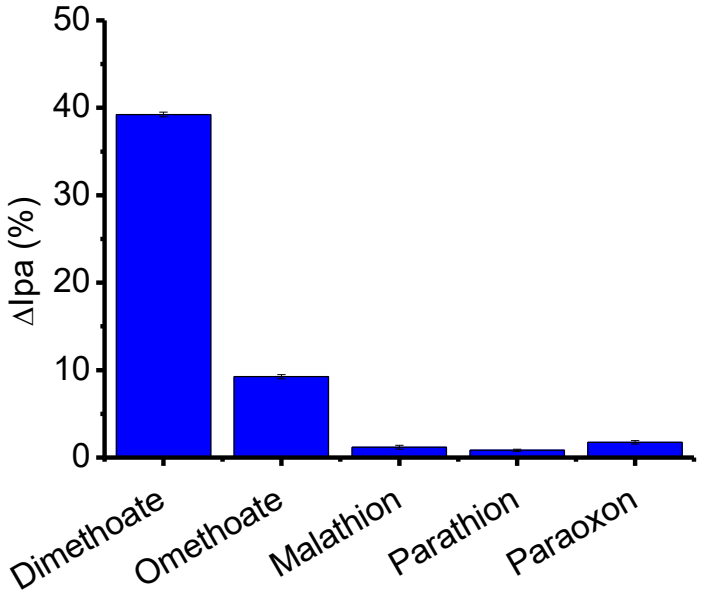

MIP-MEPS based sensing strategy for the selective assay of dimethoate. Application to wheat flour samples

UNIVERSITÀ DEGLI STUDI DI TERAMO

Wheat flour samples: MIP vs. UHPLC-MS/MS

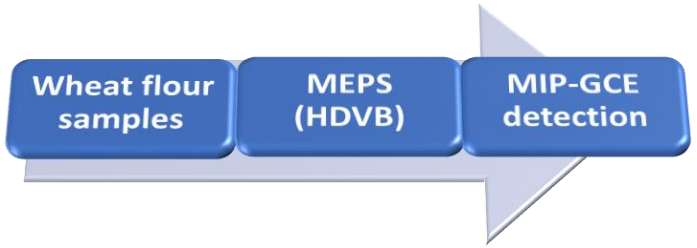

Samples	MIP-GCE RELATIVE ERROR (%) of dimethoate concentration (µg kg^{-1})	MIP-GCE SD of dimethoate concentration (µg kg^{-1})
Wheat flour spiked with dimethoate 0.5 MRL	**+13.5**	0.52
Wheat flour spiked with dimethoate 0.5 MRL + mix	**+4.6**	2.37
Wheat flour spiked with dimethoate MRL	**-21.1**	1.24
Wheat flour spiked with dimethoate MRL + mix	**-21.2**	1.36
Wheat flour spiked with dimethoate 1.5 MRL	**+16.7**	0.74
Wheat flour spiked with dimethoate 1.5 MRL + mix	**-0.4**	1.69
Wheat flour spiked with dimethoate MRL + omethoate (1:1)	**+3.5**	2.70
Wheat flour spiked with dimethoate MRL + omethoate (1:10)	**-15.5**	0.86

Chlorpyriphos

Electrochromic Molecular Imprinting Sensor for Visual and Smartphone-Based Detections

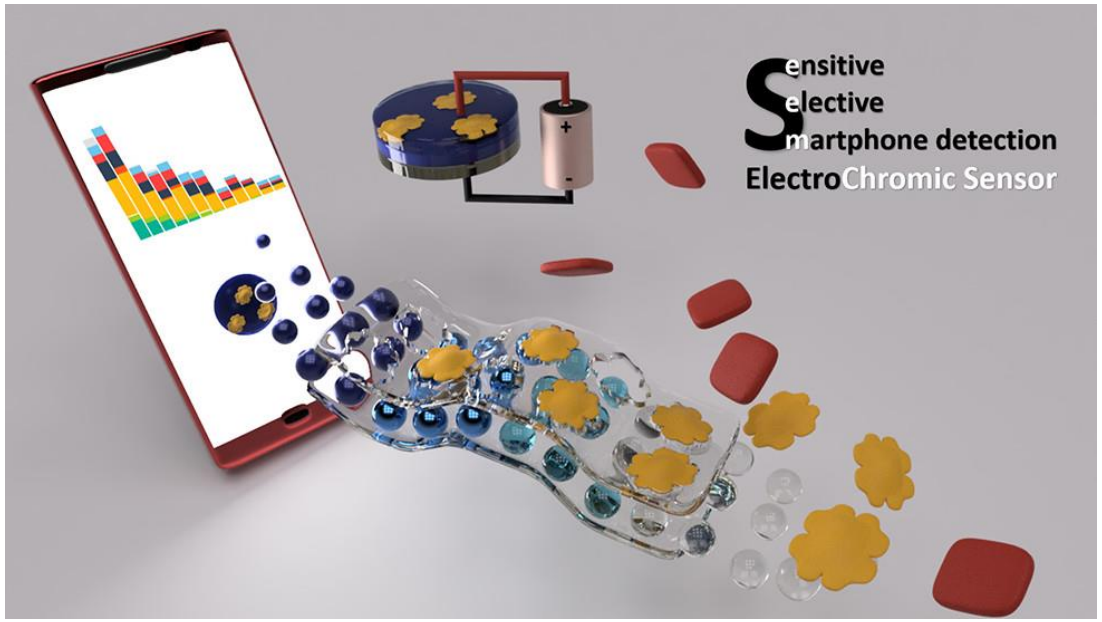

analytical chemistry
Article
Cite This: Anal. Chem. XXXX, XXX, XXX−XXX
pubs.acs.org/ac

Electrochromic Molecular Imprinting Sensor for Visual and Smartphone-Based Detections

Denise Capoferri,[†,‡,§] Ruslan Álvarez-Diduk,[†,§] Michele Del Carlo,[‡] Dario Compagnone,[‡] and Arben Merkoçi*[,†,∥]

[†]Nanobioelectronics and Biosensor Group, Catalan Institute of Nanoscience and Nanotechnology (ICN2), CSIC, The Barcelona Institute of Science and Technology, Campus UAB, Bellaterra, 08193, Barcelona, Spain
[‡]Faculty of Biosciences and Technologies for Food, Agriculture and Environment, University of Teramo, via R. Balzarini 1, 64100 Teramo, Italy
[∥]Catalan Institution for Research and Advanced Studies (ICREA), Pg. Lluís Companys 23, 08010 Barcelona, Spain

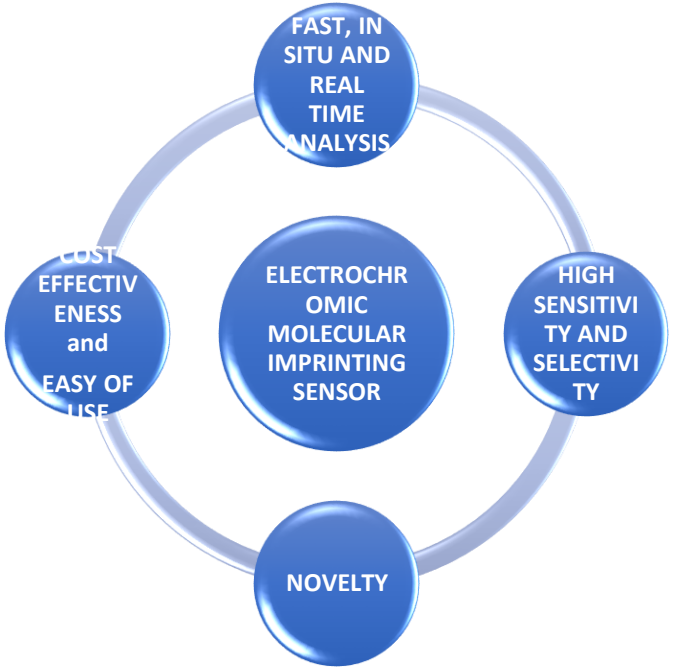

Electrochromic Molecular Imprinting Sensor for Visual and Smartphone-Based Detections

UNIVERSITÀ DEGLI STUDI DI TERAMO

Electrochromism

MIP **Strategy**

Screen-printing technology

Smartphones

CPF (chlorpyrifos)

Py

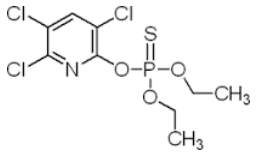

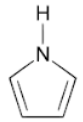

ELECTROCHROMIC MOLECULAR IMPRINTING SENSOR for an ORGANOPHOSPHATE PESTICIDE

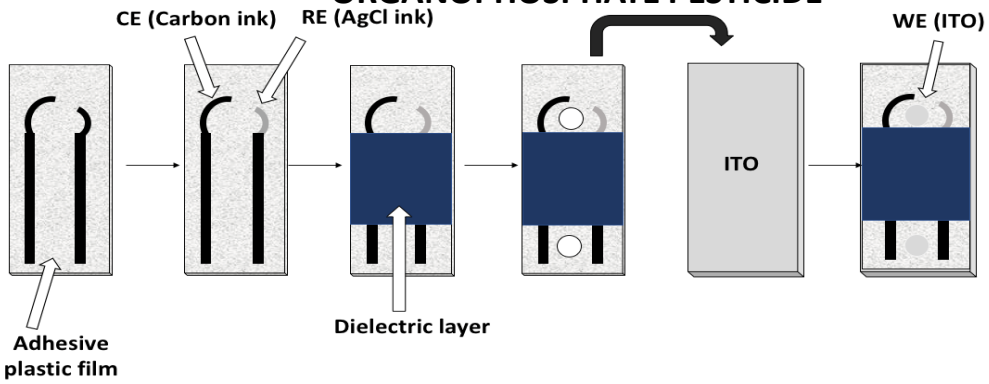

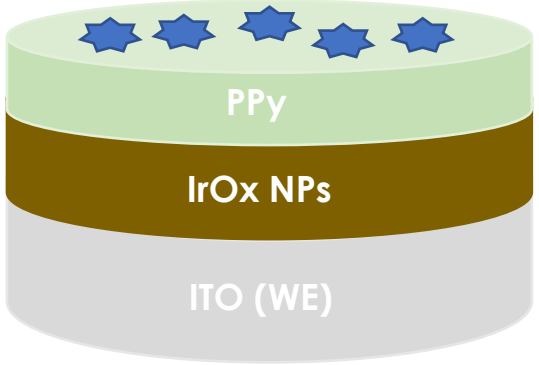

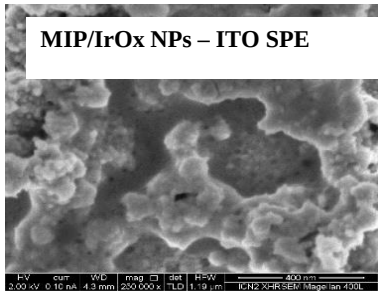

Electrochromic Molecular Imprinting Sensor for Visual and Smartphone-Based Detections

UNIVERSITÀ DEGLI STUDI DI TERAMO

WORKING PRINCIPLE

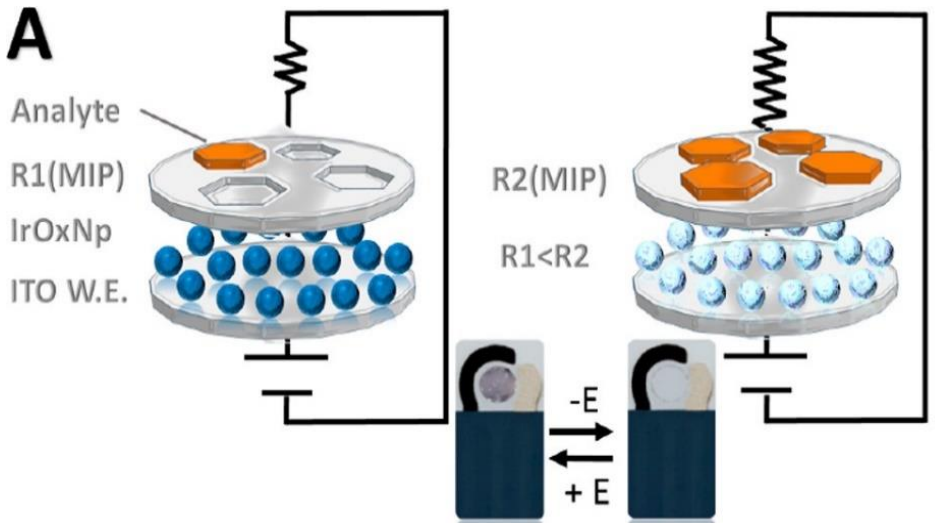

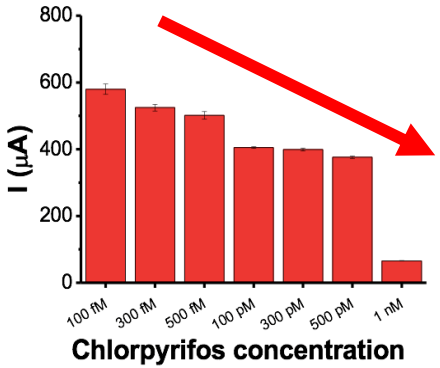

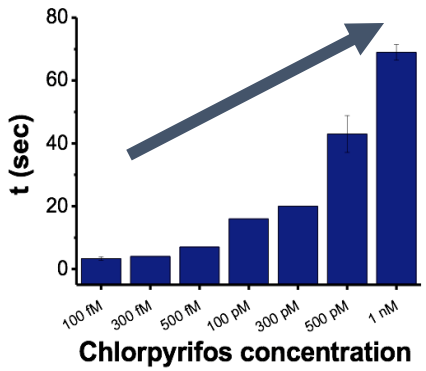

Electrochromic Molecular Imprinting Sensor for Visual and Smartphone-Based Detections

UNIVERSITÀ DEGLI STUDI DI TERAMO

VISUAL APPROACH

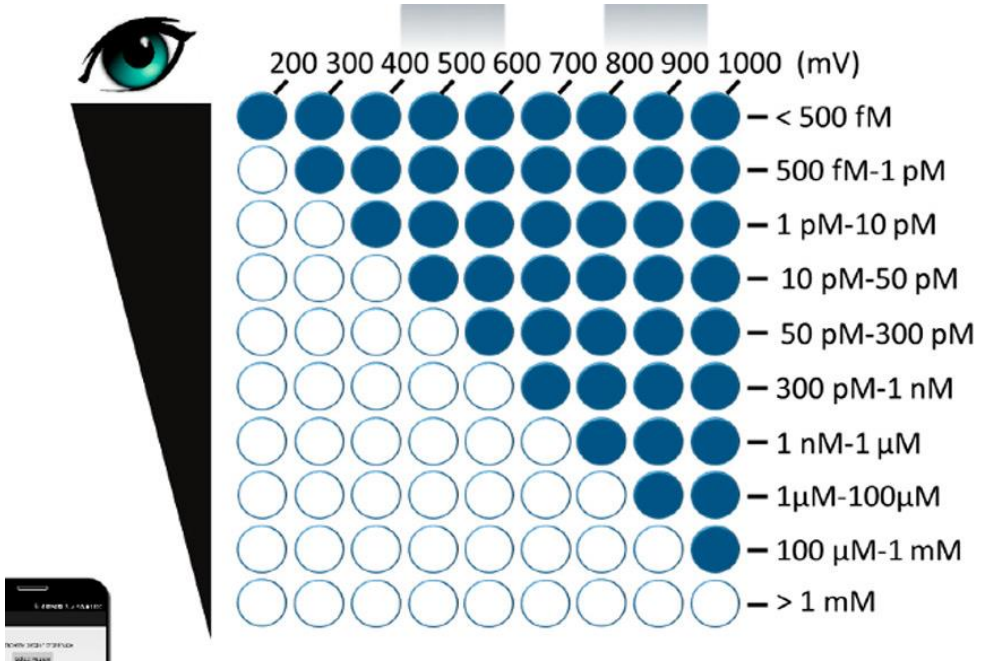

SMARTPHONE APPROACH

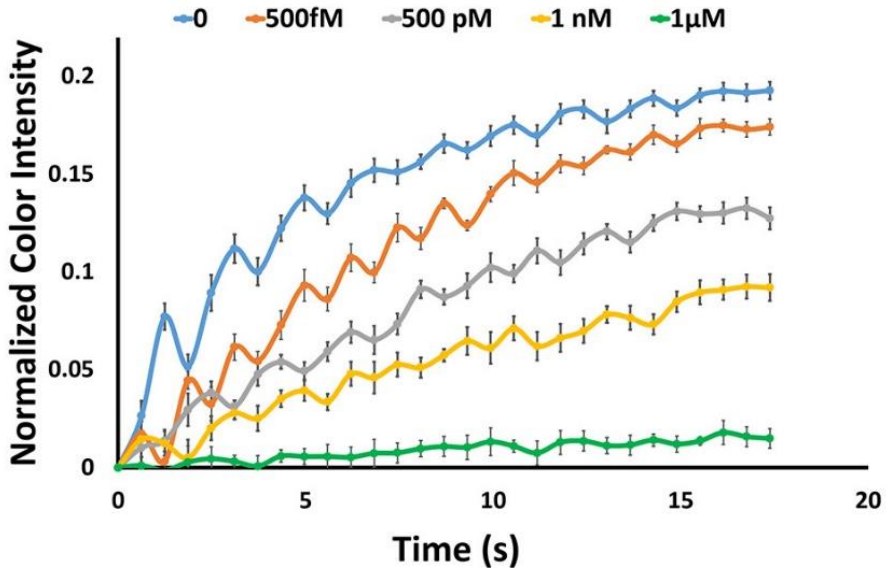

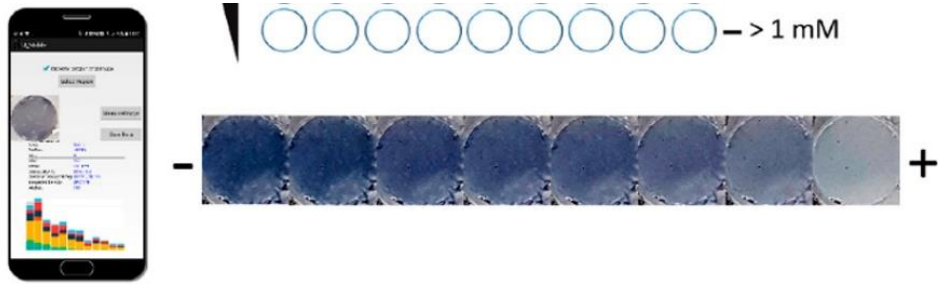

Electrochromic Molecular Imprinting Sensor for Visual and Smartphone-Based Detections

MIP vs NIP

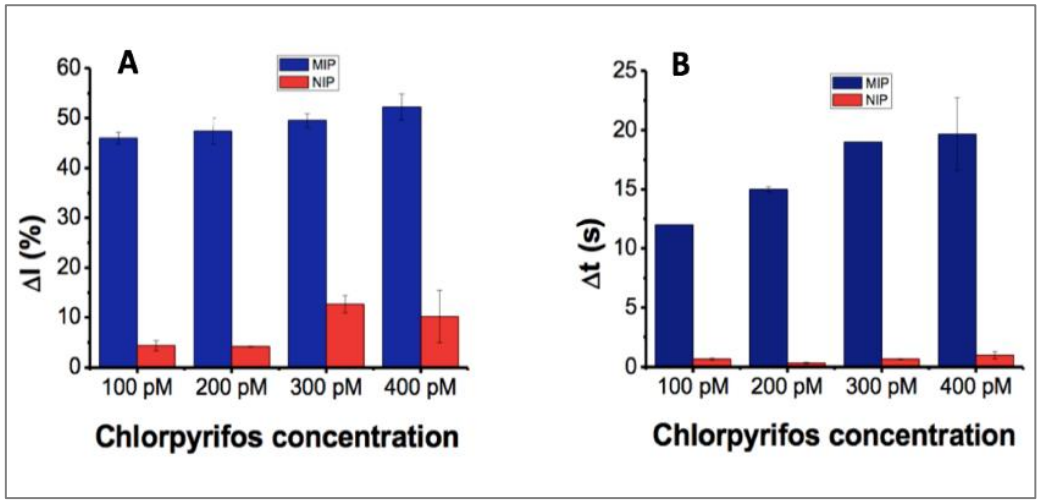

SELECTIVITY (500 mV-1000 mV)

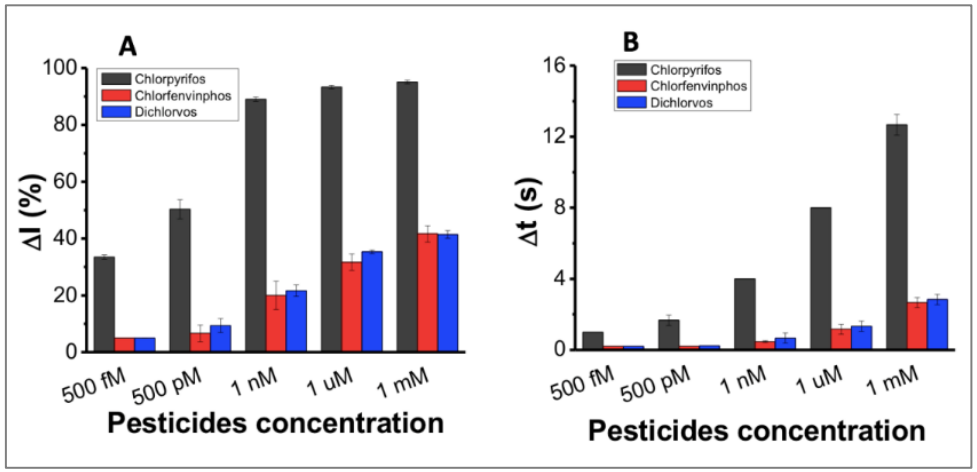

Recovery values of chlorpyrifos in spiked drinking water samples (n = 3) using the current response

Added (Spiked)	Found	Recovery (%)	RSD (%)
500 fM	517.19 fM	**103.44 ± 16.14**	15.60
500 pM	471.45 pM	**94.29 ± 17.92**	19.00
1 nM	0.99 nM	**99.50 ± 19.90**	20.00
1 µM	0.98 µM	**97.55 ± 25.87**	26.52
1 mM	1.07 mM	**106.57 ± 15.30**	14.36